Universiteit
Leiden
The Netherlands

Unraveling the auxin mechanism in 2,4-D induced somatic embryogenesis in Arabidopsis thaliana

Philipsen, C.

Citation
Philipsen, C. (2017, March 30). *Unraveling the auxin mechanism in 2,4-D induced somatic embryogenesis in Arabidopsis thaliana*. Retrieved from https://hdl.handle.net/1887/47238

Version:	Not Applicable (or Unknown)
License:	Licence agreement concerning inclusion of doctoral thesis in the Institutional Repository of the University of Leiden
Downloaded from:	https://hdl.handle.net/1887/47238

Note: To cite this publication please use the final published version (if applicable).

Cover Page

Universiteit Leiden

The handle http://hdl.handle.net/1887/47238 holds various files of this Leiden University dissertation

Author: Philipsen, Cheryl
Title: Unraveling the auxin mechanism in 2,4-D induced somatic embryogenesis in Arabidopsis thaliana
Issue Date: 2017-03-30

Unraveling the auxin mechanism in 2,4-D induced somatic embryogenesis in *Arabidopsis thaliana*

Cheryl Philipsen

Cover design by Cheryl Philipsen and Ridderprint
Lay out design by Ridderprint BV, Ridderkerk, the Netherlands

Funding statement: This work was supported by the Division for Earth and Life Sciences (ALW) with financial aid from the Netherlands Organisation for Scientific Research (NWO), through an NWO-TTI Green Genetics core project grant (NWO 828.11.004) to Dr. Remko Offringa at Leiden University and Dr. Kim Boutilier and Prof. Dr. Gerco Angement at Wageningen University & Research.

Printed by Ridderprint BV, Ridderkerk, the Netherlands

ISBN: 978-94-6299-557-4

Unraveling the auxin mechanism in 2,4-D induced somatic embryogenesis in *Arabidopsis thaliana*

Proefschrift

Ter verkrijging van
de graad van Doctor aan de Universiteit Leiden,
op gezag van Rector Magnificus Prof. mr. C.J.J.M. Stolker,
volgens besluit van het College voor Promoties
te verdedigen op 30 maart 2017
klokke 15.00 uur

door

Cheryl Philipsen

Geboren te Den Helder, Nederland
12 september 1987

Promotiecommissie

Promotor: Prof. P. J. J. Hooykaas

Co-promotor: Dr. R. Offringa

Overige leden: Prof. Dr. H. Spaink
Prof. Dr. J. J. Memelink
Prof. Dr. A. van Duijn
Dr. A. Horstman (Universiteit Wageningen)
Dr. E. Larsson (Swedish University of Agricultural Sciences, Uppsala)

Contents

Chapter 1
The role of auxin in somatic embryo induction and development 7

Chapter 2
2,4-D-induced somatic embryogenesis initiation requires a relative auxin minimum in *Arabidopsis*. 43

Chapter 3
Auxin dynamics during SE initiation is established by the tryptophan-dependent indole-3-pyruvic acid pathway in *Arabidopsis* 75

Chapter 4
Somatic embryogenesis initiation in *Arabidopsis* requires *SOLITARY ROOT/IAA14*-regulated dynamic auxin responses similar to lateral root initiation 107

Summary 143

Samenvatting 149

Dankwoord 155

Curriculum vitae 161

Chapter 1

The role of auxin in somatic embryo induction and development

Cheryl Philipsen[1,2]

[1] *Molecular and Developmental Genetics, Institute of Biology Leiden, Leiden University, Sylviusweg 72, 2333BE, Leiden, the Netherlands*
[2] *Current affiliation: Dümmen Orange, P.O. Box 26, 2678ZG, de Lier, the Netherlands*

Abstract

Vegetative propagation of plants comes in many forms such as cuttings, and shoot- and root regeneration. Alternatively, somatic embryogenesis (SE) can be employed to generate stable clonal lines of the parents. In most protocols to induce SE, the herbicide 2,4-dichlorophenoxyacetic acid (2,4-D) is used to induce the redifferentiation of embryogenic cells from somatic cells. 2,4-D is a synthetic analogue of the natural plant hormone auxin, or indole-3-acetic acid (IAA). Auxin is well known for its instructive role in many plant developmental processes and growth responses such as embryogenesis, organogenesis and tropisms. However, the exact role of auxin in the complex process of SE is still not clarified. The molecular mechanism of SE and specifically how 2,4-D, and not IAA or other auxin analogues, is able to induce this process is not yet fully understood. Here the different forms of SE and the mechanism of auxin action are reviewed, with the aim to explain how the synthetic auxin analogue 2,4-D is able to induce totipotency in somatic cells, resulting in SE, and what are potential starting points to study this interesting developmental process.

Introduction

Each living organism, whether it belongs to the bacterial-, fungal-, plant-, or animal kingdom has its own way of reproducing. Two main routes of reproduction can be distinguished, either asexual resulting in offspring that is genetically identical to the parent, or sexual requiring the production of sexual cells, or gametes, through a process of reduction division, and the subsequent fusion of gametes. These gametes can be derived from the same (hermaphrodite) parent or from different (unisexual) parents (Roach et al., 2014). Unicellular organisms such as bacteria and fungi typically reproduce asexually, as their cells divide by binary fission or form daughter cells by budding (Attar, 2016). Several higher animal and plant species have adopted a natural asexual reproduction strategy, named parthenogenesis, where embryo development occurs independent of fertilisation. Parthenogenesis includes plant reproduction strategies such as apomixis, a collective naming for asexual reproduction in plants that involves fertilisation-independent embryo development from different parts of the ovule, and results in the formation of seeds carrying embryos identical to the female parent (Koltunow, 1993; Pupilli and Barcaccia, 2012). There are two distinct apomixis strategies in plants. In the first strategy no embryo sac is produced, and the embryo originates from one or more somatic cells of the maternal ovule tissue, the nucellus or inner integument. This strategy is commonly referred to as sporophytic apomixis or adventitious embryony. The second strategy entails the formation of an unreduced embryo sac, followed by embryo development from a diploid egg cell (gametophytic apomixis). In gametophytic apomixis, the unreduced embryo sac may arise from a somatic nucellar cell (apospory) or from an unreduced megaspore mother cell (diplospory) (for a detailed overview Pupilli and Barcaccia, 2012). Apomixis-loci have been identified in *Arabidopsis* and several other species, however, due to the complexity of the trait the exact role of genes controlling apomixis remains to be resolved (Barcaccia and Albertini, 2013).

In contrast, most higher plants and animals generally produce offspring with a unique genetic basis through sexual reproduction. The latter process involves zygotic embryogenesis, which starts with the establishment of the zygote by fusion of the male and female gametes. The embryo develops from the zygote by a combination of cell division and cell differentiation. The cell migration that is essential for animal embryogenesis does not occur in plant embryos, as plant cells are fixed in a cell wall matrix (Bedzhov et al., 2014; ten Hove et al., 2015). In the dicot model species *Arabidopsis thaliana* the basic body plan is established by a more or less programmed series of cell divisions forming respectively the

radial pattern, the apical-basal axis coinciding with the establishment of the shoot- and root apical meristem (SAM and RAM) stem cell zones (Figure 1a), and finally with the initiation of the cotyledon primordia the bilateral symmetry that is typical for dicot plant embryos (Meyerowitz, 2002). In the late immature zygotic embryo (IZE) the SAM is flanked by two cotyledons and connected with the basal RAM by the hypocotyl (Figure 1b, Lau et al., 2011). After germination, the final shape of the plant is elaborated from this basal body plan by organ formation from the SAM and from the RAM-produced pericycle layer during post-embryonic development (Figure 1c,d). This final plant shape can differ considerably depending on the environmental conditions under which plants are grown. It is this stem cell zone-driven flexibility in development that allows sessile plants to adapt to sudden changes in environmental conditions. Moreover, the regenerative capacity of plant cells, especially those in the stem cell zones, has allowed the development of *in vitro* systems for clonal propagation of crop plants. Plant clonal propagation can be readily achieved in tissue culture either through stem cuttings, or by shoot- and subsequent root regeneration from tissues requiring (*de novo)* organogenesis, or by the induction of somatic embryos. The latter process requires the induction of totipotent cells from somatic cells, in order to develop somatic embryos that will contain a root-shoot axis, a vascular system and functional meristems, all produced in one single developmental step and referred to as somatic embryogenesis (SE).

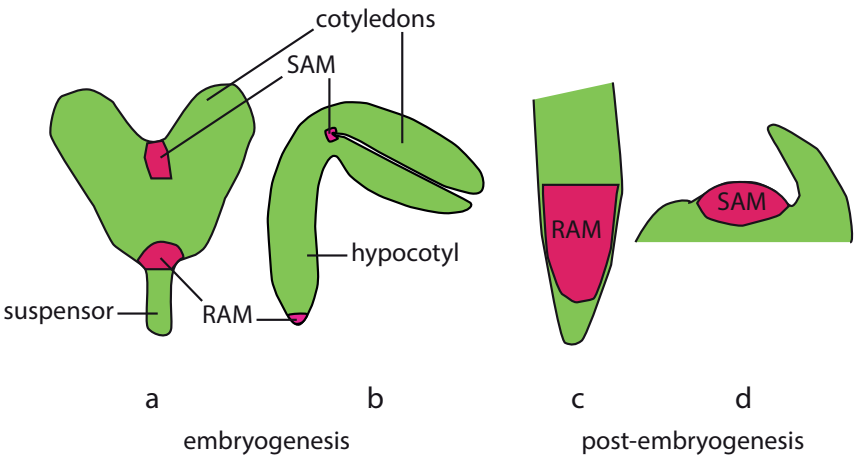

FIGURE 1 - Schematic overview of stem cell niches in Arabidopis embryos and post-embryonic tissues.
In the heart stage (a) and bent cotyledon stage embryos (b) the shoot apical meristem (SAM) is flanked by two cotyledons, whereas the root apical meristem (RAM) connects the embryo with the suspensor (a) or is located basally of the hypocotyl in the IZE (b). During post-embryonic development, the stem cell niches are located in the RAM (c) or in in the SAM of stems or leaves (d).

Both SE and apomixis are favourable in agriculture as a reproductive strategy for stable clonal propagation of heterozygous F1 crop plants, which allows for selecting gene combinations such as those showing heterosis (Pupilli and Barcaccia, 2012). Other applications include propagation of open pollinated crops, crops with long life cycles, or male sterile lines (Pupilli and Barcaccia, 2012; Barcaccia and Albertini, 2013). Propagation via SE has a number of advantages over other forms of asexual propagation or *in vitro* organogenesis in that cell cultures can be immortalized and scaled-up in bioreactors and the resulting embryos can be cryopreserved to store for later use or to establish gene banks (Timmis, 1998; Arnold et al., 2002). Moreover, as opposed to shoot/root regeneration, SE has been reported to result in limited somaclonal variation among the propagated individuals (reviewed by Gaj, 2004; Bairu et al., 2011) and can be induced on multiple types of explants, generally by using high concentrations of 2,4-dichlorophenoxy acetic acid (2,4-D), a synthetic analogue of the plant hormone auxin. In this Chapter the auxin mechanism is introduced and our current knowledge on 2,4-D induced SE and transcription factor induced SE is reviewed.

The plant hormones auxin and cytokinin in plant clonal propagation

Based on early plant tissue culture experiments, the plant hormones auxin and cytokinin have been identified as key regulators of plant regeneration. Natural cytokinins identified are adenine derivates that induce cell division and are involved in phyllotaxis and many other developmental processes (Kieber and Schaller, 2014). The first cytokinin identified, kinetin, was found in autoclaved herring sperm DNA as a potent activator of tobacco cell proliferation. In the same laboratory, another purine derivative, 6-benzylaminopurine (BA) was discovered and shown to stimulate cell division in cultured tissues (Miller et al., 1955, 1956). The most abundant naturally occurring cytokinin in plants, zeatin, was isolated for the first time from maize (Letham, 1963).

The discovery of auxin as a plant growth regulator was triggered in the late 19th century by experiments of Charles Darwin and his son Francis on the phototropic bending of oats coleoptiles (Darwin and Darwin, 1880). Following the initial isolation of the causative agent responsible for this response by Fritz Went in the 1920s, and its identification as indole-3-acetic acid (IAA) a few years later (Kögl et al., 1934), several other auxinic compounds have been identified, such as the naturally occurring indole-3-butyric acid (IBA) and the synthetic auxin analogue naphthalene acetic acid (NAA). Until now, only four naturally occurring compounds with auxin activity have been described in plants: IAA, IBA, 4-chloroindole-3-acetic acid (4-CL-IAA) and phenylacetic acid (PAA). All four are low molecular weight organic acids containing an aromatic ring (an indole

or phenyl group) with a carboxyl group attached. Over the years, compounds, such as 2,4-D, 2,4,5-trichlorophenoxyacetic acid (2,4,5-T), naphthalene-1-acetic acid (1-NAA), 4-amino-3,5,6-trichloropicolinic acid (picloram), and 2-methoxy-3,6-dichlorobenzoic acid (dicamba) were discovered to exhibit auxin-like activity (De Rybel et al., 2009; Sauer et al., 2013). Based on their toxicity at high concentrations especially for dicot plants, 2,4-D and 2,4,5-T have emerged as successful selective herbicides during the second world war (Hamner and Tukey, 1944). Because of their plant growth regulating properties and stability in tissue culture synthetic auxins have provided a useful tool to study the effects of auxin response, -homeostasis and –transport in a diverse range of plant developmental processes. Each type of auxin can result in a different developmental response depending on its concentration and the tissue it is applied to (Simon et al., 2013), resulting in growth, organogenesis, callus formation or even in SE. By controlling the ratio of auxin and cytokinin in the culture medium, either shoots, callus, or roots can be produced from the original tissue explants (Murashige and Skoog, 1962). Besides inducing organogenesis, high concentrations of the synthetic auxin 2,4-D, in several cases combined with cytokinin, can also induce SE. Hormone-induced SE was documented first in carrot cell suspension cultures (Steward et al., 1958). Since then, the production of somatic embryos has been described for various plant species, and a few model systems for SE have emerged as well as successful combinations of hormones that induce SE. In conifers 2,4-D is combined with BA (von Arnold et al., 2002; Filonova et al., 2000) and in *Medicago truncatula* SE is induced with NAA and BA (Wang et al., 2011). In the monocot model system rice, SE is induced with 2,4-D and kinetin (Verma et al., 2011; Bevitori et al., 2013) and in *Arabidopsis thaliana* 2,4-D alone is sufficient to induce SE (Luo and Koop, 1997; Gaj, 2001; Rose and Nolan, 2006; Nowak et al., 2012). To study SE in dicots, the *Arabidopsis* SE system is useful, due to its large number of available explants, high efficiency and the availability of ecotypes, reporter lines, and knock-out and overexpression mutants.

Arabidopsis somatic embryogenesis

In *Arabidopsis* SE can be induced by 2,4-D on immature zygotic embryos (IZEs), protoplasts, meristems, shoot apical tip and floral bud explants (Luo and Koop, 1997; Mordhorst et al., 1998; Gaj, 2001; Ikeda-Iwai et al., 2003). In addition, SE can be induced on IZEs or germinating seedlings in the absence of 2,4-D by the ectopic expression of specific transcription factors, such as the embryo maturation gene *LEAFY COTYLEDON 1* (*LEC1*) (Lotan et al., 1998), the shoot meristem organizer *WUSCHEL* (*WUS*) (Zuo et al., 2002), or the early embryo fate gene *BABYBOOM* (*BBM*) (Boutilier et al., 2002).

Here I review the recent advances in how 2,4-D possibly controls the SE process at the genetic, molecular and cellular levels and compare it to transcription factor induced SE to identify common targets for this complex regeneration process.
SE induction can be established via a 1-step or 2-step protocol on *Arabidopsis* IZEs. In the 1-step protocol, generally, the IZE is 14 days cultured on 2,4-D-containing medium, followed by transfer to hormone free medium for 7 days (Gaj, 2011). In this 1-step protocol, somatic embryos are considered to either develop directly from the explant and have a unicellular origin (direct SE, DSE), or to develop from a callus and thus have a multicellular origin (indirect SE, ISE) (Kurczyńska et al., 2007). Alternatively, the 2-step protocol SE is initiated by a culture period of 24 days on different types of 2,4-D-containing media, followed by a culture period on hormone free medium (Su et al., 2009; Nowak et al., 2012). In this second protocol, embryogenic calli are first established, and will only produce somatic embryos through ISE. This process is also referred to as secondary, recurrent or repetitive SE (Mordhorst et al., 1998). The protocol developed for obtaining *Picea abies* somatic embryos is exemplary: proembryogenic masses (PEMs) are first established using a mix of 2,4-D and BA, after which maturation of somatic embryos is induced by replacing 2,4-D and BA with the maturation-inducing hormone abscisic acid (ABA) (Timmis, 1998). The *Picea* PEM cultures can be cryopreserved after a period of culture on lower 2,4-D and BA concentrations, which has not been shown yet to work in *Arabidopsis*. In all described protocols for SE induction, 2,4-D is the main inducer of SE leading to cell proliferation, dedifferentiation and eventually to the initiation of somatic embryos.
In the *Arabidopsis* 1-step protocol, an initial swelling can be observed at the macroscopic level after 3 days on the abaxial and adaxial side of the cotyledons of IZEs, at which time the IZEs have unfolded from a bent cotyledon (Figure 2a) towards a "Y" shape, probably as a response to the 2,4-D treatment (Figure 2a) (Raghavan, 2004; Bassuner et al., 2006). The first extensive histological analysis of somatic embryos in *Arabidopsis* showed that the first mitotic divisions are visible as early as 2 days in culture, starting in the procambial cells at the adaxial side of the cotyledon base (Raghavan, 2004). Within 3-4 days of culture, cell divisions in the procambial cells can also be observed on the abaxial side and in epidermis and mesophyll cells on both abaxial and adaxial sides of the cotyledon (Figure 2b). Initial divisions and a higher number of cell layers are observed in the adaxial side, but the same processes can be observed on the abaxial side. Cell divisions spread through both cotyledons resulting in callus in the original mesophyll (Raghavan, 2004). The earlier study by Raghavan does not distinguish between DSE and ISE, but does describe globular embryonic structures on the epidermal cells on the adaxial side. In a later analysis, DSE and ISE were distinguished based on the origin of the cell forming the somatic embryo (Kurczynska et al. 2007) (Figure 2b,c). The ISE events from multicellular origin

are derived from both protodermal (epidermis) and subprotodermal (subepidermis) cell layers; however, a detailed analysis of the development of a somatic embryo derived through ISE is still lacking. In contrast to the earlier description of cell divisions by Raghavan (2004), Kurczyńska and coworkers (2007) state that callus mostly develops on the abaxial side, suggesting ISE preferentially occurs on this side (Figure 2b). Kurczynska and colleagues (2007) describe DSE events that can be recognized by single protodermal cells becoming enlarged and subsequently dividing periclinally and anticlinally. Additionally, multicellular embryonic structures can be observed as well. These originate from both protodermis and subprotodermis layers with similar periclinal and anticlinal divisions on the adaxial side (Figure 2c). The multicellular structures can also be recognised by thicker cell walls outlining the presumed early somatic embryos (Kurczyńska et al., 2007).

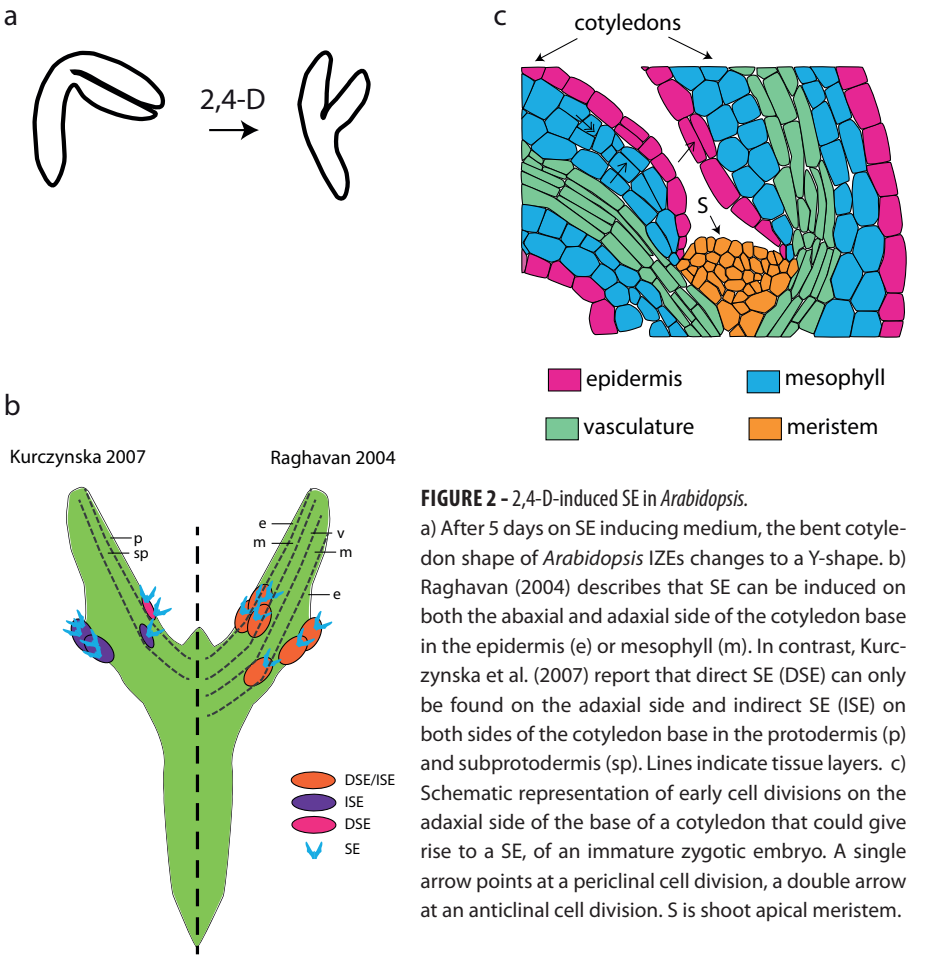

FIGURE 2 - 2,4-D-induced SE in *Arabidopsis*.
a) After 5 days on SE inducing medium, the bent cotyledon shape of *Arabidopsis* IZEs changes to a Y-shape. b) Raghavan (2004) describes that SE can be induced on both the abaxial and adaxial side of the cotyledon base in the epidermis (e) or mesophyll (m). In contrast, Kurczynska et al. (2007) report that direct SE (DSE) can only be found on the adaxial side and indirect SE (ISE) on both sides of the cotyledon base in the protodermis (p) and subprotodermis (sp). Lines indicate tissue layers. c) Schematic representation of early cell divisions on the adaxial side of the base of a cotyledon that could give rise to a SE, of an immature zygotic embryo. A single arrow points at a periclinal cell division, a double arrow at an anticlinal cell division. S is shoot apical meristem.

When somatic embryos are left to develop for 14 to 21 days on 2,4-D-containing medium followed by a hormone free period, they resemble zygotic embryos without a vascular connection to the original IZE or callus (Raghavan, 2004; Bassuner et al., 2006; Kurczyńska et al., 2007). In the 1-step protocol 73-90% of the explants used can successfully induce SE, producing on average 2 to 10 somatic embryos with normal (also described as "true"), trumpet-shaped or fused cotyledons (Gaj, 2001). It has been reported that "true" somatic embryos are attached to the IZE via a file of cells similar to a suspensor (Luo and Koop, 1997), although no evidence of suspensor identity has been provided yet. The development of somatic embryos with fused cotyledons or multiple somatic embryos fused together at the shoot to root tip complicates research on SE when determining how efficient a particular genotype is in SE. Scoring methods are mostly based on the number of somatic embryos produced per IZE (SE productivity) (Luo and Koop, 1997) and recognizing a "true" somatic embryo is proven to be difficult.

A recurrent problem in histological analysis of regenerating plant tissues is the early identification of which cells will develop into embryos, roots, shoots or callus. For example, there is insufficient evidence that the previously described thickened cell wall is only surrounding those cells that will develop into a true somatic embryo. Despite detailed histological analysis, it is therefore still difficult to draw comprehensive conclusions on the origin and preferred occurrence of somatic embryos, in part because of differences in the definitions and terms used in the above studies. Based on the two studies one can deduce that somatic embryos originate from both epidermal and mesophyll tissues, and that the somatic embryos derived from the epidermal layers are most likely a consequence of DSE. The use of cell fate specific markers and an accurate quantification of DSE and ISE events would clarify on how often and where in the IZE, DSE and ISE mostly occur.

By comparing SE with systems that use organogenesis for propagation extract a few similarities can be extracted. Similar to SE, organogenesis is established from somatic cells directly or indirectly via a callus phase. Direct organogenesis involves regeneration without a callus phase and includes the reprogramming of cells e.g. adventitious root formation (Verstraeten et al., 2014). Indirect organogenesis includes the regeneration of roots and shoots via a callus phase and can be divided into two phases. Firstly, somatic cells need to respond to exogenously applied hormones and subsequently redifferentiate to a totipotent cell state. Secondly, these cells (callus) are reprogrammed and assigned with a specific cell fate and thirdly, the completion of organ regeneration (Su and Zhang, 2014; Kareem et al., 2015). The cell divisions as described by Raghavan (2004) during SE are similar to those observed during callus- and lateral root

initiation. Assuming that ISE events result from the cell divisions in layers around the vasculature, it can be considered similar to the divisions of pericycle cells, a layer of cells surrounding the root vasculature giving rise to the lateral root (described and reviewed by De Smet 2012). Both lateral roots and somatic embryos will have to push through a layer of respectively cortex- or mesophyll cells and the epidermis. Molecular and genetic regulation enabling this development might overlap, as was shown for callus development from roots and the lateral root program (Sugimoto et al. (2010). The root identity of root-derived callus might be the key difference with embryogenic callus, of which it is assumed to be an undifferentiated mass of totipotent cells (Sugimoto et al., 2010; Sena and Birnbaum, 2010).

2,4-D, a common SE inducer

As indicated above, the most common method to induce SE is exposure of explants to synthetic derivatives of the plant growth regulator auxin, such as NAA, 2,4-D, 3,6-dichloro-2-methoxybenzoic acid (dicamba), or 4-amino-3,5,6-trichloro-2-pyridinecarboxylic acid (picloram) (Jiménez 2005). The importance of the synthetic auxin 2,4-D for the induction of SE was recognized more than 50 years ago (Steward et al., 1958; Halperin and Wetherell, 1965), and the vast majority of SE protocols, including those for *Arabidopsis*, use 2,4-D as the inducing agent (Gaj, 2001). To be able to understand its action the different components in the auxin homeostasis, transport and response pathways are introduced.

Auxin homeostasis

Typical for a hormone, the action of auxin is on the one hand determined by its concentration in the cell, which is a product of transport, biosynthesis and metabolism. On the other hand, auxin can only act if cells are sensitive to the hormone. The auxin response pathway, involving hormone receptors and downstream transcriptional regulators, determines this sensitivity. Mutant screens in *Arabidopsis thaliana* have revealed most of what it is known from the auxin pathway.

IAA is produced in meristems, young primordia, vascular tissues and reproductive organs and research in *Arabidopsis* and *Zea mays* has uncovered several IAA biosynthesis routes, which fall into two categories: i) the tryptophan (Trp)-dependent and ii) the Trp-independent routes (Woodward and Bartel, 2005). In here, I focus on the Trp-dependent route. Four Trp-dependent pathways have been uncovered and are named after the intermediate compound produced

using L-tryptophan (Trp) as a substrate: 1) the indole-3-acetaldoxime (IAOx) pathway, 2) the indoleacetamide (IAM) pathway, 3) the tryptamine pathway (TAM) and 4) the indole-3-pyruvic acid (IPyA) pathway (Figure 3) (Woodward and Bartel, 2005; Korasick et al., 2013; Ljung, 2013).

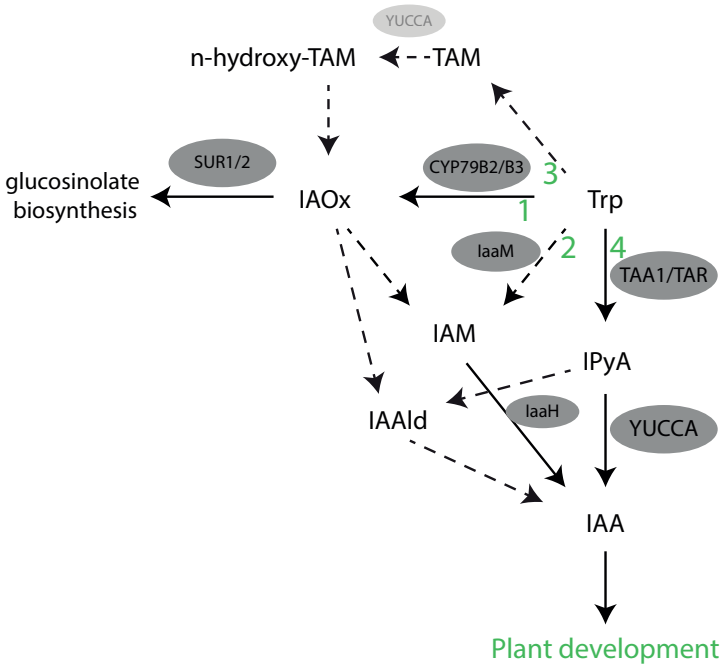

FIGURE 3 - A schematic overview of the tryptophan (Trp)-dependent auxin biosynthesis pathways.
Four Trp-dependent pathways have been suggested in the production of indole-acetic acid (IAA). (1) indole-3-acetaldoxime (IAOx) is produced from Trp by Cytochrome P450 monooxygenases CYP79B2 and CYP79B3 and can be used to produce glucosinolates by SUPERROOT1 and 2 (SUR1/2). IAOx may also be converted to indole-3-acetaldehyde (IAAld) and indoleacetamide (IAM), from which IAA is produced. (2) IAM may be produced directly from Trp by Trp monoxygenase (IaaM), which is than converted to IAA by IAM hydrolase (IaaH). (3) The conversion to tryptamine (TAM) and to n-hydroxy TAM, is possibly catalyzed by YUCCAs and results in IAOx. (4) Trp is converted to indole-3-pyruvic acid (IPyA) by TRYPTOPHAN AMINOTRANSFERASE OF ARABIDOPSIS1 / TRYPTOPHAN AMINOTRANSERASE RELATED 1 TO 4 (TAA1/TAR1-4) and subsequently to IAA by YUCCAs. Solid arrows are identified pathways, dashed arrows have not been confirmed yet and may have one or multiple steps. The scheme is based on Woodward and Bartel (2005), De Paepe et al. (2005), Korasick et al. (2013), Nishimura et al. (2014), He et al. (2001), Ljung (2013).

Typical phenotypes that results from mutants overproducing endogenous auxin are seedlings with epinastic cotyledons, elongated petioles, a shorter root, a more branched root system, or more and longer root hairs (Zhao et al., 2001). These typical auxin overproduction phenotypes were observed in mutants that ectopically express *CYP79B* as well as in knock out mutants of *SUPERROOT1 (SUR1)*

and SUR2 (Boerjan et al., 1995; Delarue et al., 1998). IAOx is produced from Trp by the Cytochrome P450 monooxygenases CYP79B2 and CYP79B3. Accumulation of IAOx by *CYP79B2* overexpression or by blocking glucosinolate biosynthesis via *SUR1* and *SUR2* disruption results in auxin overproduction, which explains the observed phenotypes (Zhao et al., 2002; Sugawara et al., 2009*;* Boerjan et al., 1995; Delarue et al., 1998) (Figure 3.1).

In the *cyp79b2 cyp79b3* double mutant, IAM levels are decreased, suggesting that IAM is likely made from IAOx (Sugawara et al., 2009). However, based on the auxin production pathway identified in the bacteria *Agrobacterium tumefaciens* and *Pseudomonas syringae* it has been hypothesized that IAM may also be produced directly from Trp by Trp monoxygenase (IaaM) (Figure 3.2). A second bacterial enzyme IAM hydrolase (IaaH) is known to convert IAM to IAA (Woodward and Bartel, 2005); however, whether this pathway exists in plants still needs further confirmation. The second possible mechanism to convert Trp to IAA is by conversion to tryptamine (TAM) (Figure 3.3). In mammalian systems, FLAVIN MONOOXGENASEs (FMOs) convert TAM to N-hydroxy-TAM (Zhao et al., 2001). A family of 11 FMO-like enzymes identified in *Arabidopsis* were proposed to fulfil a similar role and are now known as the YUCCA (YUC) family of proteins (Zhao et al., 2001; Cheng, 2006). N-hydroxy-TAM would be then converted to IAOx, followed by indole-3-acetaldehyde (IAAld) and finally to IAA (Woodward et al., 2005; Stepanova et al., 2011). However, evidence came forward that IAOx is not likely produced by YUCs (Sugawara et al., 2009) and later evidence has placed YUCs downstream of TRYPTOPHAN AMINOTRANSFERASE OF ARABIDOPSIS1 / TRYPTOPHAN AMINOTRANSERASE RELATED 1 TO 4 (TAA1/TAR1-4) family enzymes in the IPyA pathway (Stepanova et al., 2011; Won et al., 2011) (Figure 3.4). TAA1/TAR converts Trp into indole-3-pyruvic acid (IPyA), and YUCs subsequently produce IAA from IPyA by oxidative carboxylation. Together these enzymes constitute the most well researched auxin biosynthesis pathway in plants, the IPyA pathway (Won et al., 2011; Ljung, 2013; Korasick et al., 2014).

The *TAA1* gene was first discovered by study of the *wei8* loss-of-function mutant, which showed a defective ethylene response in roots. Defects in *TAA1/SHADE AVOIDANCE3/WEAK ETHYLENE INSENSITIVE8/TRANSPORT INHIBITOR RESPONSE2* (*TAA1/SAV3/WEI8/TIR2*) results in decreased free IAA (Stepanova et al., 2008; Tao et al., 2008). Since the defect could be reversed by exogenous IAA application, the TAA1 enzyme was thought to act as an aminotransferase that converts Trp into IPyA (Stepanova et al., 2008). Mutations in combinations of *TAA1* with its closest homologs *TAR1* and/or *TAR2* results in altered meristem functioning, and in defects in flowering and embryo development (Stepanova et al., 2008).

The *wei8 tar1 tar2* triple mutants fail to develop the basal part of the embryo (Stepanova et al., 2008) similar to quadruple *yuc1 yuc4 yuc10 yuc11* mutants (Cheng, 2006; Cheng et al., 2007). Based on these results the TAA1/TAR – YUCCA pathway is now considered as the most important pathway in higher plants for auxin production (Figure 5.2).

Besides free IAA, which is the active hormone, auxin can be present in the cell in several inactive storage forms. IAA can be conjugated to sugars (e.g. IAA-Glucose), amino acids (IAA-Ala, IAA-Leu, IAA-Asp, IAA-Glu, IAA-Trp), or it can be converted to other natural auxins, such as IBA (Figure 4.2) or to the inactive methyl ester form (MeIAA). IAA is converted to IBA by IBA synthase in microsomal membranes (Ludwig-Muller et al., 1995) and its conversion back to IAA is located in the peroxisome (Zolman et al., 2000; Strader et al., 2010). Most of described storage forms can be converted back to active IAA, but some forms (IAA-Asp, IAA-Glu and oxIAA) are permanently storing auxin in an inactive form (for a detailed review read Korasick et al., 2013). The role of IBA as either a storage or active form is still unclear, although it has been suggested to be a stable transport form of IAA. Long distance IBA transport was shown both in basipetal and acropetal directions similar to IAA, but how exactly remains uncharted (Simon and Petrášek, 2011; Strader and Bartel, 2011). IBA research deserves more attention as IBA constitutes 25-30% of the total auxin pool in Arabidopsis seedlings (Ludwig-Muller et al., 1993), and the compound is commonly used as a root inducing growth hormone in tissue culture.

Auxin transport

For IAA it is well-established that it is directionally transported in the plant from sites of biosynthesis to sites of action, and that this cell-to-cell transport is facilitated by in- and efflux carriers. In the 1970s, the chemiosmotic hypothesis for polar auxin transport (PAT) was proposed (Rubery and Sheldrake, 1974; Raven, 1975), which states that in the weakly acidic apoplast, 15% of the IAA molecules are protonated (IAAH) and these molecules can enter the plant cell by diffusion. The majority of the IAA molecules, however, are in the deprotonated form (IAA^-) and require active uptake by influx carriers (Figure 4.1). Once inside the more basic cytosol, the protonated auxin molecules become deprotonated, and these deprotonated auxin molecules cannot pass the membrane by diffusion, preventing auxin efflux. However, auxin efflux carriers with an asymmetric plasma membrane distribution can facilitate auxin export at one side of the cell where the partially protonated auxin can be taken up by the neighbouring cell (Swarup and Péret, 2012; Petrásek and Friml, 2009).

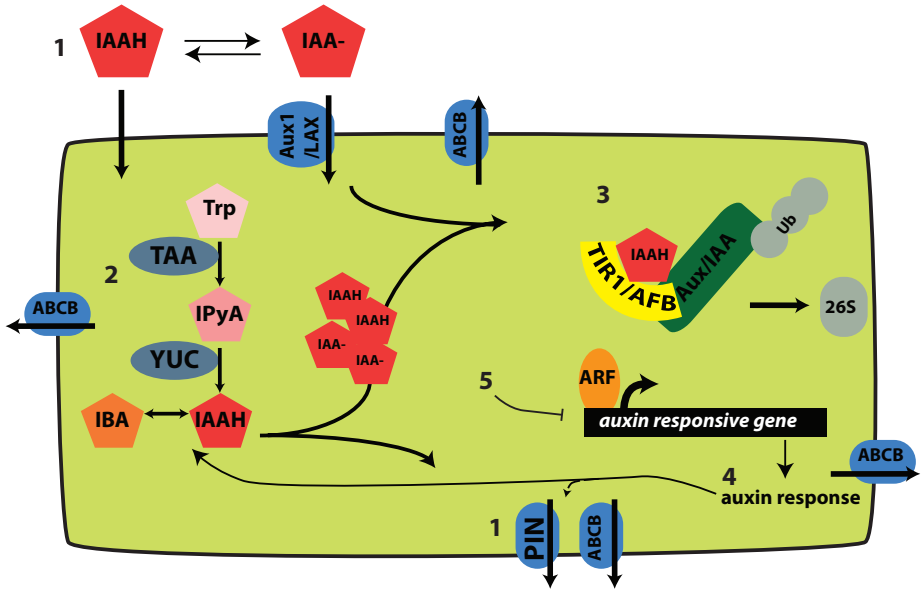

FIGURE 4 - Schematic overview of auxin homeostasis, transport and signaling in *Arabidopsis*.
Auxin homeostasis is established by 1) passive uptake of protonated IAA (IAAH) via the plasma membrane or active uptake of deprotonated IAA (IAA-) by AUX1/LIKE-AUX1 (AUX1/LAX) import carriers and efflux by PIN and ABCB export carriers. 2) Auxin is synthesized from tryptophane (Trp) to indole-3-pyruvic acid (IPyA) by the TRYPTOPHAN AMINOTRANSFERASE OF ARABIDOPSIS1/TRYPTOPHAN AMINOTRANSFERASE RELATED (TAA1/TAR) family enzymes. The final product, IAA, can be converted to the transport form indole-butyric acid (IBA) or to conjugated storage forms. Auxin signaling is established by 3) IAA-dependent recruitment of AUXIN/INDOLE-3-ACETIC ACID (Aux/IAA) repressor proteins by the TRANSPORT INHIBITOR RESPONSE1/AUXIN RECEPTOR F-BOX PROTEINS (TIR1/AFB) E3 ubiquitin ligase complex, resulting in their ubiquitination and subsequent degradation by the 26S proteasome. This releases the repression of AUXIN RESPONSE FACTOR (ARF) mediated initiation of 4) auxin responsive gene expression, which in turn may enhance auxin biosynthesis or transport, and eventually result in 5) negative feed back by the enhanced production of the Aux/IAA repressor proteins.

Research in *Arabidopsis* has identified candidate proteins for these auxin influx and efflux carriers. Auxin influx is thought to be mediated by the AUX1/LAX family of transporters, comprising the four highly conserved AUX1 and LIKE-AUX1 (LAX) proteins LAX1, LAX2 and LAX3 (Swarup and Péret, 2012). Based on auxin transport measurements in *Arabidopsis* inflorescence stems, AUX/LAX proteins are key drivers of polar auxin transport, as they load auxin into the transporting cells (Boot et al., 2016). They are known for their involvement in several developmental processes, such as gravitropism, lateral root development, vascular patterning, phyllotaxis, and embryogenesis (Swarup and Péret, 2012; Robert et al., 2015). Auxin efflux carriers have been identified through the *Arabidopsis pin formed* mutant that develops pin-like inflorescences, a phenotype that pheno-

copies treatment of *Arabidopsis* plants with inhibitors of PAT. The *Arabidopsis* genome encodes a small family of eight PIN proteins that both have overlapping and different roles in plant development (Friml et al., 2002; Benková et al., 2003; Friml et al., 2003; Blilou et al., 2005). PIN proteins consist of two regions of transmembrane domains interrupted by a hydrophilic loop (PINHL), that has recently been mapped to localize in the cytosol (Nodzyński et al., 2016). PINs with a long cytosolic loop (long PINs) are localized on the PM (PIN1, 2, 3, 4 and 7), whereas PINs with a short cytosolic loop (short PINs) are localised in the endoplasmic reticulum (ER) (PIN5 and PIN8). PIN6 contains a hydrophilic loop of intermediate length and is localised both in the ER and at the PM (Mravec et al., 2009; Sawchuk et al., 2013; Ganguly et al., 2014). Asymmetric localisation of PINs results in local dynamic auxin maxima and minima or gradients that are instructive in many developmental processes, including embryo patterning (Friml et al., 2003; Robert et al., 2015), tropic growth (Luschnig et al., 1998; Friml et al., 2002) and organ formation (Reinhardt et al., 2000; Benková et al., 2003). All the long PINs have been shown to be involved in patterning the zygotic embryo by generating dynamic auxin maxima that first mark the early embryo proper, then establish the root pole, and finally position the cotyledon primordia (Friml et al., 2003; Blilou et al., 2005).

In addition to the PIN proteins, three ABC transporters have been identified, respectively ABCB1, ABCB4 and ABCB19, that function in PAT as well, (Noh et al., 2001; Santelia et al., 2005; Cho et al., 2007). They are distributed more symmetrically than PIN proteins in the plasma membrane (Figure 4.1). They may facilitate non-polar IAA efflux to contribute to long-distance IAA transport, and thereby controlling the auxin availability to PAT (Mravec et al., 2008; Geisler and Murphy, 2006; Titapiwatanakun et al., 2009). Neither of these efflux proteins has been reported to transport other forms of auxin, besides IAA.

Several lines of evidence reveal the significance of auxin biosynthesis and transport for plant development. *Arabidopsis* seedlings with defects in combinations of YUC1, YUC2, YUC4, YUC6 and PIN1 show developmental abnormalities in embryo, leaf and flower development (Cheng et al., 2007). These are seen as the key steps in regulating organogenesis (Cheng, 2006; Stepanova et al., 2008; Robert et al., 2013; Nishimura et al., 2014). Furthermore, Robert and colleagues (2013) have shown that polar transport of localized auxin production by the IPyA pathway is necessary to establish the embryonic apical-basal axis in a spatio-temporal manner. These results illustrate the need for a well-established auxin gradient to control cell patterning and differentiation. Through the combined action of these transporters and local auxin production, dynamic auxin maxima and minima can be formed that are involved in patterning and organ formation

through cell division and differentiation (Bohn-Courseau, 2010; Marhavý et al., 2013; Xuan et al., 2015)

Auxin Response

Auxin is perceived in the nucleus to activate auxin responsive gene expression by the AUXIN RESPONSE FACTORS (ARFs) (Figure 4.3). The *Arabidopsis* genome encodes 23 ARFs (Guilfoyle and Hagen, 2007) of which five have been classified as transcriptional activators and the remaining as repressors based on the amino acid sequence in the middle region of the ARF protein (Tiwari et al., 2003). The transcriptionally activating ARFs possess a glutamine-enriched middle region that acts as activation domain (AD), whereas repressing ARFs have P-,S-, and T-rich middle region. On the N-terminal side of the middle region, a B3 DNA-binding domain (DBD) is flanked by two dimerization domains (DD) (Guilfoyle, 2015; Wright and Nemhauser, 2015; Adams-Cioaba et al., 2012). The DDs facilitate binding of ARFs as dimers to the auxin response elements (AuxREs) in the promoters of auxin responsive genes. The identification of AuxREs in many promoter regions has allowed deducing the TGTCTC and TGTCGG consensus sequences and their use to generate the artificial *DR5* and *DR5v2* promoters, respectively. These promoters have been abundantly used to monitor auxin responses in plants during cellular responses, cell- and tissue development (Ulmasov et al., 1997; Boer et al., 2014; Liao et al., 2015).

When the auxin concentration in the cell is low, transcription of auxin responsive genes is repressed by the pairing of the activating ARFs with one of the 29 family members of AUXIN/INDOLE-3-ACETIC ACID (Aux/IAA) repressor proteins in *Arabidopsis*. Aux/IAA proteins have initially been identified as the products of primary auxin response genes (Overvoorde et al., 2005). Most Aux/IAAs consist of three conserved domains: a conserved C-terminal domain that interacts with ARFs, an N-terminal domain I (DI) that recruits co-repressor proteins like TOPLESS (TPL) and is required for transcriptional repression, and the middle domain II (DII) that determines Aux/IAA protein instability through its auxin-enhanced interaction with the TRANSPORT INHIBITOR RESPONSE1/AUXIN RECEPTOR F-BOX PROTEINS (TIR1/AFB) auxin co-receptors (Wang and Estelle, 2014).

The *Arabidopsis* genome encodes 6 TIR1/AFBs proteins, which are F-box proteins that are part of $SCF^{TIR1/AFB}$ E3 ubiquitin protein ligase complexes. Auxin binding to their hydrophobic pocket stabilizes the TIR1/AFB – Aux/IAA co-receptor complex and allows the SCF^{TIR} E3 ubiquitin ligase to ubiquitinate the Aux/IAA proteins, which again targets these repressor proteins for degradation by the 26S proteasome (Maraschin et al., 2009; Dharmasiri et al., 2005a, 2005b; Parry et al., 2009). Degradation of Aux/IAA proteins releases the transcriptional repression and

allows the ARFs to activate or inactivate transcription of auxin responsive genes (Figure 4.3). The fact that the *Arabidopsis* genome encodes in total 6 TIR1/AFBs, 29 Aux/IAAs and 23 ARFs, hypothetically allows 4002 possible combinations of interactions which may lead to the same number of possible responses. In reality, however, the interactions are dependent firstly on the specific binding affinity of each TIR1/AFB for the same Aux/IAA protein (Calderón Villalobos et al., 2012; Parry et al., 2009). Secondly, each co-receptor pair has its own binding affinity for auxin, which is dependent on the efficiency (whether the molecule will bind) and specificity (the structure of the pocket) of the complex (Lee et al., 2014). Although it has been established that synthetic auxin analogues can bind the TIR1/AFB – Aux/IAA co-receptor pairs with high affinity, some analogues were shown to have higher affinity for certain co-receptor pairs, e.g. the synthetic auxin picloram (4-amino-3,5,6-trichloro-2-pyridinecarboxylic acid) has a higher affinity for the AFB5-Aux/IAA than TIR1-Aux/IAA co-receptors (Lee et al., 2014). Thirdly, an additional layer of complexity is provided by the fact that Aux/IAAs can interact with different and multiple ARFs (Figure 5). Therefore, the final response of plant cells to auxin will thus be determined by the type of auxin, the binding interaction of TIR1/AFB – Aux/IAA co-receptors with an auxin molecule and the interaction between Aux/IAAs and ARFs that will activate auxin responsive gene expression (Piya et al., 2014; Korasick et al., 2014; Bargmann et al., 2013). Auxin responsive gene expression may in turn result in the redistribution of PIN proteins (Baster et al., 2013) (Figure 4.4), or in stimulating auxin biosynthesis and metabolism (Xuan et al., 2015), which, through a negative feedback loop, can decrease the auxin response by inducing production of extra Aux/IAA proteins (Figure 4.5).

Besides the nuclear TIR1/AFB – Aux/IAA co-receptor complexes, several lines of evidence indicate the existence of other receptors that mediate rapid responses to auxin that do not necessarily require gene transcription, such as the rapid increase in cytosolic calcium ions ($[Ca^{2+}_{cyt}]$) (Monshausen et al., 2011), or the immediate inhibition of PIN endocytosis (Paciorek et al., 2005; Robert et al., 2010) upon auxin treatment. One of them is S-phase-kinase- associated protein 2 (SKP2), which is a nuclear localized protein that is proposed to regulate proteolysis of cell-cycle transcription factors as a downstream component of another possible auxin receptor, Auxin Binding Protein 1 (ABP1) (Grones and Friml, 2015). Until now, ABP1 is the only identified PM localized candidate auxin receptor, and emerging evidence suggest a pivotal role of ABP1 both in rapid cellular and in transcriptional responses (Bargmann and Estelle, 2014; Grones and Friml, 2015). Recent data, however, question the central role of ABP1 as membrane-localized receptor in auxin signalling (Gao et al., 2015; Habets and Offringa, 2015). Even

though the exact role of ABP1 in auxin signalling still needs to be clarified, it is likely that there are auxin receptors close to or at the plasma membrane that mediate rapid transcription-independent responses to auxin.

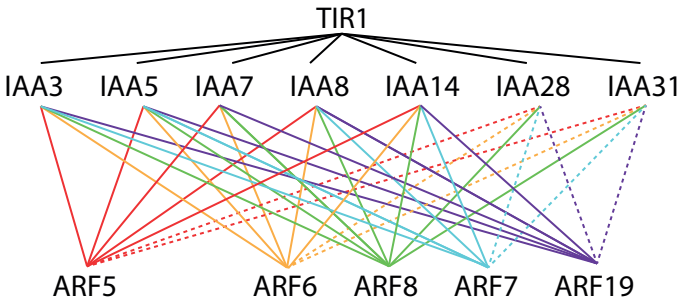

FIGURE 5 - An example of the complexity of auxin signalling.
Protein-protein interactions between TIR1 and Aux/IAAs, and between Aux/IAAs and the activating ARFs. For simplicity, interactions are only displayed for activating ARFs. The interactions are based on Y2H assays of Calderon-Villalobos et al. (2012) and Piya et al. (2014). Solid and broken lines indicate respectively strong and weak interactions.

The role of auxin during somatic embryogenesis

Synthetic auxins are notorious for their use as herbicides, killing dicot weeds, but are also famous for their use in tissue culture to induce the regeneration of shoots, adventitious roots, or somatic embryos. The success of 2,4-D application in somatic embryo culture is thought to lie in its ability to accumulate in plant cells to high levels, caused by its stability in tissue culture, and by the fact that it is not an efficient substrate for the PIN auxin efflux carriers (Delbarre et al., 1996; Petrasek, 2006). Moreover, based on its higher binding affinity to specific TIR1/AFB-Aux/IAA co-receptor pairs, 2,4-D is likely to induce a specific auxin response. There are several factors that should however be taken into account when investigating the auxin response induced by 2,4-D. Firstly, the molecular and genetic response to 2,4-D in cotyledons of the IZE that induce the transition to cells with embryo identity. Secondly, the response is likely to be cell- and tissue-type-dependent, as SE can be induced directly (in the epidermis, adaxial) or indirectly (in the mesophyll, abaxial). Thirdly, once cells with embryo identity have been established, the auxin mechanism will evolve to different responses that further coordinate the development of the somatic embryo.
Below I will discuss the effects of 2,4-D with respect to auxin transport, homeostasis and response during SE.

Auxin transport and homeostasis during SE

SE is induced by the synthetic auxin analogue 2,4-D. For the process to be induced at the molecular genetic level, 2,4-D uptake in cells is required followed by changes in auxin transport and homeostasis. Similar to the natural IAA, 2,4-D is thought to be imported into the cell by AUX1 (Marchant et al., 1999; Yang et al., 2006). However, while IAA is efficiently transported out of the cell by PIN and ABCB proteins (Friml, 2003; Tanaka et al., 2006), 2,4-D is a poor substrate for these auxin efflux carriers (Delbarre et al., 1996; Petrasek, 2006). However, experiments in *Schizosaccharomyces pombe* suggest that 2,4-D can be exported by specific PIN proteins, for example PIN2 and PIN7, but not by PIN1 (Yang and Murphy, 2009). Alternatively, evidence came forward that a member of the ABCG family of transporters ABCG37/PDR9 can function as a 2,4-D efflux transporter (Ito and Gray, 2006). Together, these characteristics allow 2,4-D to accumulate to higher amounts within plant cells compared to IAA, which may explain its toxic effects as herbicide and its efficient SE-inducing effects (Song, 2014). A few studies have shown that genotypes impaired in SE have a lower uptake of 2,4-D and show modified endogenous auxin levels (Ceccarelli et al., 2002; Su et al., 2009; Bai et al., 2013). From this I can conclude that SE induction depends on a strong auxin response. This is similar to the general assumption that an auxin maximum establishes directional growth and polarity of an organ (Bohn-Courseau, 2010), and previous reports have indicated that an auxin maximum is the main driver of SE (Michalczuk et al., 1992; Pasternak, 2002; Gaj et al., 2005; Su et al., 2015). However, somatic embryos have been shown to arise from regions of lower auxin response that co-express PIN1 and PIN4 (Bassuner et al., 2006; Su and Zhang, 2009), suggesting that a change from auxin maximum to minimum is required. Auxin response minima have been shown to contribute to organ formation in combination with oscillating mechanisms and that these are dependent on auxin transport and homeostasis (Wang et al., 2014; Xuan et al., 2015). As PINs do not transport 2,4-D efficiently, it is unlikely that they generate these auxin response minima during SE initiation. More likely, PINs are involved in the further development of the newly initiated somatic embryos, similar to zygotic embryogenesis (Friml et al., 2003; Weijers et al., 2005; Furutani, 2004). However, biosynthesis of auxin via YUCCAs has been shown to be required, as *yucs loss-of-function* mutants, *yuc1 yuc2 yuc4 yuc6* were deficient in SE and their expression was induced in SE cultures (Bai et al., 2013). Based on this observation, YUC-mediated auxin biosynthesis might be required for the dynamic auxin maxima and minima. Alternatively, it may merely provide the auxin for the PAT driven somatic embryo development (Robert et al., 2013). It will be interesting

to see what exactly generates the auxin response minima during SE initiation, and when endogenous auxin biosynthesis becomes required for SE.

The auxin response during SE

As previously described, the auxin response is elevated during SE (Pasternak, 2002; Michalczuk et al., 1992; Simon et al., 2013; Song, 2014). The dichlorophenyl ring and the two chlorines of 2,4-D structurally mimic the two rings of IAA and also fit into the TIR1/AFB-Aux/IAA auxin binding pocket, but the interaction is weaker than with IAA (Tan et al., 2007; Calderón Villalobos et al., 2012). Genetic evidence for 2,4-D mediated TIR1/AFB responses comes from the finding that the *tir1-1* mutant is resistant to 2,4-D-induced auxin responses in the root (Ruegger et al., 1998; Parry et al., 2009). In addition, mutations in *afb1*, *afb2* or *afb3* are sensitive to 2,4-D, suggesting that TIR1 is the main co-receptor for 2,4-D in the root (Parry et al., 2009). The single *tir1-1* mutant does not have a discernible zygotic embryo phenotype (Dharmasiri et al., 2005a), but in 2,4-D induced somatic embryo cultures it was described that mutations in *TIR1* are partially impaired in SE (Gliwicka et al., 2013; Su et al., 2009). Furthermore, recent transcriptome datasets reveal that multiple ARFs (*ARF5/MP, ARF6, ARF10, ARF16, ARF17*) and Aux/IAAs (*IAA16, IAA30, IAA29, IAA31*) are differentially expressed during SE. Phenotypic analysis of the *arf* loss-of-function mutants was not described, but all four corresponding *aux/iaas* loss-of-function mutants showed a reduced SE efficiency (50-70% versus 90% in wild-type), and *iaa30* even showed a reduced SE productivity (3 somatic embryos per IZE versus 4 in wild-type) (Gliwicka et al., 2013; Wickramasuriya and Dunwell, 2015).

The extensive transcriptome analysis by Gliwicka et al. (2013) shows that most of the transcription factor genes that show enhanced expression during SE are auxin-related. The *PUCHI* gene came forward as one of the highest expressed transcription factors in the early stages of SE. *PUCHI* acts together with *LATERAL ORGAN BOUNDARIES DOMAIN 16* and *18* (*LBD16*, *LBD18*), which are downstream targets of *ARF7* and *ARF19* (Kang et al., 2013). *ARF7* and *ARF19* are part of the well-established *SOLITARY ROOT(SLR)/IAA14 – ARF7 – ARF19* module involved in lateral root initiation (Fukaki et al., 2002; De Smet, 2012; Guseman et al., 2015). As mentioned earlier, callus and lateral root development are under the same genetic control and because the exact identity of embryogenic callus is still unknown, it will be interesting to learn from other callus regeneration systems (Sugimoto et al., 2010).

Taken together, multiple independent researchers have shown that 2,4-D induces a TIR1/AFB mediated auxin response and several auxin signalling components have been identified in SE. The question remains, however, which TIR1/

AFB – Aux/IAA – ARF combination is responsible for 2,4-D-induced SE initiation, including the switch from somatic to embryo cell fate identity.

Transcription factor-induced SE and intersection with auxin

In *Arabidopsis*, SE can be induced in the absence of 2,4-D by ectopic expression of specific transcription factors. *LEAFY COTYLEDON 1* (*LEC1*), *LEC2*, *BABY BOOM, RKD1/GRD,* and *WUSCHEL* (*WUS*) induce somatic embryo formation on seedlings in the absence of exogenous hormones (Lotan et al., 1998; Stone et al., 2001; Boutilier et al., 2002; Zuo et al., 2002; Köszegi et al., 2011). In this section we will highlight research on these genes in relation to SE and their link with auxin homeostasis and signaling.

LEC1 encodes a protein with sequence similarity to the B-domain of the HEME-ACTIVATED PROTEIN3 (HAP3) subunit of the CCAAT-box binding factor (CBF) (Lotan et al., 1998). The *HAP3* gene family in *Arabidopsis* comprises 36 members with the most closely related *LEC1-LIKE (L1L)* factor also being involved in seed development (Junker et al., 2012). *LEC2* and *FUS3* encode proteins with a so-called basic region 3 (B3 domain), a DNA binding motif unique to plant transcription factors with a role in developing seeds and is conserved among (*VIVIPAROUS1*) *VP1/ABI3* proteins (Luerssen et al., 1998; Stone et al., 2001). *LEC1*, *LEC2*, *ABI3*, *FUS3* and *L1L* constitute the *LAFL* gene network, key regulators of embryo morphogenesis, seed maturation and are down-regulated during seed germination (West et al., 1994; Stone et al., 2001; Braybrook et al., 2006; Braybrook and Harada, 2008; Jia et al., 2014). Defects associated with disruptive mutations in *LAFL* genes are aberrant cotyledon development, defects in storage macromolecule accumulation, altered desiccation tolerance and premature germination (Keith et al., 1994; Meinke et al., 1994; West et al., 1994; Parcy et al., 1997; Lotan et al., 1998; Stone et al., 2001). Moreover, *loss-of-function* mutants *lec1*, *lec2* and *fus3* have lost the capacity to perform SE. Fewer explants respond as well as less somatic embryos are formed per explant. Instead the explant produces watery callus and root hairs (Gaj et al., 2005). This is in line with the phenotypes of constitutively overexpressed *LEC1* and *LEC2* that leads to spontaneous SE on the shoot apical meristem and cotyledons of germinating seedlings (Lotan et al., 1998; Stone et al., 2001). However, ectopically expressed *FUS3* results in cotyledon-like leaves (Gazzarrini et al., 2004), presumably by holding the post embryonic tissues in a specific phase of the maturation process which benefits the embryogenic capacity. It was described that *LEC1* induced embryonic differentiation is dependent on ABA levels, and subsequent activation of both *LEC1* and *LEC2* leads to en-

dogenous auxin production which results in reprogramming of epidermal cells generating callus and SE (Stone et al., 2008; Junker et al., 2012). Moreover, Su et al. (2012) showed that disruption of ABA levels can alter auxin biosynthesis and transport subsequently affecting SE negatively.

Besides regulating seed maturation genes, the *LEC1* and *LEC2* transcription factors also regulate auxin biosynthesis and –signalling genes (reviewed by Jia et al., 2014) suggesting an additional mechanism for somatic embryo induction by these LAFL proteins. Both DNA binding and transcriptional regulation has only been demonstrated for a number of these target genes. LEC1 binds to the promoter of *YUC10* and activates its expression in seedlings, but only in combination with ABA (Junker et al., 2012). Similarly, LEC2 binds and activates the expression of *YUC4* in seedlings (Stone et al., 2008). LEC2 also rapidly upregulates *YUC2* and *IAA30*, but it is not clear whether these genes are direct or indirect LEC2 targets (Braybrook et al., 2006; Junker et al., 2012). Notably, indirect measurements of auxin levels through colorimetric analysis showed that auxin levels were increased upon *LEC1* and *LEC2* overexpression in seedlings, supporting their role in SE induction through auxin (Wójcikowska et al., 2013; Junker et al., 2012).

Ectopically expressed *LEC2* can outweigh for lower dosages of 2,4-D (0.1-1.0μM) or for auxins that are less efficient in somatic embryo induction, such as IAA or NAA, indicating that cells become more sensitive to auxin or that *LEC2* induces increased production of endogenous IAA (Wójcikowska et al., 2013). Conversely, overexpression of *LEC2* in combination with a 2,4-D concentration normally used to induce SE (5μM) is detrimental for somatic embryo production, with callus being produced instead of somatic embryos (Ledwoń and Gaj, 2009; Wójcikowska et al., 2013). In two different SE induction systems it was independently shown that *YUC1*, *YUC4* and *YUC10*, are differentially expressed during SE (Wójcikowska et al., 2013; Bai et al., 2013). Additionally, the 1-step protocol SE induction system showed that *TAA1* was expressed as well and the 2-step protocol showed *YUC2* and *YUC6* are also upregulated during SE (Wójcikowska et al., 2013; Bai et al., 2013). Both systems indicate that it results in enhanced endogenous auxin production. In the primary system, it was shown that *LEC2* expression clearly enhances auxin sensitivity in IZE cultures, possibly through IAA30, but the direct regulation of auxin biosynthesis or -signaling by *LEC2* remains to be solved (Braybrook et al., 2006; Wójcikowska et al., 2013).

As earlier mentioned, ectopically expressed *BBM* can also induce spontaneous SE formation. *BBM*, also known as *PLETHORA4 (PLT4)*, is one of the *PLT* family members and is expressed in developing embryos and seeds. Other *PLT* family members such as *PLT3*, *5* and *7* have been shown to coordinate shoot regenera-

tion, rhizotaxis and regulate auxin biosynthesis through *YUC1* and *YUC4* in phyllotaxis (Kareem et al., 2015; Hofhuis et al., 2013; Pinon et al., 2013). Moreover, *PLT1* and *PLT2* have not only been shown to be involved in the root development but also in callus regeneration (Galinha et al., 2007; Feng et al., 2012). The role of *PLTs* in embryogenesis was clarified through the aberrant embryonic phenotype of combined mutations in *plt1*, *plt2*, *plt3* and *bbm* (Galinha et al., 2007; Aida et al., 2004) and through dose dependent ectopically expressed PLT2 and BBM proteins that showed increase in SE capacity upon increased dosages (Horstman, 2015). Both PLT2 and BBM activate regulators of LAFL proteins (Horstman, 2015) and it was found that BBM can bind to auxin biosynthesis genes *YUC3* and *YUC8* and indirectly activate*YUC4* by binding to *STYLISH1* (*STY1*). Also auxin transport gene targets were found, i.e. efflux carriers *PIN1*, *PIN4* and *ABCB19* (Heidmann, 2015), but the exact role of BBM in regulating auxin biosynthesis and -transport during SE remains to be solved.

In conclusion, the experimental data discussed in this Chapter shows that in both 2,4-D- and TF-induced SE, auxin transport, -biosynthesis and -signaling play pivotal roles in establishing the dynamic auxin responses that are required for the initiation and development of somatic embryos.

Outline of the thesis

SE is a highly complex regeneration process that consists of multiple steps i.e. the reversion of cell fates from 'late' to adapting the new cell fate of 'early embryonic', followed by establishing the embryonic body of somatic embryos and development thereof. Auxin is involved in many plant development and regeneration processes and multiple lines of evidence, as described in this Chapter, point to an instructive role for auxin during SE.

However, despite the multiple lines of evidence, the exact genetic and molecular mechanism by which 2,4-D induces SE initiation has not been elucidated yet and this was the key objective of the research described in this PhD thesis. A better understanding of the process will enable us to induce SE more efficiently for high-throughput clonal propagation of crops.

To study cell redifferentiation, robust protocols and cellular markers are required. In Chapter 2 we first established a robust protocol for the efficient and reproducible induction of SE from *Arabidopsis* IZEs. The *pWOX2::NLS-YFP* reporter was used to mark cells that have adapted an early embryo cell fate and the *DR5::RFP* auxin response reporter was used to simultaneously monitor auxin responses. With these tools we demonstrated that for IZEs harvested 12 days after pollination

(12 dap) the SE process was most efficient and productive, and that SE initiation occurred after 5 to 7 days during SEIM incubation. As previously described, we confirmed that an auxin maximum is created but that this is followed by a local auxin minimum, in regions where somatic embryos arise. Through combined studies of mutants and inhibitors of polar auxin transport we showed that this is not caused by PIN auxin efflux carriers, but rather by auxin influx carriers AUXIN1/LIKE-AUXIN1-3 (AUX1/LAX1-3). Analysis of AUX1/LAX1-3 showed a high level of redundancy and that they create an auxin minimum possibly by retaining endogenous auxin in cells surrounding SE initiation regions.

In Chapter 3 we further investigated at what time point auxin biosynthesis is required during SE. We demonstrated that the tryptophan (Trp) to indole-3-pyruvic acid (IPyA) conversion mediated by the TAA1/TAR1-4 enzymes is contributing to the dynamic auxin response by increasing auxin levels in the entire IZE and that this is also crucial for cell development during SE initiation. By using the embryo cell fate marker *WOX2* and auxin response marker *DR5* we could show that the local auxin minimum is absent when the TAA1/TAR1-4 activity is inhibited by L-kynurenine, indicating that this enzymatic step is crucial to cell- development and redifferentation to an early embryo cell fate. Furthermore, we showed that the YUCCA family proteins, responsible for the IPyA to indole-acetic acid (IAA) conversion, function redundantly during SE and that they are crucial for survival of the IZE explants in tissue culture, but not for SE initiation.

In Chapter 4, we used the tools presented in Chapter 2 and the auxin antagonist auxinole, that blocks the binding of auxin to the TIR1/AFB-Aux/IAA co-receptors, to show that SE initiation is extremely dependent on the dynamic auxin responses established through TIR1/AFB co-receptors.. By screening reporters for the 23 *ARFs* we found that all activating *ARF* genes (*ARF5, 6, 7, 8* and *19*), are involved in SE initiation. A significant reduction in SE efficiency was observed for the *arf7 arf19* loss-of-function mutant, the *RPS5a>>miRNA167a* line in which *ARF6* and *ARF8* are knocked down, and interestingly also in the dominant negative solitary root mutant *slr-1*. These findings strongly suggest for an overlap between lateral root founder cell specification and embryonic founder cell specification. As lateral root and callus development also share similar molecular pathways, we used this fact to demonstrate that the auxin response mutants that were blocked in SE also showed a reduction in 2,4-D-induced root callus development. This phenotype seems to provide a novel and simple screen to quickly identify new candidate genes involved in SE initiation.

References

Adams-Cioaba, M.A., Li, Z., Tempel, W., Guo, Y., Bian, C., Li, Y., Lam, R., and Min, J. (2012). Crystal structures of the Tudor domains of human PHF20 reveal novel structural variations on the Royal Family of proteins. FEBS Lett. **586**: 859–865.

Aida, M., Beis, D., Heidstra, R., Willemsen, V., Blilou, I., Galinha, C., Nussaume, L., Noh, Y.S., Amasino, R., and Scheres, B. (2004). The *PLETHORA* genes mediate patterning of the *Arabidopsis* root stem cell niche. Cell **119**: 119–120.

Attar, N. (2016). Cellular microbiology: How pathogens divide. Nat. Rev. Microbiol. **14**: 604–605.

Bai, B., Su, Y.H. Yuan, J., and Zhang, X.S. (2013). Induction of somatic embryos in *Arabidopsis* requires local *YUCCA* expression mediated by the down-regulation of ethylene biosynthesis. Mol. Plant **6**: 1247–1260.

Bairu, M.W., Aremu, A.O. and van Staden, J. (2011). Somaclonal variation in plants: causes and detection methods. Plant Growth Regul. **63**: 147–173.

Barcaccia, G. and Albertini, E. (2013). Apomixis in plant reproduction: A novel perspective on an old dilemma. Plant Reprod. **26**: 159–179.

Bargmann, B.O.R. and Estelle, M. (2014). Auxin perception: in the IAA of the beholder. Physiol. Plant. **151**: 52–61.

Bargmann, B.O.R., Vanneste, S., Krouk, G., Nawy, T., Efroni, I., Shani, E., Choe, G., Friml, J., Bergmann, D.C., Estelle, M. and Birnbaum, K.D. (2013). A map of cell type-specific auxin responses. Mol. Syst. Biol. **9**: 688.

Bassuner, B.M., Lam, R., Lukowitz, W., and Yeung, E.C. (2006). Auxin and root initiation in somatic embryos of *Arabidopsis*. Plant Cell Rep. **26**: 1–11.

Baster, P., Robert, S., Kleine-Vehn, J., Vanneste, S., Kania, U., Grunewald, W., De Rybel, B., Beeckman, T., and Friml, J. (2013). SCF(TIR1/AFB)-auxin signalling regulates PIN vacuolar trafficking and auxin fluxes during root gravitropism. EMBO J. **32**: 260–274.

Bedzhov, I., Graham, S.J.L., Leung, C.Y., Zernicka-Goetz, M., and Zernicka-Goetz, M. (2014). Developmental plasticity , cell fate specification and morphogenesis in the early mouse embryo.

Benková, E., Michniewicz, M., Sauer, M., Teichmann, T., Seifertová, D., Jürgens, G., and Friml, J. (2003). Local, efflux-dependent auxin gradients as a common module for plant organ formation. Cell **115**: 591–602.

Bevitori, R., Popielarska-Konieczna, M., dos Santos, E.M., Grossi-de-Sá, M.F., and Petrofeza, S. (2013). Morpho-anatomical characterization of mature embryo-derived callus of rice (Oryza sativa L.) suitable for transformation. Protoplasma: 545–554.

Blilou, I., Xu, J., Wildwater, M., Willemsen, V., Paponov, I., Friml, J., Heidstra, R., Aida, M., Palme, K., and Scheres, B. (2005). The PIN auxin efflux facilitator network controls growth and patterning in *Arabidopsis* roots. Nature **433**: 39–44.

Boer, D.R., Freire-Rios, A., Van Den Berg, W.A.M., Saaki, T., Manfield, I.W., Kepinski, S., Lopez-Vidrieo, I., Franco-Zorrilla, J.M., De Vries, S.C., Solano, R., Weijers, D., and Coll, M. (2014). Structural basis for DNA binding specificity by the auxin-dependent ARF transcription factors. Cell **156**: 577–589.

Boerjan, W., Cervera, M.T., Delarue, M., Beeckman, T., Dewitte, W., Bellini, C., Caboche, M., Van Onckelen, H., Van Montagu, M., and Inzé, D. (1995). Superroot, a recessive mutation in *Arabidopsis*, confers auxin overproduction. Plant Cell **7**: 1405–1419.

Bohn-Courseau, I. (2010). Auxin: a major regulator of organogenesis. C. R. Biol. **333**: 290–296.

Boot, K.J.M., Hille, S.C., Libbenga, K.R., Peletier, L.A., van Spronsen, P.C., van Duijn, B., and Offringa, R. (2016). Modelling the dynamics of polar auxin transport in inflorescence stems of *Arabidopsis thaliana*. J. Exp. Bot. **67**: 649–666.

Boutilier, K., Offringa, R., Sharma, V.K., Kieft, H., Ouellet, T., Zhang, L., Hattori, J., Liu, C., van Lammeren, A.A.M., Miki, B.L.A., Custers, J.B.M., and van Lookeren Campagne, M.M. (2002). Ectopic expression of *BABY BOOM* triggers a conversion from vegetative to embryonic growth. Plant Cell **14**: 1737–1749.

Braybrook, S. and Harada, J.J. (2008). LECs go crazy in embryo development. Trends Plant Sci. **13**: 624–630.

Braybrook, S., Stone, S.L., Park, S., Bui, A.Q., Le, B.H., Fischer, R.L., Goldberg, R.B., and Harada, J.J. (2006). Genes directly regulated by *LEAFY COTYLEDON2* provide insight into the control of embryo maturation and somatic embryogenesis. Proc. Natl. Acad. Sci. USA. **103**: 3468–3473.

Calderón Villalobos, L.I.A., et al. (2012). A combinatorial TIR1/AFB-Aux/IAA co-receptor system for differential sensing of auxin. Nat. Chem. Biol. **8**: 477–485.

Ceccarelli, N., Mondin, A., Lorenzi, R., Picciarelli, P., and Schiavo, F. Lo (2002). The metabolic basis for 2,4-D resistance in two variant cell lines of carrot. Funct. Plant Biol. **29**: 575.

Cheng, Y. (2006). Auxin biosynthesis by the *YUCCA* flavin monooxygenases controls the formation of floral organs and vascular tissues in *Arabidopsis*. Genes Dev. **20**: 1790–1799.

Cheng, Y., Dai, X. and Zhao, Y. (2007). Auxin synthesized by the *YUCCA* flavin monooxygenases is essential for embryogenesis and leaf formation in *Arabidopsis*. Plant Cell Online **19**: 2430–2439.

Cho, M., Lee, S.H. and Cho, H.T. (2007). P-GLYCOPROTEIN4 displays auxin efflux transporter like action in *Arabidopsis* root hair cells and tobacco cells. **19**: 3930–3943.

Darwin, C. and Darwin, F. (1880). The power of movement in plants. J. Murray, London.

Delarue, M., Prinsen, E., Van Onckelen, H., Caboche, M., and Bellini, C. (1998). *sur2* mutations of *Arabidopsis thaliana* define a new locus involved in the control of auxin homeostasis. Plant J. **14**: 603–611.

Delbarre, A., Muller, P., Imhoff, V., and Guern, J. (1996). Comparison of mechanisms controlling uptake and accumulation of 2,4-dichlorophenoxy acetic acid, naphthalene-1-acetic acid, and indole-3-acetic acid in suspension-cultured tobacco cells. Planta **198**: 532–541.

Dharmasiri, N., Dharmasiri, S. and Estelle, M. (2005a). The F-box protein TIR1 is an auxin receptor. Nature **435**: 441–445.

Dharmasiri, N., Dharmasiri, S., Weijers, D., Lechner, E., Yamada, M., Hobbie, L., Ehrismann, J.S., Jürgens, G., and Estelle, M. (2005b). Plant development is regulated by a family of auxin receptor F box proteins. Dev. Cell **9**: 109–119.

Fehér, A. (2015). Somatic embryogenesis — Stress-induced remodeling of plant cell fate. Biochim. Biophys. Acta - Gene Regul. Mech. **1849**: 385–402.

Feng, Z., Zhu, J., Du, X. and Cui, X. (2012). Effects of three auxin-inducible *LBD* members on lateral root formation in *Arabidopsis thaliana*. Planta **236**: 1227–1237.

Filonova, L.H., Bozhkov, P. V, and von Arnold, S. (2000). Developmental pathway of somatic embryogenesis in *Picea abies* as revealed by time-lapse tracking. J. Exp. Bot. **51**: 249–264.

Friml, J. (2003). Auxin transport - Shaping the plant. Curr. Opin. Plant Biol. **6**: 7–12.

Friml, J., Benková, E., Blilou, I., Wisniewska, J., Hamann, T., Ljung, K., Woody, S., Sandberg, G., Scheres, B., and Jürgens, G. (2002). *AtPIN4* mediates sink-driven auxin gradients and root patterning in *Arabidopsis*. Cell **108**: 661–673.

Friml, J., Vieten, A., Sauer, M., Weijers, D., Schwarz, H., Hamann, T., Offringa, R., and Jürgens, G. (2003). Efflux-dependent auxin gradients establish the apical-basal axis of *Arabidopsis*. Nature **426**: 147–153.

Fukaki, H., Tameda, S., Masuda, H., and Tasaka, M. (2002). Lateral root formation is blocked by a gain-of-function mutation in the *SOLITARY-ROOT/IAA14* gene of *Arabidopsis*. Plant J. **29**: 153–168.

Furutani, M. (2004). PIN-FORMED1 and PINOID regulate boundary formation and cotyledon development in *Arabidopsis* embryogenesis. Development **131**: 5021–5030.

Gaj, M.D. (2001). Direct somatic embryogenesis as a rapid and efficient system for in vitro regeneration of *Arabidopsis thaliana*. Plant Cell. Tissue Organ Cult. **64**: 39–46.

Gaj, M.D. (2004). Factors influencing somatic embryogenesis induction and plant regeneration with particular reference to *Arabidopsis thaliana* (L.) Heynh. Plant Growth Regul. **43**: 27–47.

Gaj, M.D. (2011). Somatic embryogenesis and plant regeneration in the culture of *Arabidopsis thaliana* (L.) Heynh. immature zygotic embryos. Methods **710**: 257–265.

Gaj, M.D., Zhang, S., Harada, J.J., and Lemaux, P.G. (2005). Leafy cotyledon genes are essential for induction of somatic embryogenesis of *Arabidopsis*. Planta **222**: 977–988.

Galinha, C., Hofhuis, H., Luijten, M., Willemsen, V., Blilou, I., Heidstra, R., and Scheres, B. (2007). PLETHORA proteins as dose-dependent master regulators of *Arabidopsis* root development. Nature **449**: 1053–1057.

Ganguly, A Park, M., Kesawat, M.S., and Cho, H.-T. (2014). Functional analysis of the hydrophilic loop in intracellular trafficking of *Arabidopsis* PIN-FORMED proteins. Plant Cell **26**: 1570–1585.

Gao, Y., Zhang, Y., Zhang, D., Dai, X., Estelle, M., and Zhao, Y. (2015). AUXIN BINDING PROTEIN1 (ABP1) is not required for either auxin signaling or *Arabidopsis* development. Proc. Natl. Acad. Sci. USA **1**: 201500365.

Gazzarrini, S., Tsuchiya, Y., Lumba, S., Okamoto, M., and McCourt, P. (2004). The transcription factor *FUSCA3* controls developmental timing in *Arabidopsis* through the hormones gibberellin and abscisic acid. Dev. Cell **7**: 373–385.

Geisler, M. and Murphy, A.S. (2006). The ABC of auxin transport: The role of p-glycoproteins in plant development. FEBS Lett. **580**: 1094–1102.

Gliwicka, M., Nowak, K., Balazadeh, S., Mueller-Roeber, B., and Gaj, M.D. (2013). Extensive modulation of the transcription factor transcriptome during somatic embryogenesis in *Arabidopsis thaliana*. PLoS One **8**: e69261.

Grones, P. and Friml, J. (2015). Auxin transporters and binding proteins at a glance. J. Cell Sci. **128**: 1–7.

Guilfoyle, T.J. (2015). The PB1 domain in auxin response factor and Aux/IAA Proteins: a versatile protein interaction module in the auxin response. Plant Cell **27**: 33–43.

Guilfoyle, T.J. and Hagen, G. (2007). Auxin response factors. Curr. Opin. Plant Biol. **10**: 453–460.

Guseman, J.M., Hellmuth, A., Lanctot, A., Feldman, T.P., Moss, B.L., Klavins, E., Calderon Villalobos, L.I.A., and Nemhauser, J.L. (2015). Auxin-induced degradation dynamics set the pace for lateral root development. Development **142**: 905–909.

Habets, M.E.J. and Offringa, R. (2015). Auxin Binding Protein 1: A red herring after all? Mol. Plant **8**: 1131–-1134.

Halperin, W. and Wetherell, D.F. (1965). Ontogeny of adventive embryos of wild carrot. Science **147**: 756–758.

Hamner, C.L. and Tukey, H.B. (1944). The herbicidal action of 2,4-dichlorophenoxyacetic acid and 2,4,5-trichlorophenoxyacetic acid on bindweed. Science **100**: 154–155.

Heidmann, I. (2015). Applied and fundamental aspects of *BABY BOOM*-mediated regeneration. Thesis, Wageningen University.

Hofhuis, H., Laskowski, M., Du, Y., Prasad, K., Grigg, S., Pinon, V., and Scheres, B. (2013). Phyllotaxis and rhizotaxis in *Arabidopsis* are modified by three plethora transcription factors. Curr. Biol. **23**: 956–962.

Horstman, A. (2015). *BABY BOOM*-induced somatic embryogenesis in *Arabidopsis*. Thesis, Wageningen University.

ten Hove, C. A., Lu, K.-J., and Weijers, D. (2015). Building a plant: cell fate specification in the early *Arabidopsis* embryo. Development **142**: 420–430.

Ikeda-Iwai, M., Umehara, M., Satoh, S., and Kamada, H. (2003). Stress-induced somatic embryogenesis in vegetative tissues of *Arabidopsis thaliana*. Plant J. **34**: 107–114.

Ito, H. and Gray, W.M. (2006). A gain-of-function mutation in the *Arabidopsis* pleiotropic drug resistance transporter *PDR9* confers resistance to auxinic herbicides. Plant Physiol. **142**: 63–74.

Jia, H., McCarty, D.R. and Suzuki, M. (2013). Distinct roles of *LAFL* network genes in promoting the embryonic seedling fate in the absence of *VAL* repression. Plant Physiol. **163**: 1293–1305.

Jia, H., Suzuki, M., and Mccarty, D.R. (2014). Regulation of the seed to seedling developmental phase transition by the *LAFL* and *VAL* transcription factor networks. Wiley Interdiscip. Rev. Dev. Biol. **3**: 135–145.

Junker, A. Mönke, G., Rutten, T., Keilwagen, J., Seifert., Thi, T.M.N., Renou, J., Balzergue, S., Viehöver, P., Hähnel, U., Ludwig-Müller, J., Altschmied, L., Conrad, U., Weisshaar, B., and Bäumlein, H. (2012). Elongation-related functions of *LEAFY COTYLEDON1* during the development of *Arabidopsis thaliana*. Plant J. **71**: 427–442.

Kang, N.Y., Lee, H.W., and Kim, J. (2013). The AP2/EREBP gene *PUCHI* co-acts with *LBD16/ASL18* and *LBD18/ASL20* downstream of *ARF7* and *ARF19* to regulate lateral root development in *Arabidopsis*. Plant Cell Physiol. **54**: 1326–1334.

Kareem, A., Durgaprasad, K., Sugimoto, K., Du, Y., Pulianmackal, A.J., Trivedi, Z.B., Abhayadev, P. V., Pinon, V., Meyerowitz, E.M., Scheres, B., and Prasad, K. (2015). *PLETHORA* genes control regeneration by a two-step mechanism. Curr. Biol. **25**: 1017–1030.

Keith, K., Kraml, M., Dengler, N., and McCourt, P. (1994). *fusca3*: A heterochronic mutation affecting late embryo development in *Arabidopsis*. Plant Cell **6**: 589–600.

Kepinski, S. and Leyser, O. (2005). The F-box protein TIR1 is an auxin receptor. Nature **435**: 446–451.

Kieber, J.J. and Schaller, G.E. (2014). Cytokinins. The *Arabidopsis* Book. **12**: e0168.

Kögl, F., Erxleben, H., and Haagen-Smit, A.J. (1934). Über die Isolierung der Auxine a und b aus pflanzlichen materialien. 9. Mitteilung über pflanzliche Wachstumsstoffe. Hoppe. Seylers. Z. Physiol. Chem. **225**: 215–229.

Koltunow, A. (1993). Apomixis: embryo sacs and embryos formed without meiosis or fertilization in ovules. Plant Cell **5**: 1425–1437.

Korasick, D. A., Enders, T. A., and Strader, L.C. (2013). Auxin biosynthesis and storage forms. J. Exp. Bot. **64**: 2541–2555.

Korasick, D. A, Westfall, C.S., Lee, S.G., Nanao, M.H., Dumas, R., Hagen, G., Guilfoyle, T.J., Jez, J.M., and Strader, L.C. (2014). Molecular basis for AUXIN RESPONSE FACTOR protein interaction and the control of auxin response repression. Proc. Natl. Acad. Sci. USA. **111**: 5427–5432.

Köszegi, D., Johnston, A.J., Rutten, T., Czihal, A., Altschmied, L., Kumlehn, J., Wüst, S.E.J., Kirioukhova, O., Gheyselinck, J., Grossniklaus, U., and Bäumlein, H. (2011). Members of the RKD transcription factor family induce an egg cell-like gene expression program. Plant J. **67**: 280–291.

Kurczyńska, E.U., Gaj, M.D., Ujczak, A., and Mazur, E. (2007). Histological analysis of direct somatic embryogenesis in *Arabidopsis thaliana* (L.) Heynh. Planta **226**: 619–28.

Lau, S., Slane, D., Herud, O., Kong, J., and Jürgens, G. (2011). Early embryogenesis in flowering plants: setting up the basic body pattern. Annu. Rev. Plant Biol. **63**: 483–506.

Ledwoń, A. and Gaj, M.D. (2009). *LEAFY COTYLEDON2* gene expression and auxin treatment in relation to embryogenic capacity of *Arabidopsis* somatic cells. Plant Cell Rep. **28**: 1677–1688.

Lee, S., Sundaram, S., Armitage, L., Evans, J.P., Hawkes, T., Kepinski, S., Ferro, N., and Napier, R.M. (2014). Defining binding efficiency and specificity of auxins for SCF TIR1/AFB -Aux/IAA co-receptor complex formation. ACS Chem. Biol. **9**: 673–682.

Letham, D.S. (1963). Zeatin, a factor inducing cell division isolated from Zea mays. Life Sci. **8**: 569–573.

Liao, C., Smet, W., Brunoud, G., Yoshida, S., Vernoux, T., and Weijers, D. (2015). Reporters for sensitive and quantitative measurement of auxin response. Nat. Methods **12**: 1–6.

Ljung, K. (2013). Auxin metabolism and homeostasis during plant development. Development **140**: 943–950.

Lotan, T., Ohto, M., Yee, K.M., West, M. A, Lo, R., Kwong, R.W., Yamagishi, K., Fischer, R.L., Goldberg, R.B., and Harada, J.J. (1998). *Arabidopsis LEAFY COTYLEDON1* is sufficient to induce embryo development in vegetative cells. Cell **93**: 1195–205.

Ludwig-Muller, J., Sass, S., Sutter, E.G., Wodner, M., and Epstein, E. (1993). Indole-3-butyric acid in *Arabidopsis thaliana*. Plant Growth Regul. **13**: 179–187.

Ludwig-Muller, J., Hilgenberg, W., and Epstein, E. (1995). The in vitro biosynthesis of indole-3 butyric acid In *Maize*. Phytochem. . Sep **40**: 61–68.

Luerssen, H., Kirik, V., Herrmann, P., and Miséra, S. (1998). FUSCA3 encodes a protein with a conserved VP1/AB13-like B3 domain which is of functional importance for the regulation of seed maturation in *Arabidopsis thaliana*. Plant J. **15**: 755–764.

Luo, Y. and Koop, H.U. (1997). Somatic embryogenesis in cultured immature zygotic embryos and leaf protoplasts of *Arabidopsis thaliana* ecotypes. Planta **202**: 387–396.

Luschnig, C., Gaxiola, R.A., Grisafi, P., and Fink, G.R. (1998). EIR1, a root specific protein involved in auxin transport, is required for gravitropism in *Arabidopsis thaliana*. Genes Dev. **12**: 2175–2187.

Maraschin, F.D.S., Memelink, J., and Offringa, R. (2009). Auxin-induced, SCF(TIR1)-mediated poly-ubiquitination marks AUX/IAA proteins for degradation. Plant J. **59**: 100–109.

Marchant, A, Kargul, J., May, S.T., Muller, P., Delbarre, a, Perrot-Rechenmann, C., and Bennett, M.J. (1999). AUX1 regulates root gravitropism in *Arabidopsis* by facilitating auxin uptake within root apical tissues. EMBO J. **18**: 2066–2073.

Marhavý, P., Vanstraelen, M., De Rybel, B., Zhaojun, D., Bennett, M.J., Beeckman, T., and Benková, E. (2013). Auxin reflux between the endodermis and pericycle promotes lateral root initiation. EMBO J. **32**: 149–158.

Meinke, D.W., Franzmann, L.H., Nickle, T.C., and Yeung, E.C. (1994). Leafy cotyledon mutants of *Arabidopsis*. Plant Cell **6**: 1049–1064.

Meyerowitz, E.M. (2002). Plants compared to animals: the broadest comparative study of development. Science **295**: 1482–1485.

Michalczuk, L., Ribnicky, D.M., Cooke, T.J., and Cohen, J.D. (1992). Regulation of indole-3-acetic acid biosynthetic pathways in carrot cell cultures. Plant Physiol. **100**: 1346–1353.

Miller, C.O., Skoog, F., F.S., O., M.H., S., and Strong, F.M. (1956). Isolation, structure and synthesis of kinetin, a substance promoting cell division. J. Am. Chem. Soc.: 1345–1350.

Miller, C.O., Skoog, F., H., von S.M., and Strong, F.M. (1955). Kinetin, a cell division factor from deoxyribonucleic acid. J. Am. Chem. Soc.: 1392.

Monshausen, G.B., Miller, N.D., Murphy, A.S., and Gilroy, S. (2011). Dynamics of auxin-dependent Ca 2+ and pH signaling in root growth revealed by integrating high-resolution imaging with automated computer vision-based analysis. Plant J. **65**: 309–318.

Mordhorst, A.P., Voerman, K.J., Hartog, M. V., Meijer, E.A., van Went, J., Koornneef, M., and de Vries, S.C. (1998). Somatic embryogenesis in *Arabidopsis thaliana* is facilitated by mutations in genes repressing meristematic cell divisions. Genetics **149**: 549–563.

Mravec, J. et al. (2009). Subcellular homeostasis of phytohormone auxin is mediated by the ER-localized PIN5 transporter. Nature **459**: 1136–1140.

Mravec, J., Kubes, M., Bielach, A., Gaykova, V., Petrásek, J., Skůpa, P., Chand, S., Benková, E., Zazímalová, E., and Friml, J. (2008). Interaction of PIN and PGP transport mechanisms in auxin distribution-dependent development. Development **135**: 3345–3354.

Murashige, T. and Skoog, F. (1962). A revised medium for rapid growth and bio assays with tobacco tissue cultures. Physiol. Plant. **15**: 473–497.

Nishimura, T., Hayashi, K.-I., Suzuki, H., Gyohda, A., Takaoka, C., Sakaguchi, Y., Matsumoto, S., Kasahara, H., Sakai, T., Kato, J.-I., Kamiya, Y., and Koshiba, T. (2014). Yucasin is a potent inhibitor of YUCCA, a key enzyme in auxin biosynthesis. Plant J. **77**: 352–366.

Nodzyński, T., Vanneste, S., Zwiewka, M., Pernisová, M., Hejátko, J., and Friml, J. (2016). Enquiry into the topology of plasma membrane localized PIN auxin transport components. Mol. Plant: 1504–1519.

Noh, B., Murphy, A.S., and Spalding, E.P. (2001). Multidrug resistance-like genes of *Arabidopsis* required for auxin transport and auxin-mediated development. Plant Cell **13**: 2441–2454.

Nowak, K., Wojcikowska, B., Szyrajew, K., and Gaj, M.D. (2012). Evaluation of different embryogenic systems for production of true somatic embryos in *Arabidopsis*. Biol. Plant. **56**: 401–408.

Overvoorde, P.J., Okushima, Y., Alonso, J.M., Chan, A., Chang, C., Ecker, J.R., Hughes, B., Liu, A., Onodera, C., Quach, H., Smith, A., YU, G., and Theologis, A. (2005). Functional genomic analysis of the *AUXIN/INDOLE-3-ACETIC ACID* gene family members in *Arabidopsis thaliana*. Plant Cell **17**: 3282–3300.

Paciorek, T., Zazímalová, E., Ruthardt, N., Petrásek, J., Stierhof, Y.-D., Kleine-Vehn, J., Morris, D.A., Emans, N., Jürgens, G., Geldner, N., and Friml, J. (2005). Auxin inhibits endocytosis and promotes its own efflux from cells. Nature **435**: 1251–1256.

Parcy, F., Valon, C., Kohara, a, Miséra, S., and Giraudat, J. (1997). The *ABSCISIC ACID-INSENSITIVE3*, *FUSCA3*, and *LEAFY COTYLEDON1* loci act in concert to control multiple aspects of *Arabidopsis* seed development. Plant Cell **9**: 1265–1277.

Parry, G., Calderon-Villalobos, L.I.A., Prigge, M., Peret, B., Dharmasiri, S., Itoh, H., Lechner, E., Gray, W.M., Bennett, M., and Estelle, M. (2009). Complex regulation of the TIR1/AFB family of auxin receptors. Proc. Natl. Acad. Sci. USA. **106**: 22540–22545.

Pasternak, T.P. (2002). The role of auxin, pH, and stress in the activation of embryogenic cell division in leaf protoplast-derived cells of Alfalfa. Plant Physiol. **129**: 1807–1819.

Petrasek, J. (2006). PIN proteins perform a rate-limiting function in cellular auxin efflux. Science. **312**: 914–918.

Petrásek, J. and Friml, J. (2009). Auxin transport routes in plant development. Development **136**: 2675–2688.

Pinon, V., Prasad, K., Grigg, S.P., Sanchez-Perez, G.F., and Scheres, B. (2013). Local auxin biosynthesis regulation by *PLETHORA* transcription factors controls phyllotaxis in *Arabidopsis*. Proc. Natl. Acad. Sci. USA. **110**: 1107–1112.

Piya, S., Shrestha, S.K., Binder, B., Stewart, C.N., and Hewezi, T. (2014). Protein-protein interaction and gene co-expression maps of *ARFs* and *Aux/IAAs* in *Arabidopsis*. Front. Plant Sci. **5**: 1–9.

Pupilli, F. and Barcaccia, G. (2012). Cloning plants by seeds: inheritance models and candidate genes to increase fundamental knowledge for engineering apomixis in sexual crops. J. Biotechnol. **159**: 291–311.

Raghavan, V. (2004). Role of 2,4-dichlorophenoxyacetic acid (2,4-D) in somatic embryogenesis on cultured zygotic embryos of *Arabidopsis*: cell expansion, cell cycling, and morphogenesis during continuous exposure of embryos to 2,4-D. Am. J. Bot. **91**: 1743–1756.

Raven, J.A. (1975). Transport of indoleacetic acid in plant cells in relation to pH and electrical potential gradients, and its significance for polar IAA transport. New Phytol.: 163–172.

Reinhardt, D., Mandel, T., and Kuhlemeier, C. (2000). Auxin regulates the initiation and radial position of plant lateral organs. Plant Cell. **12**: 507–518.

Roach, K.C., Feretzaki, M., Sun, S., and Heitman, J. (2014). Unisexual reproduction. Advances in Genetics. **85:** 255-305.

Robert, H.S., Grones, P., Stepanova, A.N., Robles, L.M., Lokerse, A.S., Alonso, J.M., Weijers, D., and Friml, J. (2013). Local auxin sources orient the apical-basal axis in *Arabidopsis* embryos. Curr. Biol. **23**: 2506–2512.

Robert, H.S., Grunewald, W., Sauer, M., Cannoot, B., Soriano, M., Swarup, R., Weijers, D., Bennett, M., Boutilier, K., and Friml, J. (2015). Plant embryogenesis requires *AUX/LAX*-mediated auxin influx. Development **142**: 702–711.

Robert, S. Kleine-Vehn, J., Barbez, E., Sauer, M., Paciorek, T., Baster, P., Vanneste, S., Zhang, J., Sibu Simon, S., Covanová, M ,Hayashi, K., Dhonukshe, P., Yang, Z., Bednarek, S.Y., Jones, A.M., Luschnig, C., Aniento, F., Zažímalová, E., and Friml, J. (2010). *ABP1* mediates auxin inhibition of clathrin-dependent endocytosis in *Arabidopsis*. Cell 143: 111–121.

Rose, R.J. and Nolan, K.E. (2006). Invited review: Genetic regulation of somatic embryogenesis with particular reference to *Arabidopsis thaliana* and *Medicago truncatula*. Vitr. Cell. Dev. Biol. - Plant **42**: 473–481.

Rubery, P.H. and Sheldrake, A.R. (1974). Carrier-mediated auxin transport. Planta **118**: 101–121.

Ruegger, M., Dewey, E., Gray, W.M., Hobbie, L., Turner, J., and Estelle, M. (1998). The TIR1 protein of *Arabidopsis* functions in auxin response and is related to human SKP2 and yeast Grr1p. Genes Dev. **12**: 198–207.

Ruzicka, K., Simásková, M., Duclercq, J., Petrásek, J., Zazímalová, E., Simon, S., Friml, J., Van Montagu, M.C.E., and Benková, E. (2009). Cytokinin regulates root meristem activity via modulation of the polar auxin transport. Proc. Natl. Acad. Sci. USA. **106**: 4284–4289.

De Rybel, B., Audenaert, D., Beeckman, T., and Kepinski, S. (2009). The past, present, and future of chemical biology in auxin research. ACS Chem. Biol. **4**: 987–998.

Santelia, D., Vincenzetti, V., Azzarello, E., Bovet, L., Fukao, Y., Düchtig, P., Mancuso, S., Martinoia, E., and Geisler, M. (2005). MDR-like ABC transporter AtPGP4 is involved in auxin-mediated lateral root and root hair development. FEBS Lett. **579**: 5399–5406.

Sauer, M., Robert, S., and Kleine-Vehn, J. (2013). Auxin: simply complicated. J. Exp. Bot. **64**: 2565–2577.

Sawchuk, M.G., Edgar, A., and Scarpella, E. (2013). Patterning of leaf vein networks by convergent auxin transport pathways. PLoS Genet. **9**: e1003294.

Sena, G. and Birnbaum, K.D. (2010). Built to rebuild: In search of organizing principles in plant regeneration. Curr. Opin. Genet. Dev. **20**: 460–465.

Simon, S., Kubeš, M., Baster, P., Robert, S., Dobrev, P.I., Friml, J., Petrášek, J., and Zažímalová, E. (2013). Defining the selectivity of processes along the auxin response chain: a study using auxin analogues. New Phytol. **200**: 1034–1048.

Simon, S. and Petrášek, J. (2011). Why plants need more than one type of auxin. Plant Sci. **180**: 454–460.

De Smet, I. (2012). Lateral root initiation: one step at a time. New Phytol. **193**: 867–873.

Song, Y. (2014). Insight into the mode of action of 2,4-dichlorophenoxyacetic acid (2,4-D) as an herbicide. J. Integr. Plant Biol. **56**: 106–113.

Stepanova, A.N., Robertson-Hoyt, J., Yun, J., Benavente, L.M., Xie, D.-Y., Dolezal, K., Schlereth, A., Jürgens, G., and Alonso, J.M. (2008). *TAA1*-mediated auxin biosynthesis is essential for hormone crosstalk and plant development. Cell **133**: 177–191.

Stepanova, A.N., Yun, J., Robles, L.M., Novak, O., He, W., Guo, H., Ljung, K., and Alonso, J.M. (2011). The *Arabidopsis YUCCA1* flavin monooxygenase functions in the indole-3-pyruvic acid branch of auxin biosynthesis. Plant Cell **23**: 3961–3973.

Steward, F.C., Mapes, M.O., and Mears, K. (1958). Growth and organized development of cultured cells. II. Organization in cultures grown from freely suspended cells. Am. J. Bot. **45**: 705–708.

Stone, S.L., Braybrook, S. A, Paula, S.L., Kwong, L.W., Meuser, J., Pelletier, J., Hsieh, T.-F., Fischer, R.L., Goldberg, R.B., and Harada, J.J. (2008). *Arabidopsis LEAFY COTYLEDON2* induces maturation traits and auxin activity: Implications for somatic embryogenesis. Proc. Natl. Acad. Sci. USA **105**: 3151–3156.

Stone, S.L., Kwong, L.W., Yee, K.M., Pelletier, J., Lepiniec, L., Fischer, R.L., Goldberg, R.B., and Harada, J.J. (2001). *LEAFY COTYLEDON2* encodes a B3 domain transcription factor that induces embryo development. Proc. Natl. Acad. Sci. USA. **98**: 11806–11811.

Strader, L.C. and Bartel, B. (2011). Transport and metabolism of the endogenous auxin precursor indole-3-butyric acid. Mol. Plant **4**: 477–486.

Strader, L.C., Chen, G.L., and Bartel, B. (2010). Ethylene directs auxin to control root cell expansion. Plant J **64**: 874–884.

Su, Y.H., Liu, Y.B., Bai, B., and Zhang, X.S. (2015). Establishment of embryonic shoot-root axis is involved in auxin and cytokinin response during *Arabidopsis* somatic embryogenesis. Front. Plant Sci. **5**: 1–9.

Su, Y.H., Su, Y.X., Liu, Y.G., and Zhang, X.S. (2013). Abscisic acid is required for somatic embryo initiation through mediating spatial auxin response in *Arabidopsis*. Plant Growth Regulation. **69:** 167–176.

Su, Y.H. and Zhang, X.S. (2009). Auxin gradients trigger de novo formation of stem cells during somatic embryogenesis. Plant Signal. Behav. **4**: 574–576.

Su, Y.H. and Zhang, X.S. (2014). The hormonal control of regeneration in plants. Curr. Top. Dev. Biol. **108**: 35–69.

Su, Y.H., Zhao, X.Y., Liu, Y.B., Zhang, C.L., O'Neill, S.D., and Zhang, X.S. (2009). Auxin-induced *WUS* expression is essential for embryonic stem cell renewal during somatic embryogenesis in *Arabidopsis*. Plant J. **59**: 448–460.

Sugawara, S., Hishiyama, S., Jikumaru, Y., Hanada, A., Nishimura, T., Koshiba, T., Zhao, Y., Kamiya, Y., and Kasahara, H. (2009). Biochemical analyses of indole-3-acetaldoxime-dependent auxin biosynthesis in *Arabidopsis*. Proc. Natl. Acad. Sci. USA. **106**: 5430–5435.

Sugimoto, K., Jiao, Y., and Meyerowitz, E.M. (2010). *Arabidopsis* regeneration from multiple tissues occurs via a root development pathway. Dev. Cell **18**: 463–471.

Swarup, R. and Péret, B. (2012). *AUX/LAX* family of auxin influx carriers—an overview. Front. Plant Sci. **3**: 1–11.

Tan, X., Calderon-Villalobos, L.I. a, Sharon, M., Zheng, C., Robinson, C. V, Estelle, M., and Zheng, N. (2007). Mechanism of auxin perception by the TIR1 ubiquitin ligase. Nature **446**: 640–645.

Tanaka, H., Dhonukshe, P., Brewer, P.B., and Friml, J. (2006). Spatiotemporal asymmetric auxin distribution: a means to coordinate plant development. Cell. Mol. Life Sci. **63**: 2738–2754.

Tao, Y., Ferrer, J., Ljung, K. (2008). Rapid synthesis of auxin via a new tryptophan-dependent pathway is required for shade avoidance in plants. Cell **133**: 164–176.

Timmis, R. (1998). Bioprocessing for tree production in the forest industry: conifer somatic embryogenesis. Biotechnol. Prog. **14**: 156–166.

Titapiwatanakun, B., Blakeslee, J.J., Bandyopadhyay, A., Yang, H., Mravec, J., Sauer, M., Cheng, Y., Adamec, J., Nagashima, A., Geisler, M., Sakai, T., Friml, J., Peer, W.A., Murphy, A.S. (2009). ABCB19/PGP19 stabilises PIN1 in membrane microdomains in *Arabidopsis*. Plant J. **57**: 27–44.

Tiwari, S.B., Hagen, G., and Guilfoyle, T.J. (2003). The roles of auxin response factor domains in auxin-responsive transcription. Plant Cell **15**: 533–543.

Ulmasov, T., Murfett, J., Hagen, G., and Guilfoyle, T.J. (1997). Aux/IAA proteins repress expression of reporter genes containing natural and highly active synthetic auxin response elements. Plant Cell **9**: 1963–1971.

Verma, D., Joshi, R., Shukla, A., and Kumar, P. (2011). Protocol for in vitro somatic embryogenesis and regeneration of rice (Oryza sativa L.). Indian J. Exp. Biol. **49**: 958–963.

Verstraeten, I., Schotte, S., and Geelen, D. (2014). Hypocotyl adventitious root organogenesis differs from lateral root development. Front. Plant Sci. **5**: 1–13.

von Arnold, S., Sabala, I., Bozhkov, P., Dyachok, J., and Filonova, L. (2002). Developmental pathways of somatic embryogenesis. Plant Cell. Tissue Organ Cult. **69**: 233–249.

Wang, Q., Kohlen, W., Rossmann, S., Vernoux, T., and Theres, K. (2014). Auxin depletion from the leaf axil conditions competence for axillary meristem formation in *Arabidopsis* and Tomato. Plant Cell **26**: 2068–2079.

Wang, R. and Estelle, M. (2014). Diversity and specificity: auxin perception and signaling through the TIR1/AFB pathway. Curr. Opin. Plant Biol. **21C**: 51–58.

Wang, X.-D., Nolan, K.E., Irwanto, R.R., Sheahan, M.B., and Rose, R.J. (2011). Ontogeny of embryogenic callus in *Medicago truncatula*: the fate of the pluripotent and totipotent stem cells. Ann. Bot. **107**: 599–609.

Weijers, D., Sauer, M., Meurette, O., Friml, J., Ljung, K., Sandberg, G., Hooykaas, P.J.J., and Offringa, R. (2005). Maintenance of embryonic auxin distribution for apical-basal patterning by PIN-FORMED-dependent auxin transport in *Arabidopsis*. Plant Cell **17**: 2517–2526.

West, M., Yee, K., Danao, J., Zimmerman, J., Fischer, R., Goldberg, R., and Harada, J. (1994). *LEAFY COTYLEDON1* is an essential regulator of late embryogenesis and cotyledon identity in *Arabidopsis*. Plant Cell **6**: 1731–1745.

Wickramasuriya, A.M. and Dunwell, J.M. (2015). Global scale transcriptome analysis of *Arabidopsis* embryogenesis in vitro. BMC Genomics **16**: 1–23.

Wójcikowska, B., Jaskóła, K., Gąsiorek, P., Meus, M., Nowak, K., and Gaj, M.D. (2013). *LEAFY COTYLEDON2 (LEC2)* promotes embryogenic induction in somatic tissues of *Arabidopsis*, via *YUCCA*-mediated auxin biosynthesis. Planta **238**: 425–440.

Won, C., Shen, X., Mashiguchi, K., Zheng, Z., Dai, X., Cheng, Y., Kasahara, H., Kamiya, Y., Chory, J., and Zhao, Y. (2011). Conversion of tryptophan to indole-3-acetic acid by *TRYPTOPHAN AMINOTRANSFERASES* and *YUCCAs* in *Arabidopsis*. Proc. Natl. Acad. Sci. USA. **108**: 18518–18523.

Woodward, A.W. and Bartel, B. (2005). Auxin: regulation, action, and interaction. Ann. Bot. **95**: 707–735.

Woodward, C., Bemis, S.M., Hill, E.J., Sawa, S., Koshiba, T., and Torii, K.U. (2005). Interaction of auxin and *ERECTA* in elaborating *Arabidopsis* inflorescence architecture revealed by the activation tagging of a new member of the *YUCCA* family putative flavin monooxygenases. Plant Physiol. **139**: 192–203.

Wright, R.C. and Nemhauser, J.L. (2015). New tangles in the auxin signaling web. F1000Prime Rep. **7**: 7–19.

Xuan, W., Audenaert, D., Parizot, B., Möller, B.K., Njo, M.F., De Rybel, B., De Rop, G., Van Isterdael, G., Mähönen, A.P., Vanneste, S., and Beeckman, T. (2015). Root cap-derived auxin pre-patterns the longitudinal axis of the *Arabidopsis* root. Curr. Biol. **25**: 1381–1388.

Yang, H. and Murphy, A.S. (2009). Functional expression and characterization of *Arabidopsis* ABCB, AUX1 and PIN auxin transporters in *Schizosaccharomyces pombe*. Plant J. **59**: 179–191.

Yang, Y., Hammes, U.Z., Taylor, C.G., Schachtman, D.P., and Nielsen, E. (2006). High-affinity auxin transport by the AUX1 Influx Carrier Protein. Curr. Biol. **16**: 1123–1127.

Zhao, Y., Christensen, S.K., Fankhauser, C., Cashman, J.R., Cohen, J.D., Weigel, D., and Chory, J. (2001). A role for flavin monooxygenase-like enzymes in auxin biosynthesis. Science **291**: 306–309.

Zhao, Y., Hull, A.K., Ecker, J.R., Normanly, J., Chory, J., and Celenza, J.L. (2002). Trp-dependent auxin biosynthesis in. Genes Dev.: 3100–3112.

Zolman, B.K., Yoder, A., and Bartel, B. (2000). Genetic analysis of indole-3-butyric acid responses in *Arabidopsis thaliana* reveals four mutant classes. Genetics **156**: 1323–1337.

Zuo, J., Niu, Wu, Q.-W., Frugis, G., and Chua, N-H. (2002). The *WUSCHEL* gene promotes vegetative-to-embryonic transition in *Arabidopsis*. Plant J. **30**: 349–359.

Chapter 2

2,4-D-induced somatic embryogenesis initiation requires a relative auxin minimum in *Arabidopsis*.

Cheryl Philipsen[1,2],
Remko Offringa[1]

[1.] *Molecular and Developmental Genetics, Institute of Biology Leiden, Universiteit Leiden, Sylviusweg 72, 2333BE, Leiden, Nederland*
[2] *Current affiliation: Dümmen Orange, P.O. Box 26, 2678ZG, de Lier, the Netherlands*

Abstract

Techniques for clonal plant propagation are important to high economically valued crops and ornamentals and it comes in many forms, including the process of somatic embryogenesis (SE). In *Arabidopsis*, SE can be efficiently induced by treatment of immature zygotic embryos (IZEs) with the synthetic auxin analog 2,4-dichlorophenoxyacetic acid (2,4-D). The natural auxin indole-3-acetic acid (IAA) and its cellular transport play an important role in zygotic embryogenesis (ZE) as well as organogenesis; however, the involvement of IAA in 2,4-D induced SE initiation is yet unclear. To investigate this we established a standardized system for SE initiation and outgrowth of somatic embryos using 12 days old *Arabidopsis* IZEs. In this system, *pWOX2::NLS-YFP* was used as a marker for embryonic cell fate and the first *WOX2-YFP*-reported embryonic cell clusters could be observed after 5 to 7 days of culture in somatic embryogenesis inducing medium (SEIM). Interestingly, these clusters were located in regions of low auxin response. Studies using inhibitors of cellular auxin transport indicated an important role for auxin influx in SE initiation, whereas auxin efflux only seemed to be important for establishment of the embryonic body pattern later during SE. In fact, *aux1 lax* loss-of-function mutant IZEs showed enhanced shoot/root regeneration at the cost of SE. Expression of AUX1 influx carriers directly next to the SE initiation sites suggested that auxin influx might be necessary for generating the low auxin response regions that are important for SE initiation.

Introduction

Clonal plant propagation can be achieved by simple stem-, leaf- or root cuttings, or by more elaborate tissue culture-based methods where shoots and subsequently roots, or even complete embryos are regenerated from plant tissues. In the latter process, referred to as somatic embryogenesis (SE), somatic plant cells derived from late embryogenic or vegetative tissues develop into embryos. In contrast to zygotic embryogenesis (ZE), SE does not require fertilization as an initial trigger, but it still results in an embryo with a complete root-shoot axis, vascular system and functional meristems (Pupilli and Barcaccia, 2012; Fehér, 2015). SE is desirable as a strategy for stable clonal propagation, of for example F1 hybrid crops, since the resulting embryos can be cryopreserved for later use or to establish gene banks (Timmis, 1998; Arnold et al., 2002) and it allows the production of unlimited numbers of normal individuals using bioreactors (Timmis, 1998). Moreover, as opposed to shoot/root regeneration, SE has been reported to result in limited somaclonal variation among the propagated individuals, (reviewed by Gaj, 2004; Bairu et al., 2011). SE is also used as an alternative method to study ZE in species that have a long reproduction cycle and with economic relevance, such as spruce (*Pinacea*) (Timmis, 1998; FAO, 2015). SE provides the advantage of producing a high number of individual somatic embryos and thus the process of embryogenesis can be studied on a large scale within a shorter time frame. One has to keep in mind, however, that SE and ZE are different processes that are initiated by different signals.

Several genes have been identified as key regulators of SE. These include *LEAFY COTYLEDON1 (LEC1)* and *LEC2, FUSCA3 (FUS3), BABY BOOM (BBM)* and *WUSCHEL (WUS)* (Lotan et al., 1998; Stone et al., 2001; Boutilier et al., 2002; Zuo et al., 2002). *LEC1, ABA INSENSITIVE3* (*ABI3*), *FUS3, and LEC2* constitute the *LAFL* gene network, that was initially identified based on its role in seed maturation and the transition from embryo to seedling development (Jia et al., 2013). Later, it was shown that *lec1*, *lec2* and *fus3* loss-of-function mutants are impaired in their competence to form somatic embryos (Gaj et al., 2005), whereas constitutive overexpression of *LEC1* and *LEC2* leads to spontaneous SE on the shoot apical meristem and cotyledons of germinating seedlings (Lotan et al., 1998; Stone et al., 2001). Overexpression of *FUS3* leads to development of cotyledon-like leaves by holding these post embryonic tissues in a phase that benefits the embryogenic capacity (Gazzarrini et al., 2004). The action of the *LAFL* genes seems to depend on levels of the seed maturation hormone abscisic acid (ABA). ABA is required for *LEC1*- and *LEC2*-induced embryonic differentiation, which subsequently activates

endogenous auxin production and results in reprogramming of epidermal cells generating callus and somatic embryos (Stone et al., 2008; Junker et al., 2012).

The induction of SE in different plant species often requires treatment of somatic tissues with 2,4-dichlorophenoxyacetic acid (2,4-D), a synthetic analog of the plant hormone auxin, indole-3-acetic-acid (IAA). The natural IAA generally cannot induce this process, which is surprising in view of the important role of this signalling molecule during early zygotic embryogenesis (Friml et al., 2003; Rademacher et al., 2012), and the importance of an elevated auxin response downstream of the *LAFL* gene network and ABA in inducing SE (Michalczuk et al., 1992; Pasternak, 2002; Gaj et al., 2005; Su et al., 2015). In zygotic embryogenesis the auxin responses patterning the embryo are governed by differential distribution of auxin by polar cel-to-cell transport of auxin (Weijers et al., 2005; Robert et al., 2013, 2015b). Here, we investigated the role of auxin transporters in regulating auxin responses during 2,4-D induced SE initiation from *Arabidopsis* immature zygotic embryos (IZEs).

Polar auxin transport (PAT) involves the activity of three families of membrane proteins (Petrásek and Friml, 2009; Swarup and Péret, 2012). In line with the chemiosmotic hypothesis that was initially proposed to provide a mechanistic basis for the cell-to-cell auxin flow (Rubery and Sheldrake, 1974; Raven, 1975; Goldsmith, 1977), auxin can diffuse over the plasma membrane in its protonated form, but its uptake is also facilitated by AUX1/LIKE AUX1 (AUX1/LAX) influx carriers that form a small family of four proteins in *Arabidopsis* (AUX1, LAX1, LAX2 and LAX3). AUX/LAX proteins are thought to enhance the steady-state concentration of auxin in plant cells, and were found to be important drivers of PAT (Swarup et al., 2005; Jones et al., 2009; Boot et al., 2015). AUX1 and LAX3 function in gravitropism (Swarup et al., 2001) and lateral root development (Marchant et al., 2002; De Smet et al., 2007; Swarup et al., 2008), LAX2 regulates vascular patterning in cotyledons (Peret et al., 2012) and AUX1, LAX1 and LAX2 are required in different stages in zygotic embryo development (Ugartechea-Chirino et al., 2010; Peret et al., 2012; Robert et al., 2015b). The role of AUX/LAX in SE is not well established yet.

The chemiosmotic hypothesis for PAT predicts that due to the basic pH inside plant cells auxin is mostly deprotonated, and that as a negatively charged ion, auxin can only pass the plasmamembrane (PM) with the help of efflux carriers. Asymmetric distribution of these efflux carriers on the PM of the cell generates a polar cell-to-cell flow of auxin. Research in *Arabidopsis* has identified two types of auxin efflux carrier. First, the PIN-FORMED (PIN) proteins that have been shown to be the rate limiting components that direct PAT through their asymmetric distribution at the PM of the cell (Petrásek et al., 2006; Wisniewska, 2006). Secondly,

the ABCB/MULTIDRUG RESISTANCE/P-GLYCOPROTEIN class of transporters that do not exhibit polarity and have been proposed to determine the amount of auxin available for PIN-mediated PAT (Geisler and Murphy, 2006; Mravec et al., 2008). In *Arabidopsis thaliana*, PIN proteins are encoded by a small gene family of eight members. The protein structure of PINs is highly conserved and consists of two transmembrane domain regions separated by a hydrophilic loop that varies in length (Friml et al., 2002; Benková et al., 2003; Friml et al., 2003; Blilou et al., 2005; Mravec et al., 2009). PINs with a long hydrophilic loop (long PINs) are localized on the PM (PIN1, 2, 3, 4 and 7) whereas PINs with a short hydrophilic loop (short PINs) are localised in the endoplasmatic reticulum (ER) (PIN5 and PIN8). PIN6 contains a hydrophilic loop of intermediate length and is localised both in the ER and at the PM (Mravec et al., 2009; Sawchuk et al., 2013; Ganguly et al., 2014). Asymmetric localisation by PINs results in local dynamic auxin maxima and minima or gradients that are instructive in many developmental processes, including embryo patterning (Friml et al., 2003; Robert et al., 2015b), tropic growth (Luschnig et al., 1998; Friml et al., 2002) and organ formation (Reinhardt et al., 2000; Benková et al., 2003). All the long PINs have been shown to be involved in patterning the zygotic embryo by generating auxin maxima that first mark the early embryo proper, then organise the root pole, and finally position the cotyledon primordia (Friml et al., 2003; Blilou et al., 2005). During SE PIN1 is proposed to act by mediating auxin transport from areas with high auxin towards areas of low auxin prior to establishment of the somatic embryo (Su et al., 2009), and PIN4 was shown to be uniformly expressed in cell clusters and restricted to the embryonic root as development progresses (Bassuner et al., 2006). These findings suggest a developmental role for PINs during SE.

In order to test the involvement of PAT in SE, we first optimized the *Arabidopsis* system for 2,4-D-induced SE from IZEs for our culture conditions. By making use of the embryonic cell fate reporter *pWOX2::NLS-YFP* (Breuninger et al., 2008; Haecker et al., 2004) and combining this with the well-known *DR5* auxin response reporter (Ulmasov et al., 1997), we could show that SE is initiated in IZEs between 5 and 7 days after the start of 2,4-D treatment in areas of low *DR5* response. This is in contrast to the auxin maxima that mark the positions of lateral organ initiation in the shoot meristem and in the root (Reinhardt et al., 2003; Benková et al., 2003) (Reinhard 2003, Benkova 2003). Inhibitor studies indicated that auxin influx rather than efflux is crucial for SE initiation. The expression of the AUX1 influx carrier in cells next to the SE initiation sites suggested that auxin influx is required to generate the relative auxin response minimum that allows SE initiation.

Results

A standardized procedure for SE induction and scoring on Arabidopsis IZEs

Even though several protocols have been published on 2,4-D induced SE on *Arabidopsis* IZEs (Gaj et al., 2005; Su et al., 2009; Nowak et al., 2012), we experienced quite some variation in the efficiency of SE per experiment. Since comparing different treatments and *Arabidopsis* mutants for SE efficiency required a robust and reproducible protocol, we decided to optimize the protocol for our laboratory conditions. Thus far, most protocol optimizations have focused on medium composition. Here we mainly considered the workflow (Figure 1) of the SE protocol, with a focus on the culture time and the developmental stage and the physiology of the IZEs, (Luo and Koop, 1997; Gaj, 2001; Jiménez, 2005). Most protocols use 'late' IZEs, where the two cotyledons are folded beside the hypocotyl-root. Since the 'folded' phenotype is rather a subjective criterion, we aimed at culturing IZEs for which the development was synchronized by harvesting them at 9, 11, 12, 14 and 15 days after pollination (dap), on solid somatic embryogenesis inducing medium (SEIM) for 14 days, and on hormone free medium for 7 days. Experiments were either scored for SE efficiency, which is the number of IZE explants producing somatic embryos and embryonic structures, or for SE productivity, where we determined the average number of somatic embryos formed per IZE. The SE efficiency appeared to be a stable parameter that allowed to assess SE between experiments, whereas SE productivity varied strongly between experiments (0.2 – 3.8 somatic embryos/IZE, Figure S1) and was more dependent on the observer and it is therefore important to always include an untreated or wild-type control into the experiment. To improve uniformity in SE productivity scoring, we defined more clearly the structures that developed during culturing and were taken along in the score. For SE productivity, only individual somatic embryos were counted that showed a smooth green surface, developed their own vascular system (Bassuner et al., 2006), and were only connected to the IZE explant at the root tip (Figure 2a,b).

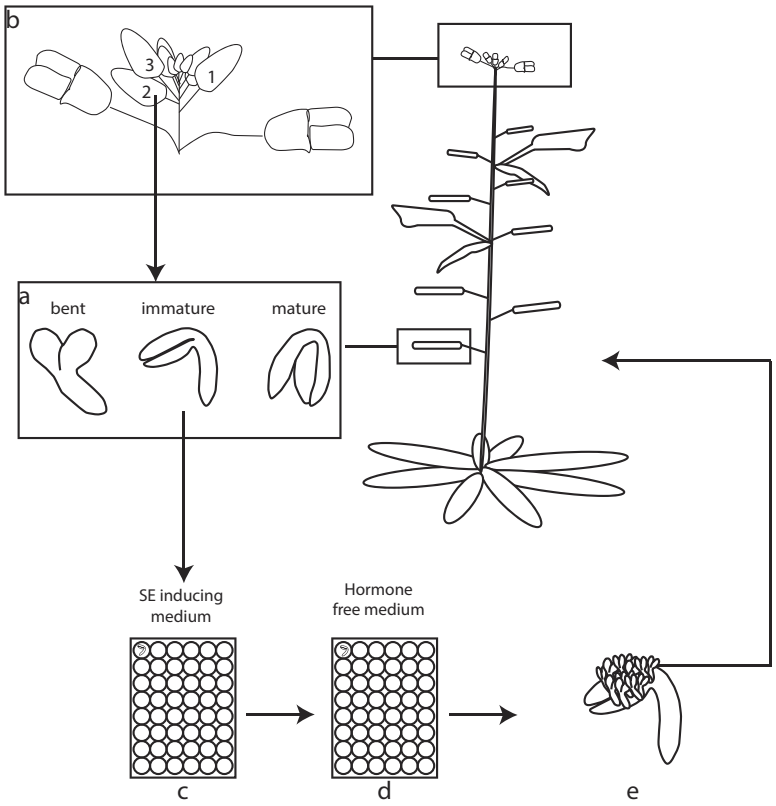

FIGURE 1 - Workflow of somatic embryogenesis (SE) on *Arabidopsis thaliana* immature zygotic embryos (IZEs).
IZEs were either harvested from siliques and size-selected (a), or the three most mature closed flower buds were emasculated and pollinated and IZEs were harvested at specific days after pollination (b). SE was induced by culturing the IZEs on SEIM for 14 days (c), after which they were transferred to hormone free medium for 7 days to allow outgrowth of the somatic embryos to facilitate scoring (d). Somatic embryos germinated and grew out to a full mature plant when detached from the explant and germinated on hormone free medium (e).

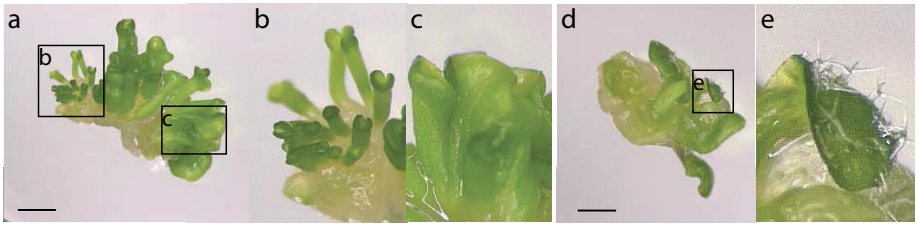

FIGURE 2 - Overview of the different tissues developing from *Arabidopsis* IZEs.
a) and d) two *Arabidopsis* (Col-0) IZEs after standard SE culture (see M&M). b) and c) are enlargements of the indicated regions in a), showing either individual somatic embryos with an individual root pole (b) or fused embryonic structures (c). e) Detail of the region in c) showing a shoot-like structure with a rough green surface and trichomes. Scale bar represents 1mm.

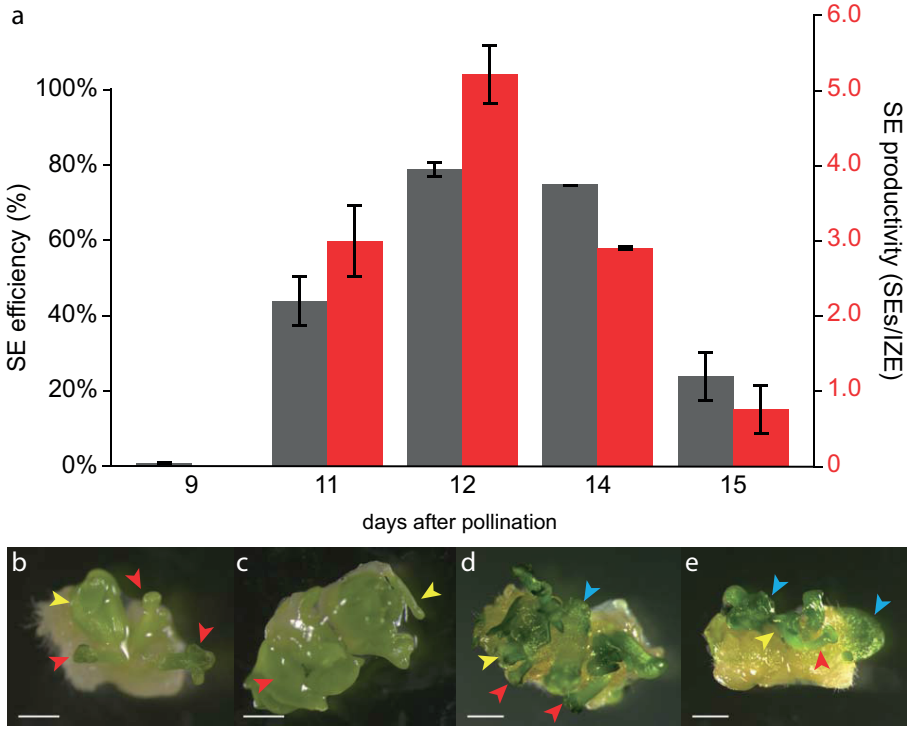

FIGURE 3 - SE efficiency and productivity strongly depend on the age of the *Arabidopsis* IZEs.
a) SE efficiency (grey bars) and SE productivity (red bars) of *Arabidopsis* IZEs after standard SE culture. SE efficiency is expressed as the number of IZEs producing embryonic callus and somatic embryos and SE productivity is expressed as number of individual somatic embryos produced per IZE. Bars represent average of duplicate experiments, with n=48. Error bars indicate the standard error of the mean (SEM). $\chi 2$ test for association showed that the SE efficiency is significantly determined by the age of the IZE ($\chi 2$=85.6, p<0.05). b-e) *Arabidopsis* IZEs harvested at 11 (b), 12 (c), 14 (d), or 15 dap (e) after standard SE culture. Red arrowheads indicate individual somatic embryos, yellow arrowheads indicate embryonic structures, and blue arrow heads point out shoot-like structures. Scale bar represents 1mm.

Somatic embryos fused along the hypocotyl-cotyledon axis into embryonic structures were too difficult to accurately count and were therefore only taken along for the SE efficiency (Figure 2a,c). By scoring this way, we took into account that the SE productivity provided an underestimate of the total number of somatic embryos per explant. Obviously, shoot-like structures that exhibited a rougher darker green surface and trichomes (Figure 2d,e) were not scored as somatic embryos. Using these criteria, we observed the highest SE efficiency with IZEs that were harvested 12 or 14 dap, and the highest SE productivity in 12 dap IZEs (Figure 3a). Although some 11 dap IZEs were capable of producing individual somatic embryos (Figure 3b,c), most of the IZEs died during culturing on SEIM in the first 7 days, resulting in a low SE efficiency. IZEs of 9 dap mostly died during culture, and most 15 dap IZEs produced shoot-like structures rather than somatic embryos (Figure 3e). A χ^2 test for association showed that the SE efficiency depends on the IZE age ($p<0.05$). Since both SE productivity and SE efficiency were high at 12 dap, this time point was selected for IZE harvesting.

SE initiation in IZEs requires 5 days 2,4-D induction

With the SE protocol optimized using 12 dap IZEs, our next aim was to use a reporter to identify embryonic cells during SE initiation. Several embryonic cell reporters have been described previously (Haecker et al., 2004; Soriano et al., 2013), but some of these reporters marked the suspensor rather than the embryo proper during zygotic embryogenesis. In contrast, the *pWOX2::NLS-YFP* reporter specifically marked the zygotic embryos from early stages on (Haecker et al., 2004; Breuninger et al., 2008, Figure S2), and seemed ideal for the purpose of tracing the initiation and early phases of SE. Time lapse imaging of IZEs by confocal microscopy every 24 hours starting from day 8 in culture showed that *pWOX2::NLS-YFP* expressing cells could already be observed at day 8 (Figure 4a), and over days 10 to 14 these cells grew out to *pWOX2::NLS-YFP* expressing protuberances that resembled globular shaped zygotic embryos (Figure 4b-d). *pWOX2::NLS-YFP* expressing cells were observed on both adaxial and abaxial sides of the cotyledons, mostly located at the base of the cotyledons (the proximal area). The *pWOX2::NLS-YFP* expressing protuberances developed on top of callus tissue that did not express *pWOX2::NLS-YFP* or only at a low level (Figure 4d). Based on this observation, the fact that the *WOX2-YFP* reporter marks the early zygotic embryo (Breuninger et al., 2008), and that the expressing protuberances grew out to somatic embryos when followed in time we concluded that *pWOX2::NLS-YFP* is a suitable marker to track SE from initiation to development of the somatic embryo and thereby as a marker for cells that revert their cell fate from 'late' embryogenic to 'early' embryogenic.

Next, we looked at earlier time points to more accurately determine the minimum 2,4-D exposure time required of SE initiation by incubating *pWOX2::NLS-YFP* IZEs for 3, 5 or 7 days on SEIM, and subsequently for 48hr to hormone free medium (Figure 4e-i). Incubation on SEIM for 5 and 7 days, but not 3 days, resulted in *pWOX2::NLS-YFP* expressing cells in the proximal region of the cotyledons (Figure 4e,f,g). However, these positive cells did not develop into strong foci of YFP expression, but instead YFP positive cells remained more dispersed in the proximal region of the cotyledons compared to their controls (Figure 4h,i). This suggested that the patterning programme of the somatic embryo is abolished after transfer to hormone free medium. A phenotypic study of IZEs that were grown for 3, 5 or 7 days on SEIM and subsequently transferred to hormone free medium to allow somatic embryos to develop for a subsequent 7 days (Figure 4j-m) showed that IZEs grown for 3 days on SEIM continued to germinate after transfer to hormone free medium and developed into seedlings with aberrations (Figure 4l). IZEs incubated for 5 days on SEIM showed mostly seedling growth, but on average 53% developed embryonic structures (Figure 4k). The 7 days SEIM incubation resulted in a similar SE efficiency (76%) as the standard 14 days protocol, whereas the SE productivity lagged behind considerably (Figure 4j). A χ^2 test for association showed that the SE efficiency was significantly dependent on the duration of 2,4-D treatment ($p < 0.05$). These results indicated that 5 days 2,4-D exposure was sufficient for IZE cells to be reprogrammed and revert their cell fate, but also that a longer 2,4-D exposure is required to establish multiple stable foci of *WOX2* expression that give rise to a reasonable number of individual somatic embryos.

2,4-D induced somatic embryos occur in areas of relatively low auxin response

To investigate the correlation between early somatic embryo initiation and auxin response we combined the *pWOX2::NLS-YFP* embryo marker with the *DR5::RFP* auxin response reporter. At 3 and 4 days after 2,4-D treatment, the auxin response was relatively low throughout the entire IZE (Figure 5a,b). At day 5, however, the auxin response increased both in the cotyledons (Figure 5c) and the hypocotyl (Figure 5e,f,i). *pWOX2::NLS-YFP* expression was again first observed at day 5, mostly in cells in the proximal region on both adaxial and abaxial sides of the cotyledons and in a few cells in the hypocotyl (Figure 5c-f). Simultaneously, we observed that the auxin response was overall increasing, but that local auxin response minima developed on day 5, coinciding with cells expressing *pWOX2::NLS-YFP* (Figure 5d-f). Remarkably, this is in contrast to lateral organogenesis in the shoot apical meristem (SAM) or root, where auxin maxima mark the onset of organ initiation (Benková et al., 2003; Friml et al., 2003; Heisler et al., 2005; Marhavý et al., 2013). These findings suggest that the auxin response

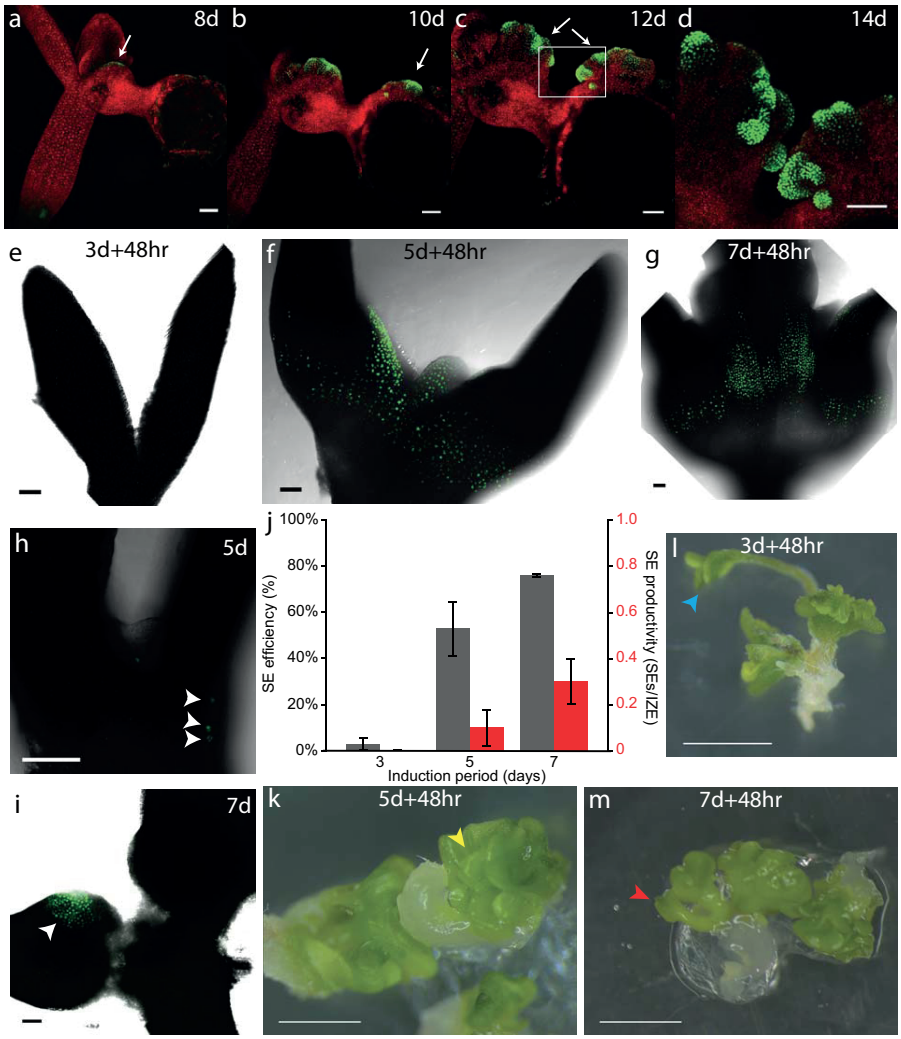

FIGURE 4 - SE in *Arabidopsis* IZEs is initiated between 5 and 7 days of culture.
a - d) Timelapse of *pWOX2::NLS-YFP* (green) expression in *Arabidopsis* IZEs after 8 (a), 10 (b), 12 (c) or 14 (d) days of culture on SEIM. Chlorophyl in red, arrows point to cells expressing *pWOX2::NLS-YFP*, scale bar represents 100µm. e-i) *pWOX2::NLS-YFP* (green) expression in IZEs after 3 days SEIM + 48hr hormone free (e) 5 days SEIM + 48hr hormone free (f) 7 days SEIM + 48hrs hormone free (g), controls of 5 days SEIM in (h) and 7 days SEIM in (i), white arrow heads point at cells expressing *pWOX2::NLS-YFP*. j - m) phenotype study of hormone free treatment with j) SE efficiency (grey bars) and productivity (red bars) for each initiation period. Bars represent average of duplicate experiments, with n=48. Error bars are SEM, $\chi 2$ test for association was used, $\chi 2=70.7$, $p=0.05$. l-m) Phenotypes of IZEs with SEIM induction for l) 3 days k) 5 days m) 7 days. Red arrowhead point at individual somatic embryos, yellow arrowhead point at embryonic like structures and blue arrowhead are dedicated to shoot like structures. Scale bar is 1mm.

is regulated in a spatiotemporal manner during SE initiation. To investigate whether this dynamic auxin response was required for SE initiation, we stopped SE induction after three days by transferring IZEs to hormone free medium and incubating them for 48 hours. We noticed that the auxin response was lost, both in cotyledons (Figure 5g vs 5h) and in the hypocotyl (Figure 5i vs 5j). Simultaneously, *pWOX2::NLS-YFP* was also absent in the cotyledons, confirming that SE initiation was inhibited. Interestingly, during incubation on hormone free medium, an increase in *pWOX2::NLS-YFP* expression could be observed in the hypocotyl, indicating that the cells in the hypocotyl maintained their embryonic identity, and suggesting that 2,4-D is required to downregulate this *WOX2* expression in the hypocotyl and to reprogram cells in the cotyledons to induce SE.

Auxin response minima coinciding with SE initiation require auxin influx proteins

The auxin dynamics in the cell reported by the *DR5::RFP* marker is the sum of auxin homeostasis (biosynthesis, conjugation and turn over), transport and signalling. All three pathways have been reported to be important for zygotic embryogenesis (Hardtke and Berleth, 1998; Friml et al., 2003; Cheng, 2006; Weijers et al., 2006; Rademacher et al., 2012; Robert et al., 2013, 2015b). To study auxin transport, we used the inhibitors N-1-napthylphthalamic acid (NPA) (Noh et al., 2001) or 1-naphthoxyacetic acid (1-NOA) (Parry et al., 2001) to chemically block respectively auxin efflux- or auxin influx activity from the start (0d), before establishment of the first embryonic cells (3d) or during establishment of the first embryonic cells (5d). As controls, we included IZEs continuously grown on SEIM (0d ctrl) or IZEs that were transferred to fresh SEIM plates after 5 days of culture on SEIM (5d ctrl). Blocking active auxin efflux with 100µM NPA did not affect SE initiation as severely as was expected based on genetic data on zygotic embryogenesis (Figure 6a) (Friml et al., 2003; Blilou et al., 2005). NPA treated IZEs developed both individual somatic embryos as well as embryonic structures (Figure 6g-i). However, the derived somatic embryos appeared to be smaller and more often fused compared to the control. Only NPA treatment of IZEs from the start of their incubation on SEIM resulted in a significant reduction in SE efficiency (60%), but the SE productivity, i.e. the development of the individual somatic embryos, was significantly reduced for day 0 (0.7 somatic embryos/IZE) and day 3 (0.7 somatic embryos/IZE) compared to the control (1.3-1.5 somatic embryos/IZE). Examination of the *WOX2 DR5* reporters showed no obvious perturbation in the spatiotemporal distribution of the auxin response in NPA treated IZEs. NPA treatment still allowed SE initiation to occur in local relative auxin minima (Figure 6f), similar to the control (Figure 6b). In conclusion, auxin efflux is not responsible for generating such local auxin response minima.

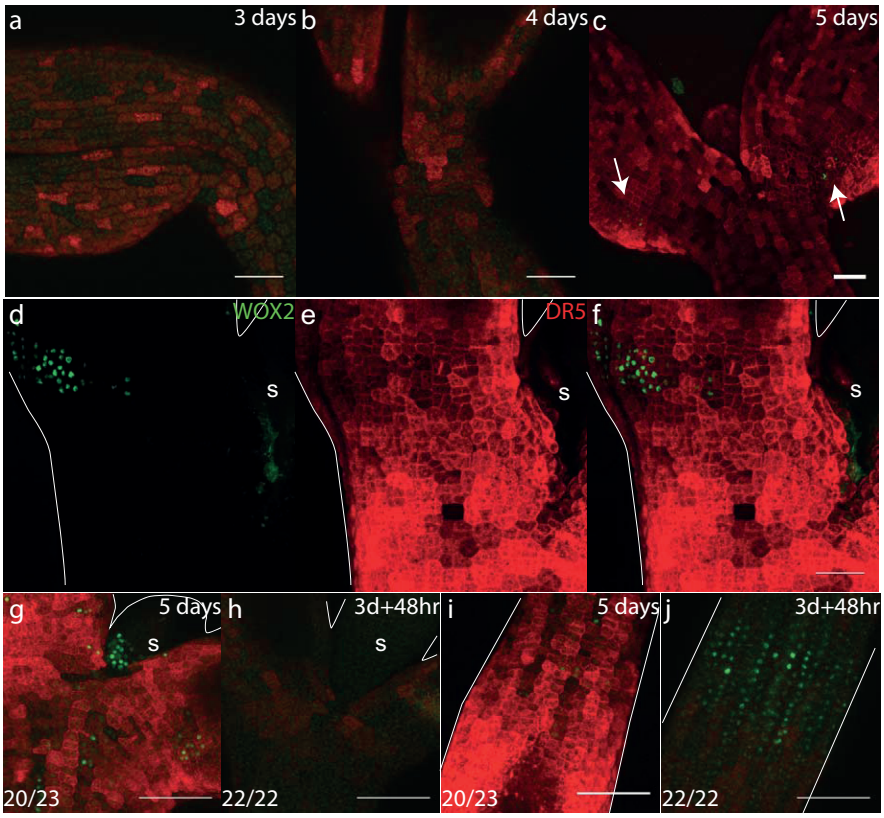

FIGURE 5 - Dynamic auxin responses during SE initiation in *Arabidopsis* IZEs.
Representative CLSM images of *pWOX2::NLS-YFP* (green) *DR5::RFP* (red) IZEs, cultured on SEIM for 3 days (a,g,h,j), 4 days (b) and 5 days (c,d-f,i). Images in (a-c, f, g-j) show both the YFP and RFP signal, whereas (d) and (e) represent respectively the separate YFP and RFP signals in (f). g,i) An IZE with 5 days SEIM induction vs h,j) is an IZE with 3 days induction + 48 hr hormone free treatment. Observation frequencies are indicated in the left bottom, scale bar is 50um (a-c) or 100µm (g-j).

In contrast, treatment with the auxin influx inhibitor NOA resulted in a significant reduction of the SE efficiency and -productivity for all three time points (Figure 6a). The NOA-treated IZEs mostly developed small whitish calli with dark green leaf-like structures or an occasional embryo-like structure (Figure 6k-m). These findings are supported by the *WOX2-YFP* expression, showing that no embryonic cell fate was initiated (Figure 6j). The auxin response was still strong upon treatment with 1-NOA, but in contrast to the control, this response seemed more evenly distributed without the generation of local auxin minima. Our observations suggest that auxin influx is necessary for embryonic cell fate initiation by creating local auxin minima, and that auxin efflux rather plays a role in the further development of these cells into somatic embryos.

A recent publication has indicated the involvement of auxin influx in zygotic embryogenesis, where the AUX1, LAX1 and LAX2 influx carriers are the main contributors that supply the PAT system with auxin (Robert et al., 2015b). To investigate which influx carriers are required and to confirm our findings with 1-NOA we

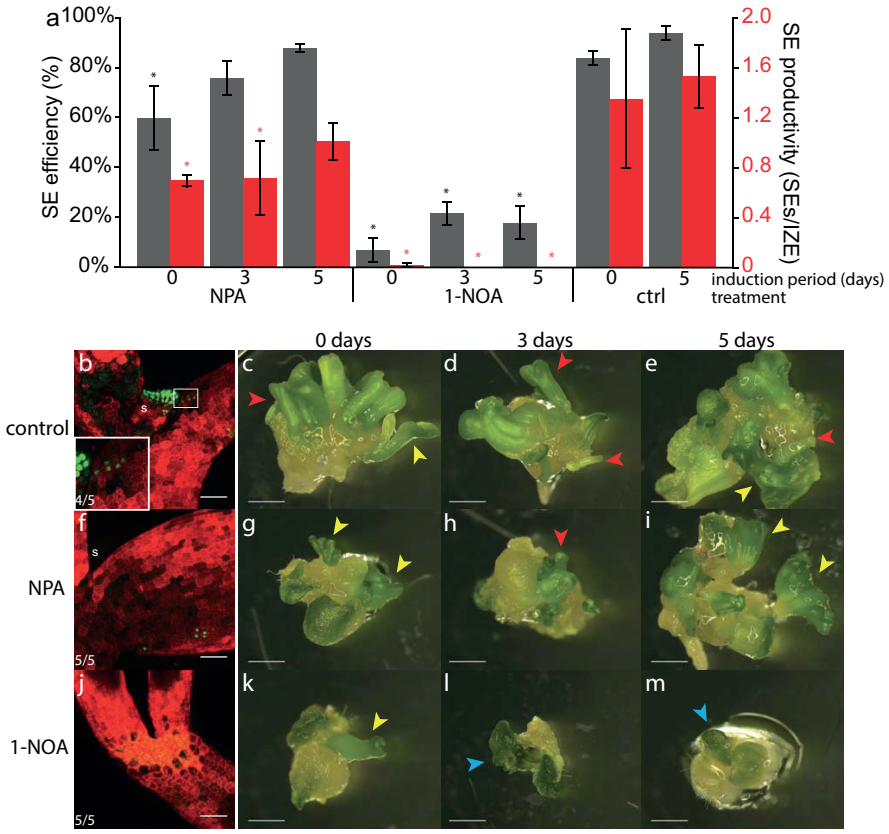

FIGURE 6 - Auxin influx rather than -efflux is essential for SE initiation in *Arabidopsis* IZEs.

a) SE efficiency (grey bars) and productivity (red bars) of IZEs incubated on SEIM to which 100uM NPA or 1-NOA was added at the start or at 3 or 5 days after the start of the incubation. Control IZEs were incubated on SEIM without (0) or with transfer to fresh SEIM after 5 days (5). Bars represent values of duplo experiments with n = 48, error bars indicate SEM. Asterisks denote statistical difference between control and treatment. SE efficiencies were compared using the $\chi 2$ test ($p<0.05$), and SE productivities were compared using the Welch *t*-test ($p<0.05$). b, e, h) Representative CLSM images of *pWOX2::NLS-YFP* (green) *DR5::RFP* (red) IZEs cultured for 3 days on SEIM followed by 48hr on hormone free medium, in the absence (b) or presence of 100µM NPA (f) or 100µM 1-NOA (j). Scale bar represents 50µm. Numbers represent observation frequencies (c-e). Phenotype of control treatment (2,4-D) with (c) 0 days (d) 3 days (e) 5 days. Phenotype of NPA with (g) 0 days (h) 3 days (i) 5 days. (k - m) phenotype of 1-NOA with (k) 0 days (l) 3 days (m) 5 days. Red arrow heads point at individual somatic embryos, yellow arrow heads pointed at embryogenic structures and blue arrow heads indicate shoot-like structures, observation frequencies are indicated the bottom right corner, scale bar represents 1mm.

determined the SE efficiency of the *Arabidopsis aux1 lax1*, *aux1 lax2* and *aux1 lax3* double mutants and compared this to wild type (Figure 7). In these experiments we noticed that many of the mutant IZEs produced shoot and root structures next to embryogenic structures and individual somatic embryos (Figure 7b-e). For this reason, we also scored the shoot/root regeneration efficiency (number of IZEs producing shoots and/or roots; Figure 7a). In the wild type, the SE efficiency reached 94%, 11% of the IZEs produced shoot/roots, and on average 0.73 somatic embryos were produced per IZE. In the *aux1 lax1* double mutant both SE efficiency and SE productivity were significantly decreased (respectively 74% and 0.29) and interestingly, the shoot/root regeneration was significantly increased (51%). For the *aux1 lax2* and *aux1 lax3* double mutants the SE efficiency was not significantly reduced, but the SE productivity was, and these IZEs produced significantly more shoot and roots, (Figure 7a). These findings show that the AUX1/LAX influx proteins act redundantly during SE and are required for SE initiation.

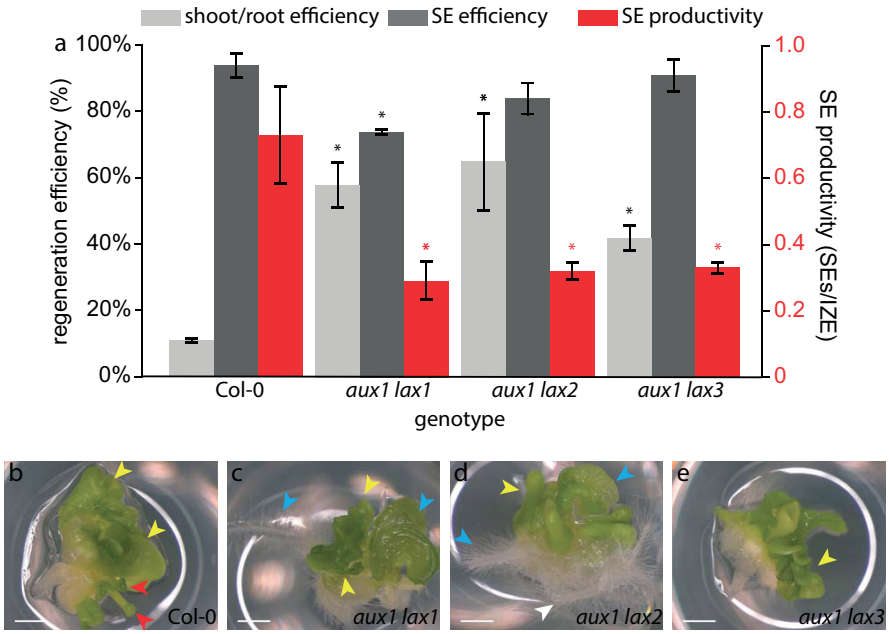

FIGURE 7 - Reduced SE and enhanced shoot/root regeneration in aux1 *lax* loss-of-function mutants.
a) Regeneration efficiencies in wild-type (Col-0), *aux1* lax1, *aux1 lax2,* and *aux1 lax3* IZEs. Bars represent shoot and root efficiency (light gray), SE efficiency (dark grey), and SE productivity (solid red) values of duplo experiments with n = 48. Error bars indicate the SEM. Asterisks denote statistical difference between wild-type control and mutant. For SE efficiency and productivity respectively a $\chi 2$ test and a Welch t-test were used ($p<0.05$) b-e). Phenotypes of b) Col-0 c) *aux1 lax1* d) *aux1 lax2* e) *aux1 lax3* IZEs after standard culture. Red arrow heads point at individual somatic embryos, yellow arrow heads point at embryogenic structures and blue arrow heads indicate shoot- or root-like structures. Scale bar represents 1mm.

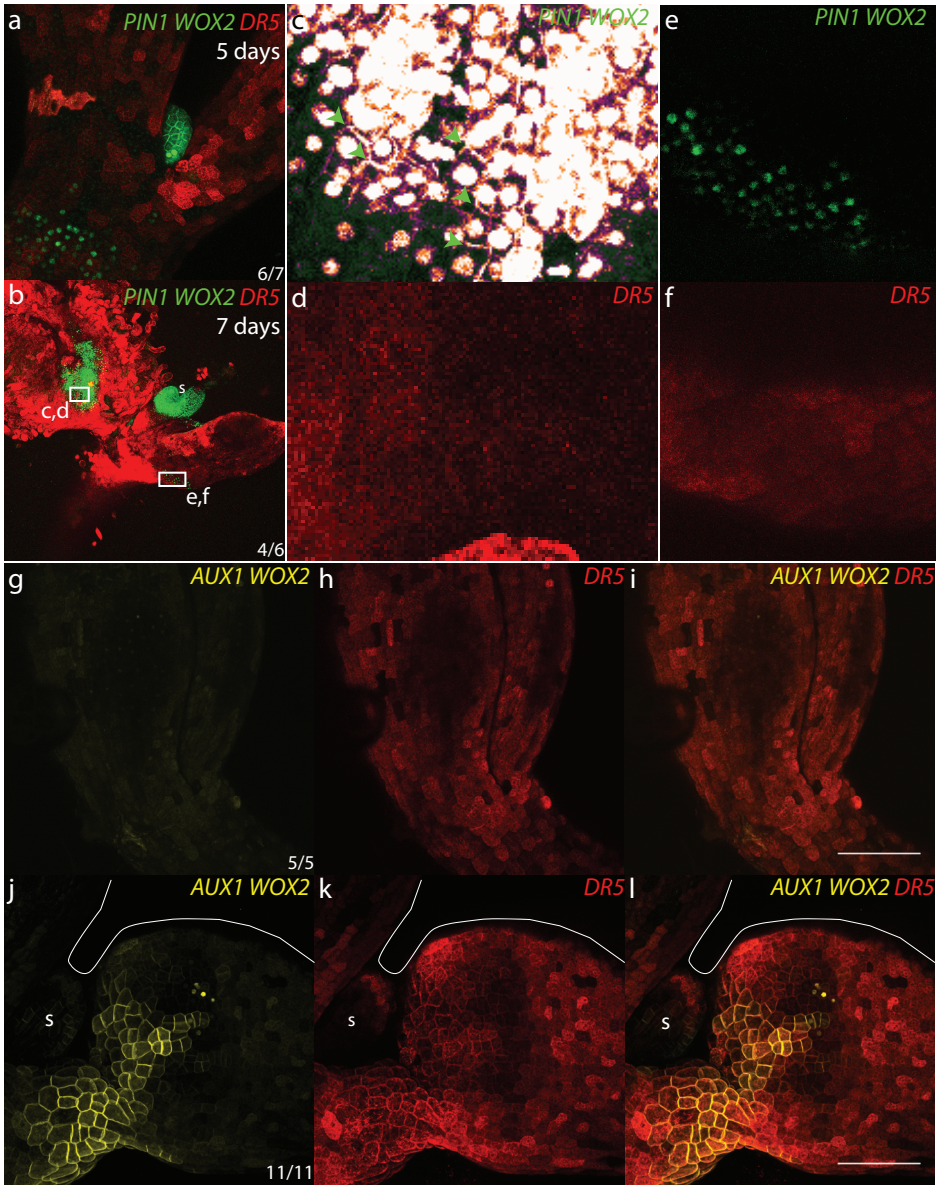

FIGURE 8 - Expression and localisation of PIN1 and AUX1 during 2,4-D induced SE initiation.
a-f) Representative CLSM images of *pPIN1::PIN1:GFP pWOX2::NLS-YFP DR5::RFP* IZEs cultured for a) 5 days and b) 7 days on SEIM. c-f) Enlargements of the boxed regions in (b) with c) a false coloured image of *PIN1* (localised on the membrane, green arrows) and *WOX2* (nuclear localisation) for enhanced contrast and d) *DR5*. e-f) is box 2 with e) *PIN1 WOX2* and f) *DR5*. *PIN1* and *WOX2* are in green, *DR5* in red. g-l) IZEs of *pAUX1::AUX1:YFP pWOX2::NLS-YFP DR5::RFP* cultured on SEIM for g-i) 3 days and j-l) 5 days. *AUX1* and *WOX2* in yellow and *DR5* in red. The shoot apical meristem is marked with an S, observation frequencies are indicated the bottom right corner, scale bar represents 100µm.

Auxin influx is needed to generate auxin response minimum for SE initiation

The previous results suggested that auxin efflux does not contribute to initiation of SE, but rather to the development of the somatic embryo similar to zygotic embryogenesis by establishing the embryo body pattern. To test this hypothesis we studied somatic embryo initiation events in the proximal region of cotyledons of *pPIN1::PIN1-GFP pWOX2::NLS-YFP DR5:RFP* IZEs after 5 and 7 days of culture on SEIM. On day 5, *PIN1::PIN1-GFP* expression was mostly observed in the SAM of the IZE and not in the *WOX2::NLS-YFP* expressing regions where somatic embryos were initiated (Figure 8a). On day 7, however, clusters of *PIN1::PIN1-GFP WOX2::NLS-YFP* positive cells could be observed, and *DR5::RFP* expression in these cell clusters was always low (Figure 8b,c,d). In some areas of low *DR5::RFP* expression we observed cell clusters showing weaker *WOX2::NLS-YFP* and no *PIN1::PIN1-GFP* expression (Figure 8e,f), similar to the *WOX2::NLS-YFP* clusters observed at day5 (Figure 8a). These results are in line with the NPA studies, and indicate that areas of low auxin response that seem to coincide with initiation of SE occur independent of *PIN1* expression, and that *PIN1* only becomes expressed at a later time point after SE initiation, where it is required for embryo patterning. In IZEs that combined the *pAUX1::AUX1:YFP* construct (Swarup et al., 2005) with the *WOX2::NLS-YFP* and *DR5::RFP* reporters no expression of *pAUX1::AUX1:YFP* nor *pWOX2::NLS-YFP* could be detected after 3 days on SEIM (Figure 8g-i). However, after 5 days on SEIM patches of *pAUX1::AUX1:YFP* expressing cells could be observed close to *pWOX2::NLS-YFP* marked cells (Figure 8j-l). The cells expressing *pWOX2::NLS-YFP* were present in low auxin zones, whereas the *pAUX1::AUX1:YFP* expressing cells were part of a zone with a relatively higher auxin response (Figure 8j-l). This finding supports our hypothesis that AUX1/LAX carriers cause local auxin minima in the cotyledons of the IZE resulting into initiation of SE marked by the expression of the *WOX2-YFP* reporter.

Discussion

Somatic embryogenesis is an important tissue culture tool that is used for the stable asexual propagation of economically important crops and ornamentals, and for studying the embryo initiation process for plant species with a long reproductive cycle. For many plant species SE can be induced by treatment of plant tissues with the synthetic auxin analog 2,4-D. Detailed knowledge on the molecular mechanism by which 2,4-D induces SE is lacking, and to gain more insight we optimized the *Arabidopsis* SE system that uses IZEs as explants (Gaj, 2011; Nowak et al., 2012), and studied the role of auxin transport in SE initiation.

A narrow time window for SE induction

Our results showed that the highest and most reproducible SE efficiencies could be obtained using IZEs synchronized in development by manual pollination, and preferably harvested at 12 dap. Opposed to what previous papers report (Luo and Koop, 1997; Gaj, 2004), we experienced that IZEs harvested at earlier time points do not survive when cultured on SEIM. Apparently, sufficient maturation of the IZE is important for its survival in tissue culture. Several lines of evidence back up this idea as the embryogenic capacity of tissues is enhanced by dehydration and osmotic stresses (Ikeda-Iwai et al., 2003; Gazzarrini et al., 2004). The well-known spontaneous SE phenotypes of seedlings ectopically expressing *LEC1*, *LEC2* or *FUS3* also support the idea that tissue maturation is a central mechanism in SE. These *LAFL* genes have initially been identified because of their role in seed maturation and their dependency on seed maturation hormone ABA. By ectopically expressing *LEC1*, *LEC2* and *FUS3*, the seedling development is arrested and most likely reverted to the embryo maturation phase, resulting in prolonged embryo identity and SE initiation (Stone et al., 2008; Junker et al., 2012; Su et al., 2012; Jia et al., 2013). In contrast to these systems, in our 2,4-D SE inducible system, in which SE efficiency is dependent on the age of the IZE, it is necessary to take other factors into account. One of them is, the maternal environment in which seeds develop, as it determines the vigour of the IZEs (Finch-Savage and Bassel, 2016). For reproducible SE efficiencies the growth conditions should therefore be kept constant.

With our optimised culture system we were able to show, using the *pWOX2::NLS-YFP* reporter as embryonic cell marker (Breuninger et al., 2008), that the first reversions from somatic to embryonic cell identity occurred between 5 and 7 days in culture. Our results showed that the development of the somatic embryo could be traced from single cells to globular shaped embryos and the earliest embryonic cell clusters could be observed after 5 days of 2,4-D induction. However, transfer to hormone free medium at this time point resulted in loss of *WOX2* expression and reverted the tissue to the germination programme. Thus there is a narrow time frame in which IZEs can be used as explants for SE efficiently, between 12 and 14 dap, and a minimum time of 5 days on SEIM is required to induce SE. Our system allows for studying real-time dynamic molecular responses as opposed to classic histology studies, which have relied on destructive methods (Raghavan, 2004; Bassuner et al., 2006; Kurczyńska et al., 2007; Soriano et al., 2013). Other reports have shown the use of the *WUSCHEL (WUS)* shoot apical meristem (SAM) stem cell fate reporter, as a marker for SE (Su and Zhang, 2009), but this reporter would only show cells that have already adapted the stem cell

fate (Mayer et al., 1998; Strable and Scanlon, 2016) and is therefore not accurate to identify the transition from late to early embryogenic cell fate.

An auxin minimum is compulsory for SE initiation

Previous reports have indicated that, similar to ZE, dynamic auxin responses starting with an auxin maximum are the main drivers of SE (Michalczuk et al., 1992; Pasternak, 2002; Gaj et al., 2005; Su et al., 2015). In line with these reports, by combining the *pWOX2::NLS-YFP* marker with the *DR5::RFP* auxin reporter, we were able to show that after 5 days of culture the overall auxin response in IZEs was elevated. Surprisingly, however, local auxin minima were established in which cells acquired embryo identity. Our results showed that PINs were not required for SE initiation and that the observed local auxin response minima were not produced by coordinated PIN mediated auxin efflux. This is contradictory to a previous hypothesis in which it was proposed that PIN1 mediates auxin from high to low areas in order to induce SE (Su et al., 2009). It is also in contrast to the auxin maximum marking the early embryo proper during ZE, and to the PIN generated auxin maxima that are initiation points for lateral organ development such as leaves and flowers on the shoot- or inflorescence meristems, and lateral roots on the root pericycle (Benková et al., 2003; Reinhardt et al., 2003). Treatment of IZEs with the polar auxin transport inhibitor NPA did result in aberrant, fused embryonic structures, indicating that, similar to ZE, PIN driven PAT is rather involved in development and patterning of the somatic embryo (Friml et al., 2003; Robert et al., 2013).

Interestingly, in contrast to auxin efflux, the AUX1/LAX auxin influx proteins appeared to be required for SE initiation. The role of AUX1/LAX is well established during root growth and development (Bennett et al., 1996;; Peret et al., 2012), in phyllotaxis (Reinhardt 2003; Bainbridge et al., 2008), and also in ZE (Robert et al., 2015b). However, except for recent evidence that *LAX3* is expressed during SE (Revalska et al., 2015), no role for the AUX1/LAX proteins during SE has yet been reported The proposed function of the AUX/LAX proteins is to keep auxin contained in cells, and recent auxin transport measurements confirmed an important role for AUX1/LAX proteins in loading auxin into the PAT system (Boot et al., 2016). Similarly, we hypothesize that the coordinated expression of AUX/LAX proteins keeps endogenous auxin contained in specific cells of the IZE, thereby enhancing auxin response in these cells and simultaneously causing an auxin response minimum in other regions of the IZE. In the absence of auxin minima in 1-NOA and 2,4-D treated IZEs, the balance shifted from SE to organ regeneration, which confirms the importance of auxin minima for the induction of embryonic cell identity, and is in line with the requirement of auxin maxima

for organ initiation (Benkova, et al., 2003, Reinhardt et al., 2003). We cannot point out AUX1/LAX-mediated auxin influx as the sole responsible mechanism for SE initiation. Evidence is emerging that oscillating auxin responses resulting from dynamic changes in auxin signalling, -biosynthesis or -metabolism contribute to organ initiation, meristem establishment and embryo patterning (Xuan et al., 2015; Wang et al., 2014; Robert et al., 2013).

Methods

Plant lines

All *Arabidopsis thaliana* lines described below are in Columbia (Col-0) background. The *pWOX2::NLS-YFP* line was kindly donated by Thomas Laux and is resistant to phosphinothricin (ppt) (Breuninger et al., 2008). The *DR5::RFP* line was donated by Eva Benkova and is resistant to hygromycin (hyg) (Marhavý et al., 2011). *AUX1::AUX1-YFP* harbours kanamycin (kan) resistance and was donated by Malcom Bennet (Swarup et al., 2005). *PIN1::PIN1-GFP* (kan) was a gift from Jiri Friml (Benková et al., 2003). The *aux1 lax* double mutants were a gift from Ranjan Swarup (Peret et al., 2012). The *aux1* mutation was verified by growing seedlings on 0.1µM 2,4-D and seedlings were selected based on their resistance to 2,4-D. The other mutations were confirmed by genotyping.

Genotyping

Sequences of DNA primers used for genotyping of the *aux lax* double mutants are in listed in Table S1. All PCR reactions were performed using DreamTaq DNA polymerase (ThermoFisher Scientific, EP0705) on genomic DNA isolated as described by Giraudat (2003), Tm = 61°C, and At = 60s, unless otherwise stated.

Tissue culture and growth conditions

Arabidopsis seeds were surface sterilized and germinated on MA medium (Masson and Paszkowski, 1992) complemented with 1% (w:v) sucrose, and 0.8% (w:v) Daishin agar, pH5.8. For antibiotic selection ppt, hyg or kan was added to the medium after autoclaving at a final concentration of 20mg/mL for ppt and hyg, and of 50mg/mL for kan. Seven to ten days after germination (dag), seedlings were transferred to a mixture of soil and sand, 2 per pot, and grown under a 16hr. photoperiod and 70% relative humidity. IZEs were harvested from plants 1-2 weeks after flowering. The siliques were surface sterilized with a 20% bleach/70% ethanol solution for 5min. and rinsed at least three times with sterile water.

SE-inducing medium (SEIM) consisted of B5 medium, with 4.5µM 2,4-D, 2% (w:v) sucrose and 0.8% (w:v) Daishin agar (Gaj, 2011; Nowak et al., 2012). Hormone free medium was MA medium (Masson and Paszkowski, 1992). Media were sterilized by autoclaving at 120°C for 20min. SE was performed in sterile 48-wells plates (Greiner cellstar art. nr. 677180) that were filled with 400µL SEIM or hormone free medium using a repeater pipet. IZEs were placed on SEIM (one per well) and incubated overnight at 4°C in the dark followed by incubation at 21°C under a 16hr photoperiod for a standard period of 14 days, followed by 7 days incubation on hormone free medium (standard SE culture). NPA (CAS 132-66-1) and 1-NOA (CAS 2976-75-1) were ordered from Sigma and were added to SEIM from a 50mM stock solution in DMSO to a final concentration of 100µM.

For the inhibitor and phenotypic studies, IZEs synchronized in their developmental stage were obtained by manual pollination. For this purpose, the 2 or 3 oldest, but still closed, flower buds of primary inflorescence stems were emasculated and pollinated and 12 days after pollination (dap) IZEs were excised from the ovule using a dissecting microscope. Per two parent plants, 2-3 sets of 2-3 closed flower buds were emasculated.

To keep data comparable between inhibitor experiments, large-scale experiments were set up as follows: each replicate consisted of 100µM NPA, 100µM 1-NOA and control treatments with 2,4-D induction periods for 0, 3 and 5 days. Per treatment, 48 IZEs were used, one IZE per well in a 48-wells plate. For the 3 and 5 days induction, a large pool of IZEs was cultured in multiple 48-wells plates. At day 3 and day 5 48 IZEs were selected randomly out of the different plates for each treatment and transferred to plates containing 2,4-D and 100µM inhibitor. The day 0 treatments were set up differently: 1 silique was used to take 12 IZEs for each treatment; this required 4 siliques in total to compile 1 plate per treatment.

The mutant studies were performed by culturing 48 IZEs per genotype in duplicates.

For confocal or light microscopy analysis non-synchronized late IZEs from more or less the same developmental stage were selected based on their size as described by (Gaj, 2011). Broken or damaged IZEs were discarded and not used.

Statistics of somatic embyogenesis

To quantify SE, four categories were used to score 1) embryogenic tissue (also referred to as embryogenic callus), if no individual somatic embryos were found but embryogenic tissue developed. Embryogenic tissue was defined as smooth green structures without trichomes, that either looked like fused cotyledons or like fused zygotic embryos 2) SE forming IZEs, if individual somatic embryos

were observed that were attached to the IZE by their root pole. In that case, the number of individual somatic embryos was counted. 3) Non-embryogenic callus forming IZEs, if callus was formed that remained white-yellowish without developing somatic embryos or embryogenic tissue 4) Dead IZEs that turned white, if the tissue turned white, showed no growth and maintained their original size.

Category 1 and 2 were merged to quantify the number of responding IZEs that produced embryogenic tissue. The SE efficiency was then calculated as (Luo and Koop, 1997)

$$SE\ efficiency = \frac{N_r}{N_t} \quad 100\%$$

N_r = the number of responding explants. N_t = total number of explants tested.

SE productivity was calculated as

$$SE\ productivity = \frac{N_i}{N_t}$$

N_i = the number of individual somatic embryos observed. N_t = the total number of IZEs that were tested (including the ones that died).

Statistics for SE efficiency were performed in Microsoft Excel, using the χ^2-test for association (Holmes et al., 2011). For SE productivity, a Welch *t*-test was performed in Rstudio (Pace, 2015).
For inhibitor studies we compared the control treatments to check whether refreshment of SEIM would contribute to SE efficiency and productivity. The two controls were not statistically different for SE efficiency and productivity (respectively χ^2_{calc}=2.9, and *t*-test p-value 0.524, described in Chapter 2) and for this reason we performed all statistical tests between the treatment and the 0 days control.

Microscopy

Confocal Laser Scanning Microscopy (CLSM) was performed with a ZEISS LSM510 exciter equipped with argon and helium/neon lasers. GFP and YFP were detected using a 488nm band pass filter for excitation and a 500-530nm band pass (BP) filter for emission. Simultaneously, chlorophyll background fluorescence was captured with a long pass (LP) 650nm emission filter. RFP was excited at 530nm and was captured with a BP 550-600nm emission filter. Images were captured with ZEISS ZEN2009 software. Samples were prepared on a microscope slide by

embedding IZEs in a thin layer of 0.5% low melting point agarose, and adding a droplet of water before covering with a cover slip.
Phenotype images were obtained using a Leica DC 500 stereomicroscope with the Leica Application Suite v2.8.1 software or with a MRc5 (ZEISS) microscope with DIC/Nomarski ZEISS AxioCam using AxioVision40 V4.7.2.0 software.

Acknowledgements

C.P. was supported by an NWO-TTI-Green Genetics core project grant (NWO 828.11.004) to R.O. from the Earth and Life Sciences Division with financial support from the Netherlands Organisation for Scientific Research (NWO). We thank Gerda Lamers for her help with microscopy.

Supplemental Information

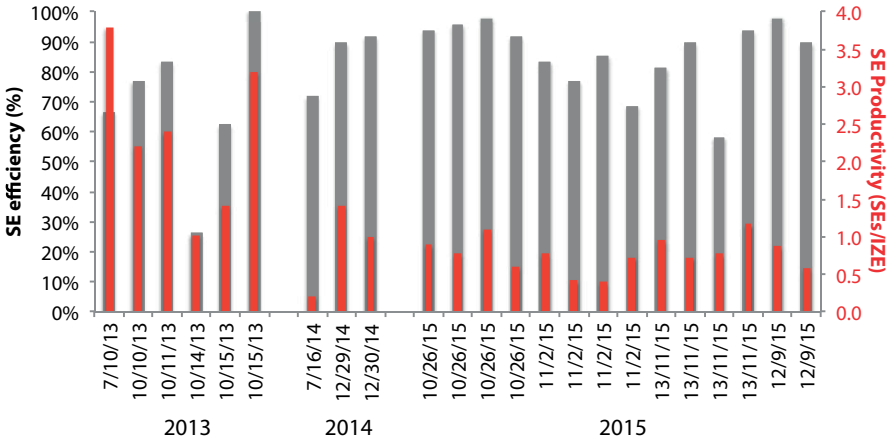

FIGURE S1 - Variation in SE efficiency and SE productivity. Per experiment SE efficiency (grey bars and left axis) and SE productivity (red bars and right axis) are indicated. Values are given for experiments in the course of 2013, 2014 and 2015.

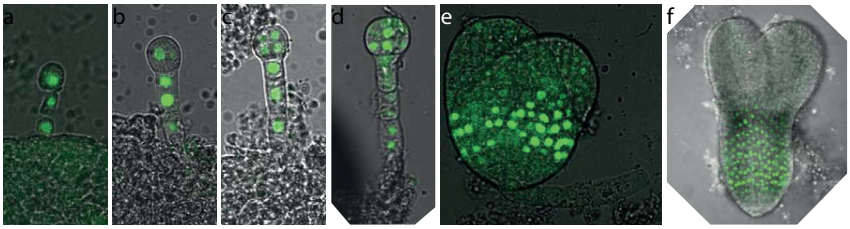

FIGURE S2 - Expression pattern of the embryo cell fate marker WOX2-YFP in Arabidopis. Representative CSLM images of pWOX2::NLS-YFP (green) in the 1-cellstage (a), 2-cell stage (b), octant- cell stage (c), early globular stage (d), late heart stage (e), torpedo stage (f). WOX2-YFP was observed from the zygotic stage onwards, in the entire embryo and suspensor. In later stages, expression diminishes and becomes limited to the hypocotyl area.

TABLE S1 - Primer sequences for genotyping. GSP is gene specific primer, BP is border specific primer. All reactions were carried out with genomic DNA, DreamTaq polymerase, Tm = 61°C, At = 60s, unless otherwise stated.

GENE	PRIMER ORIENTATION	SEQUENCE (5' - 3')	REMARKS
lax1	GSP left	ATATGGTTGCAGGTGGCACA	
	GSP right	GTAACCGGCAAAAGCTGCA	
	Border	AAGCACGACGGCTGTAGAATAG	in combination with GSP left primer for transposon insertion
lax2	GSP left	ATGGAGAACGGTGAGAAAGCAGC	
	GSP right	CGCAGAAGGCAGCGTTAGCG	
	Border	AAGCACGACGGCTGTAGAATAG	in combination with GSP left primer for transposon insertion
lax3	GSP left	TACTTCACCGGAGCCACCA	
	GSP right	TGATTGGTCC GAAAAAGG	
	Border	AAGCACGACGGCTGTAGAATAG	in combination with GSP left primer for transposon insertion

References

Arnold, S. von, Sabala, I., Bozhkov, P., Dyachok, J., and Filonova, L. (2002). Developmental pathways of somatic embryogenesis. Plant Cell. Tissue Organ Cult. **69**: 233–249.

Bainbridge, K., Guyomarc'h, S., Bayer, E., Swarup, R., Bennett, M., Mandel, T., and Kuhlemeier, C. (2008). Auxin influx carriers stabilize phyllotactic patterning. Genes Dev. **22**: 810–823.

Bairu, M.W., Aremu, A.O., and van Staden, J. (2011). Somaclonal variation in plants: causes and detection methods. Plant Growth Regul. **63**: 147–173.

Bassuner, B.M., Lam, R., Lukowitz, W., and Yeung, E.C. (2006). Auxin and root initiation in somatic embryos of *Arabidopsis*. Plant Cell Rep. **26**: 1–11.

Benková, E., Michniewicz, M., Sauer, M., Teichmann, T., Seifertová, D., Jürgens, G., and Friml, J. (2003). Local, efflux-dependent auxin gradients as a common module for plant organ formation. Cell **115**: 591–602.

Blilou, I., Xu, J., Wildwater, M., Willemsen, V., Paponov, I., Friml, J., Heidstra, R., Aida, M., Palme, K., and Scheres, B. (2005). The PIN auxin efflux facilitator network controls growth and patterning in *Arabidopsis* roots. Nature **433**: 39–44.

Boot, K.J.M., Hille, S.C., Libbenga, K.R., Peletier, L.A., van Spronsen, P.C., van Duijn, B., and Offringa, R. (2015). Modelling the dynamics of polar auxin transport in inflorescence stems of *Arabidopsis* thaliana. J. Exp. Bot. **67:** 649-666.

Boutilier, K., Offringa, R., Sharma, V.K., Kieft, H., Ouellet, T., Zhang, L., Hattori, J., Liu, C., van Lammeren, A.A.M., Miki, B.L.A., Custers, J.B.M., and van Lookeren Campagne, M.M. (2002). Ectopic expression of *BABY BOOM* triggers a conversion from vegetative to embryonic growth. Plant Cell **14**: 1737–1749.

Breuninger, H., Rikirsch, E., Hermann, M., Ueda, M., and Laux, T. (2008). Differential expression of WOX Genes mediates apical-basal axis formation in the *Arabidopsis* embryo. Dev. Cell **14**: 867–876.

Cheng, Y. (2006). Auxin biosynthesis by the YUCCA flavin monooxygenases controls the formation of floral organs and vascular tissues in *Arabidopsis*. Genes Dev. **20**: 1790–1799.

FAO (2015). 2014 Global forest products facts and figures. Food Agric. Organ. United Nations: 1–17.

Fehér, A. (2015). Somatic embryogenesis — Stress-induced remodeling of plant cell fate. Biochim. Biophys. Acta - Gene Regul. Mech. **1849**: 385–402.

Finch-Savage, W.E. and Bassel, G.W. (2016). Seed vigour and crop establishment: extending performance beyond adaptation. J. Exp. Bot. **67**: 567–591.

Friml, J., Benková, E., Blilou, I., Wisniewska, J., Hamann, T., Ljung, K., Woody, S., Sandberg, G., Scheres, B., and Jürgens, G. (2002). AtPIN4 mediates sink-driven auxin gradients and root patterning in *Arabidopsis*. Cell **108**: 661–673.

Friml, J., Vieten, A., Sauer, M., Weijers, D., Schwarz, H., Hamann, T., Offringa, R., and Jürgens, G. (2003). Efflux-dependent auxin gradients establish the apical-basal axis of *Arabidopsis*. Nature **426**: 147–153.

Gaj, M.D. (2001). Direct somatic embryogenesis as a rapid and efficient system for in vitro regeneration of *Arabidopsis* thaliana. Plant Cell. Tissue Organ Cult. **64**: 39–46.

Gaj, M.D. (2004). Factors influencing somatic embryogenesis induction and plant regeneration with particular reference to *Arabidopsis* thaliana (L.) Heynh. Plant Growth Regul. **43**: 27–47.

Gaj, M.D. (2011). Somatic embryogenesis and plant regeneration in the culture of *Arabidopsis thaliana* (L.) Heynh. immature zygotic embryos. Methods **710**: 257–265.

Gaj, M.D., Zhang, S., Harada, J.J., and Lemaux, P.G. (2005). Leafy cotyledon genes are essential for induction of somatic embryogenesis of *Arabidopsis*. Planta **222**: 977–988.

Ganguly, A., Park, M., Kesawat, M.S., and Cho, H.-T. (2014). Functional analysis of the hydrophilic loop in intracellular trafficking of *Arabidopsis* PIN-FORMED proteins. Plant Cell **26**: 1570–1585.

Gazzarrini, S., Tsuchiya, Y., Lumba, S., Okamoto, M., and McCourt, P. (2004). The transcription factor *FUSCA3* controls developmental timing in *Arabidopsis* through the hormones gibberellin and abscisic acid. Dev. Cell **7**: 373–385.

Geisler, M. and Murphy, A.S. (2006). The ABC of auxin transport: The role of p-glycoproteins in plant development. FEBS Lett. **580**: 1094–1102.

Giraudat, J. (2003). Practical course on genetic and molecular analysis of *Arabidopsis*. In EMBO course, J. Giraudat, ed (EMBO), pp. 1–21.

Goldsmith, M.H.M. (1977). The polar transport of auxin. Annu. Rev. Plant Physiol. **28**: 439–478.

Haecker, A., Gross-Hardt, R., Geiges, B., Sarkar, A., Breuninger, H., Herrmann, M., and Laux, T. (2004). Expression dynamics of *WOX* genes mark cell fate decisions during early embryonic patterning in *Arabidopsis thaliana*. Development **131**: 657–668.

Hardtke, C.S. and Berleth, T. (1998). The *Arabidopsis* gene *MONOPTEROS* encodes a transcription factor mediating embryo axis formation and vascular development. EMBO J. **17**: 1405–1411.

Heisler, M.G., Ohno, C., Das, P., Sieber, P., Reddy, G. V, Long, J. A, and Meyerowitz, E.M. (2005). Patterns of auxin transport and gene expression during primordium development revealed by live imaging of the *Arabidopsis* inflorescence meristem. Curr. Biol. **15**: 1899–1911.

Holmes, D., Moody, P., and Dine, D. (2011). Research methods for biosciences 2nd ed. O. university Press, ed (Oxford University Press).

Ikeda-Iwai, M., Umehara, M., Satoh, S., and Kamada, H. (2003). Stress-induced somatic embryogenesis in vegetative tissues of *Arabidopsis thaliana*. Plant J. **34**: 107–114.

Jia, H., McCarty, D.R., and Suzuki, M. (2013). Distinct roles of *LAFL* network genes in promoting the embryonic seedling fate in the absence of *VAL* repression. Plant Physiol. **163**: 1293–1305.

Jiménez, V.M. (2005). Involvement of plant hormones and plant growth regulators on in vitro somatic embryogenesis. Plant Growth Regul. **47**: 91–110.

Jones, A.R., Kramer, E.M., Knox, K., Swarup, R., Bennett, M.J., Lazarus, C.M., Leyser, H.M.O., and Grierson, C.S. (2009). Auxin transport through non-hair cells sustains root-hair development. Nat. Cell Biol. **11**: 78–84.

Junker, A. Mönke, G., Rutten, T., Keilwagen, J., Seifert., Thi, T.M.N., Renou, J., Balzergue, S., Viehöver, P., Hähnel, U., Ludwig-Müller, J., Altschmied, L., Conrad, U., Weisshaar, B., and Bäumlein, H. (2012). Elongation-related functions of *LEAFY COTYLEDON1* during the development of *Arabidopsis thaliana*. Plant J. **71**: 427–442.

Kurczyńska, E.U., Gaj, M.D., Ujczak, A., and Mazur, E. (2007). Histological analysis of direct somatic embryogenesis in *Arabidopsis thaliana* (L.) Heynh. Planta **226**: 619–628.

Lotan, T., Ohto, M., Yee, K.M., West, M. A, Lo, R., Kwong, R.W., Yamagishi, K., Fischer, R.L., Goldberg, R.B., and Harada, J.J. (1998). *Arabidopsis LEAFY COTYLEDON1* is sufficient to induce embryo development in vegetative cells. Cell **93**: 1195–1205.

Luo, Y. and Koop, H.U. (1997). Somatic embryogenesis in cultured immature zygotic embryos and leaf protoplasts of *Arabidopsis thaliana* ecotypes. Planta **202**: 387–96.

Luschnig, C., Gaxiola, R.A., Grisafi, P., and Fink, G.R. (1998). EIR1, a root specific protein involved in auxin transport, is required for gravitropism in *Arabidopsis* thaliana. Genes Dev. **12**: 2175–2187.

Marchant, A., Bhalerao, R., Casimiro, I., Eklöf, J., Casero, P.J., Bennett, M., and Sandberg, G. (2002). AUX1 promotes lateral root formation by facilitating indole-3-acetic acid distribution between sink and source tissues in the *Arabidopsis* seedling. Plant Cell **14**: 589–97.

Marhavý, P., Bielach, A., Abas, L., Abuzeineh, A., Duclercq, J., Tanaka, H., Pařezová, M., Petrášek, J., Friml, J., Kleine-Vehn, J., and Benková, E. (2011). Cytokinin modulates endocytic trafficking of PIN1 auxin efflux carrier to control plant organogenesis. Dev. Cell **21**: 796–804.

Marhavý, P., Vanstraelen, M., De Rybel, B., Zhaojun, D., Bennett, M.J., Beeckman, T., and Benková, E. (2013). Auxin reflux between the endodermis and pericycle promotes lateral root initiation. EMBO J. **32**: 149–158.

Mayer, K.F.X., Schoof, H., Haecker, A., Lenhard, M., Jürgens, G., and Laux, T. (1998). Role of *WUSCHEL* in regulating stem cell fate in the *Arabidopsis* shoot meristem. Cell **95**: 805–815.

Michalczuk, L., Ribnicky, D.M., Cooke, T.J., and Cohen, J.D. (1992). Regulation of indole-3-acetic acid biosynthetic pathways in carrot cell cultures. Plant Physiol. **100**: 1346–1353.

Mravec, J., Petr Skupa, Bailly, A., Hoyerova, K., Křeček, Bielach, A., Petrášek, J., Zhang, J., Gaykova, V., Stierhof, Y-D., Dobrev P.I., Schwarzerova, K., Rolčík, J., Seifertová, D., Luschnig, C., Benková, E., Zažímalova, E., Geisler, M., Friml, J. (2009). Subcellular homeostasis of phytohormone auxin is mediated by the ER-localized PIN5 transporter. Nature **459**: 1136–1140.

Mravec, J., Kubes, M., Bielach, A., Gaykova, V., Petrásek, J., Skůpa, P., Chand, S., Benková, E., Zazímalová, E., and Friml, J. (2008). Interaction of PIN and PGP transport mechanisms in auxin distribution-dependent development. Development **135**: 3345–3354.

Noh, B., Murphy, A.S., and Spalding, E.P. (2001). Multidrug resistance-like genes of *Arabidopsis* required for auxin transport and auxin-mediated development. Plant Cell **13**: 2441–2454.

Nowak, K., Wojcikowska, B., Szyrajew, K., and Gaj, M.D. (2012). Evaluation of different embryogenic systems for production of true somatic embryos in *Arabidopsis*. Biol. Plant. **56**: 401–408.

Pace, L. (2015). Beginning R: an introduction to statistical programming (Apress).

Parry, G., Delbarre, A., Marchant, A., Swarup, R., Napier, R., Perrot-Rechenmann, C., and Bennett, M.J. (2001). Novel auxin transport inhibitors phenocopy the auxin influx carrier mutation aux1. Plant J. **25**: 399–406.

Pasternak, T.P. (2002). The role of auxin, pH, and stress in the activation of embryogenic cell division in leaf protoplast-derived cells of Alfalfa. Plant Physiol. **129**: 1807–1819.

Péret, B., Swarup, K., Ferguson, A., Seth, M., Yang, Y., Dhondt, S., James, N., Casimiro, I., Perry, P., Syed, A., Yang, H., Reemmer, J., Venison, E., Howells, C., Perez-Amador, M-A., Yun, J., Alonso, J., Beemster, G.T.S., Laplaze, L., Murphy, A., Bennett, M.J., Nielsen, E., and Swarup, R. (2012). AUX/LAX genes encode a family of auxin influx transporters that perform distinct functions during *Arabidopsis* development. Plant Cell **24**: 2874–2885.

Petrášek, J., Mravec, J., Bouchard, R., Blakeslee, J.J., Abas, M., Seifertová , D., Wiśniewska, J., Tadele, Z., Kubeš, M., Cővanová., M., Dhonukshe, P., Skupa, P., Benková, E., Perry, L., Křeček, P., Lee, O.K.., Fink, G.R., Geisler, M., Murphy, A.S., Luschnig, L., Zažímalova, E., and Friml, J. (2006). PIN proteins perform a rate-limiting function in cellular auxin efflux. Science **312**: 914–918.

Petrásek, J. and Friml, J. (2009). Auxin transport routes in plant development. Development **136**: 2675–88.

Pupilli, F. and Barcaccia, G. (2012). Cloning plants by seeds: inheritance models and candidate genes to increase fundamental knowledge for engineering apomixis in sexual crops. J. Biotechnol. **159**: 291–311.

Rademacher, E.H., Lokerse, A.S., Schlereth, A., Llavata-Peris, C., Bayer, M., Kients, M., Rios, A.F., Borst, J.W., Lukowitz, W., Jürgens, G., and Weijers, D. (2012). Different auxin response machineries control distinct cell fates in the early plant embryo. Dev. Cell **22**: 211–222.

Raghavan, V. (2004). Role of 2,4-dichlorophenoxyacetic acid (2,4-D) in somatic embryogenesis on cultured zygotic embryos of *Arabidopsis*: cell expansion, cell cycling, and morphogenesis during continuous exposure of embryos to 2,4-D. Am. J. Bot. **91**: 1743–1756.

Raven, J.A. (1975). Transport of indoleacetic acid in plant cells in relation to pH and electrical potential gradients, and its significance for polar IAA transport. New Phytol.: 163–172.

Reinhardt, D., Mandel, T., and Kuhlemeier, C. (2000). Auxin regulates the initiation and radial position of plant lateral organs. Plant Cell **12**: 507–518.

Reinhardt, D., Pesce, E.-R., Stieger, P., Mandel, T., Baltensperger, K., Bennett, M., Traas, J., Friml, J., and Kuhlemeier, C. (2003). Regulation of phyllotaxis by polar auxin transport. Nature **426**: 255–260.

Revalska, M., Vassileva, V., Zechirov, G., and Iantcheva, A. (2015). Is the auxin influx carrier *LAX3* essential for plant growth and development in the model plants *Medicago truncatula*, *Lotus japonicus* and *Arabidopsis thaliana* Biotechnol. Biotechnol. Equip. **29**: 786–797.

Robert, H.S., Crhak Khaitova, L., Mroue, S., and Benkova, E. (2015a). The importance of localized auxin production for morphogenesis of reproductive organs and embryos in *Arabidopsis*. J. Exp. Bot. **66**: 5029–5042.

Robert, H.S., Grunewald, W., Sauer, M., Cannoot, B., Soriano, M., Swarup, R., Weijers, D., Bennett, M., Boutilier, K., and Friml, J. (2015b). Plant embryogenesis requires AUX/LAX-mediated auxin influx. Development **142**: 702–711.

Robert, H.S., Grones, P., Stepanova, A.N., Robles, L.M., Lokerse, A.S., Alonso, J.M., Weijers, D., and Friml, J. (2013). Local auxin sources orient the apical-basal axis in *Arabidopsis* embryos. Curr. Biol. **23**: 2506–2512.

Rubery, P.H. and Sheldrake, A.R. (1974). Carrier-mediated auxin transport. Planta **118**: 101–121.

Sawchuk, M.G., Edgar, A., and Scarpella, E. (2013). Patterning of leaf vein networks by convergent auxin transport pathways. PLoS Genet. **9**: e1003294.

De Smet, I., Tetsumura, T., De Rybel, B., Frei dit Frey, N., Laplaze, L., Casimiro, I., Swarup, R., Naudts, M., Vanneste, S., Audenaert, D., Inzé, D., Bennet, M.J., and Beeckman, T. (2007). Auxin-dependent regulation of lateral root positioning in the basal meristem of *Arabidopsis*. Development 134: 681–690.

Soriano, M., Li, H., and Boutilier, K. (2013). Microspore embryogenesis: establishment of embryo identity and pattern in culture. Plant Reprod. **26**: 181–196.

Stone, S.L., Braybrook, S. a, Paula, S.L., Kwong, L.W., Meuser, J., Pelletier, J., Hsieh, T.-F., Fischer, R.L., Goldberg, R.B., and Harada, J.J. (2008). *Arabidopsis LEAFY COTYLEDON2* induces maturation traits and auxin activity: Implications for somatic embryogenesis. Proc. Natl. Acad. Sci. **105**: 3151–3156.

Stone, S.L., Kwong, L.W., Yee, K.M., Pelletier, J., Lepiniec, L., Fischer, R.L., Goldberg, R.B., and Harada, J.J. (2001). *LEAFY COTYLEDON2* encodes a B3 domain transcription factor that induces embryo development. Proc. Natl. Acad. Sci. USA **98**: 11806–11811.

Strable, J. and Scanlon, M.J. (2016). Meristems take their cues from organ primordia. Nat. Genet. **48**: 704–705.

Su, Y.H., Liu, Y.B., Bai, B., and Zhang, X.S. (2015). Establishment of embryonic shoot-root axis is involved in auxin and cytokinin response during *Arabidopsis* somatic embryogenesis. Front. Plant Sci. **5**: 1–9.

Su, Y.H., Su, Y.X., Liu, Y.G., and Zhang, X.S. (2012). Abscisic acid is required for somatic embryo initiation through mediating spatial auxin response in *Arabidopsis*. Plant Growth Regul.

Su, Y.H. and Zhang, X.S. (2009). Auxin gradients trigger de novo formation of stem cells during somatic embryogenesis. Plant Signal. Behav. **4**: 574–576.

Su, Y.H., Zhao, X.Y., Liu, Y.B., Zhang, C.L., O'Neill, S.D., and Zhang, X.S. (2009). Auxin-induced *WUS* expression is essential for embryonic stem cell renewal during somatic embryogenesis in *Arabidopsis*. Plant J. **59**: 448–60.

Swarup, K., Benková, E., Swarup, R., Casimiro, I., Péret, B., Yang, Y., Parry, G., Nielsen, E., De Smet, I., Vanneste, S., Levesque, M.P., Carrier, D., James, N., Calvo, V., Ljung, K., Kramer, E., Roberts, R., Graham, N., Marillonnet, S., Patel, K., Jones, J.D.G., Taylor, G., Schachtman, D.P., May, S., Sandberg, G., Benfey, P., Friml, J., Kerr, I., Beeckman, T., Laplaze, L., and Bennet, M.J. (2008). The auxin influx carrier LAX3 promotes lateral root emergence. Nat. Cell Biol. **10**: 946–954.

Swarup, R., Friml, J., Marchant, A., Ljung, K., Sandberg, G., Palme, K., and Bennett, M. (2001). Localization of the auxin permease AUX1 suggests two functionally distinct hormone transport pathways operate in the *Arabidopsis* root apex. Genes Dev. **15**: 2648–2653.

Swarup, R., Kramer, E.M., Perry, P., Leyser, O., Knox, K., Beemster, G.T.S., Haseloff, J., Bhalerao, R., and Bennett, M.J. (2005). Root gravitropism requires lateral root cap and epidermal cells for transport and response to a mobile auxin signal. Nat. Cell Biol. **7**: 1057–1065.

Swarup, R. and Péret, B. (2012). *AUX/LAX* family of auxin influx carriers—an overview. Front. Plant Sci. **3**: 1–11.

Timmis, R. (1998). Bioprocessing for tree production in the forest industry: conifer somatic embryogenesis. Biotechnol. Prog. **14**: 156–166.

Ugartechea-Chirino, Y., Swarup, R., Swarup, K., Péret, B., Whitworth, M., Bennett, M., and Bougourd, S. (2010). The *AUX1/LAX* family of auxin influx carriers is required for the establishment of embryonic root cell organization in *Arabidopsis thaliana*. Ann. Bot. **105**: 277–289.

Ulmasov, T., Murfett, J., Hagen, G., and Guilfoyle, T.J. (1997). Aux/IAA proteins repress expression of reporter genes containing natural and highly active synthetic auxin response elements. Plant Cell **9**: 1963–71.

Wang, Q., Kohlen, W., Rossmann, S., Vernoux, T., and Theres, K. (2014). Auxin depletion from the leaf axil conditions competence for axillary meristem formation in *Arabidopsis* and *Tomato*. Plant Cell **26**: 2068–2079.

Weijers, D., Sauer, M., Meurette, O., Friml, J., Ljung, K., Sandberg, G., Hooykaas, P., and Offringa, R. (2005). Maintenance of embryonic auxin distribution for apical-basal patterning by PIN-FORMED-dependent auxin transport in *Arabidopsis*. Plant Cell **17**: 2517–2526.

Weijers, D., Schlereth, A., Ehrismann, J.S., Schwank, G., Kientz, M., and Jürgens, G. (2006). Auxin triggers transient local signaling for cell specification in *Arabidopsis* embryogenesis. Dev. Cell **10**: 265–270.

Wisniewska, J. (2006). Polar PIN localization directs auxin flow in plants. Science (80-.). **312**: 883–883.

Xuan, W., Audenaert, D., Parizot, B., Möller, B.K., Njo, M.F., De Rybel, B., De Rop, G., Van Isterdael, G., Mähönen, A.P., Vanneste, S., and Beeckman, T. (2015). Root cap-derived auxin pre-patterns the longitudinal axis of the *Arabidopsis* root. Curr. Biol. **25**: 1381–1388.

Zuo, J., Niu, Wu, Q.-W., Frugis, G., and Chua, N-H. (2002). The *WUSCHEL* gene promotes vegetative-to-embryonic transition in *Arabidopsis*. Plant J. **30**: 349–359.

Chapter 3

Auxin dynamics during SE initiation is established by the tryptophan-dependent indole-3-pyruvic acid pathway in *Arabidopsis*.

Cheryl Philipsen[1],
Kadir Akdeniz[1,3],
Paulina Zwijnenburg[1],
Remko Offringa[1]

[1] *Molecular and Developmental Genetics, Institute of Biology Leiden, Leiden University, Sylviusweg 72, 2333BE, Leiden, the Netherlands*
[2] *Current affiliation: Dümmen Orange, P.O. Box 26, 2678ZG, de Lier, the Netherlands*
[3] *Current affiliation: Erasmus MC, 's-Gravendijkwal 230, 3015 CE Rotterdam*

Abstract

Somatic embryogenesis (SE) in *Arabidopsis* can be efficiently induced by treatment of immature zygotic embryos (IZEs) with the synthetic auxin analog 2,4-dichlorophenoxyacetic acid (2,4-D). The exact involvement of the natural auxin, indole acetic acid (IAA), and its biosynthesis in 2,4-D-induced SE initiation is yet to be solved. IAA is mostly produced in the root and shoot apical meristem via L-tryptophan (Trp)-dependent or -independent pathways. The best-characterized Trp-dependent pathway is the indole-3-pyruvic acid (IPyA) pathway, which includes two enzymatic steps that successively convert Trp into IPyA and IPyA to IAA. The first step comprises the TRYPTOPHAN AMINOTRANSFERASE OF ARABIDOPSIS1 / TRYPTOPHAN AMINOTRANSERASE RELATED1-4 (TAA1/TAR1-4) family of enzymes. The second step includes the YUCCA1-11 (YUC1-11) family enzymes. We used combinations of chemical biology, genetics and reporter studies to unravel the Trp-dependent pathway during 2,4-D induced SE initiation. Our results suggest that YUC activity is rather required for development of the embryo and that TAA1/TARs are required to establish a dynamic auxin response to initiate SE.

Introduction

The plant hormone auxin, or indole-3-acetic acid (IAA), controls many aspects of plant development, from early zygotic embryogenesis to later patterning events such as leaf venation and phyllotaxis (Sawchuk and Scarpella, 2015; Reinhardt et al., 2003). The discovery of auxin, its activity and auxin-like compounds have led to the application and many uses of auxins in research and tissue culture (De Rybel et al., 2009; Song, 2014). The natural auxins IAA and indole-butyric-acid (IBA) and synthetic auxin analogs 1-naphthaleneacetic acid (1-NAA) and 2,4-dichlorophenoxyacetic acid (2,4-D) are abundantly used in tissue culture to induce rooting on plant cuttings, or to obtain plant regeneration by induction of callus, shoots or even embryos on vegetative plant tissues (Gaj, 2001; Su and Zhang, 2014). The latter process, referred to as somatic embryogenesis, in most cases requires long-term incubation of competent plant tissues on 2,4-D (Su and Zhang, 2014). In *Arabidopsis*, somatic embryos can be efficiently induced by incubating immature zygotic embryos on 2,4-D-containing SE induction medium (SEIM). Although this protocol was established some time ago (Gaj, 2001; Nowak et al., 2012), the mechanism by which 2,4-D induces SE initiation and acts on endogenous IAA biosynthesis in this process, has not been elucidated yet. Studies on the effect of 2,4-D on plant cells and tissues show that the auxin response is elevated (Pasternak, 2002; Michalczuk et al., 1992; Simon et al., 2013; Song, 2014) and in Chapter 2 we have shown that prior to SE initiation the auxin response is elevated followed by a local minimum in foci of embryogenic cells. This chapter focuses on the role of auxin biosynthesis in causing the subsequent 2,4-D-induced auxin response maxima and minima that lead to SE.

Auxin responses are tightly controlled by its biosynthesis and metabolism, transport and signaling. Auxin is produced mainly in developing tissues in the shoot and root and through polar auxin transport IAA is redistributed from the source to locations where IAA is required to steer plant development (Robert et al., 2015). Research in *Arabidopsis* and *Zea mays* (maize) has uncovered several IAA biosynthesis routes, which fall into two categories: the tryptophan (Trp)-dependent and the Trp-independent routes. Four Trp-dependent pathways have been uncovered and named after the intermediate compound produced using L-tryptophan (Trp) as a substrate: i) the indole-3-acetaldoxime (IAOx) pathway, ii) the indoleacetamide (IAM) pathway, iii) the tryptamine pathway (TAM) and iv) the indole-3-pyruvic acid (IPyA) pathway (Woodward and Bartel, 2005; Korasick et al., 2013; Ljung, 2013). Genetic and biochemical evidence indicates that the IPyA pathway, which includes a two-step enzymatic conversion of Trp to IAA, is the major auxin biosynthesis route in plants (Zhao et al., 2012). The first step

involves the TRYPTOPHAN AMINOTRANSFERASE OF ARABIDOPSIS1 / TRYPTOPHAN AMINOTRANSERASE RELATED 1-4 (TAA1/TAR1-4) family of enzymes that convert Trp to IPyA (Stepanova et al., 2011; Won et al., 2011; Tao et al., 2008). In the second step the YUCCA (YUC) family of proteins convert IPyA to IAA (Zhao et al., 2001; Cheng, 2006; Cheng et al., 2007).

Mutations in the *TAA1* gene and its closest homologs *TAR1* and *TAR2* result in altered meristem functioning, defects in flowering and embryo development (Stepanova et al., 2008). The *wei8 tar1 tar2* triple mutants display *monopteros* (*mp*)-like phenotypes: they fail to establish the basal part of the embryo and often develop a single cotyledon (Stepanova et al., 2008). The quadruple mutant *yuc1 yuc4 yuc10 yuc11* displays similar phenotypes as the triple *wei8 tar1 tar2* mutant (Cheng, 2006; Cheng et al., 2007). More embryonic defects were discovered in knock out combinations of *yuc3*, *yuc4*, and *yuc9*. Local auxin production was proposed to act in conjunction with PIN-FORMED1 (PIN1) driven polar auxin transport to establish auxin gradients that steer pattern development in the *Arabidopsis* embryo (Robert et al., 2013).

Despite sufficient genetic evidence that the IPyA auxin biosynthesis route is important for zygotic embryogenesis in *Arabidopsis*, its role in 2,4-D-induced SE has only superficially been touched. In an *Arabidopsis* 2,4-D-induced secondary SE culture system (Bai et al., 2013) expression of *YUC1*, *YUC2*, *YUC4*, *YUC6* was shown to be enhanced following SE initiation by transfer of embryonic calli to 2,4-D free medium. In this system, single and higher order mutants of *yuc1, yuc2, yuc4,* and *yuc6* were not affected in their SE capacity. In contrast, *yuc1 yuc4 yuc10 yuc11* quadruple mutant embryonic calli showed a significant reduction in the SE capacity (Bai et al., 2013). A major disadvantage of the secondary SE culture system is that somatic embryos are derived from pre-existing embryonic calli in the absence of 2,4-D (Nowak et al., 2012), and therefore the early events that lead to the induction of embryo identity by 2,4-D cannot be studied.

Here, we studied the role of auxin biosynthesis in our primary 2,4-D induced SE on *Arabidopsis* IZEs, first by using two chemical inhibitors, L-kynurenine (kyn) (He et al., 2011) and yucasin (yuc) (Nishimura et al., 2014) that respectively block the Trp → IPyA and IPyA → IAA conversions, and secondly by studying the effect of loss-of-function mutations and the expression of *TAA/TAR* and *YUC* genes during 2,4-D induced SE. Surprisingly, our data shows that the YUCCA-mediated IPyA → IAA conversion is not required for SE initiation, but only for later development of the somatic embryos, whereas the Trp → IPyA conversion step, as regulated by TAA1/TARs enzymes, is crucial for this process.

Results

YUCCAs are not essential for SE initiation, but are required for somatic embryo development

Based on the results of Bai and coworkers (2013) suggesting the important role of the *YUC* genes in 2,4-D-induced SE initiation, we tested the inhibitor yucasin, which specifically blocks the IPyA → IAA conversion by the YUCCA monooxygenases, in our primary *Arabidopsis* SE system. Earlier experiments showed that the first *pWOX2::YFP*-marked embryonic cells could be observed after 5 days, but not yet after 3 days of incubation on SEIM (Chapter 2). We have demonstrated in Chapter 2 that it was possible to identify at which stage an auxin related pathway has a role by applying chemical inhibitors prior (day 0), during (day 3) or after (day 5) the establishment of these first embryogenic cells. In previous control experiments (Chapter 2) we observed that the transfer to fresh SEIM medium does not affect SE. By applying 100µM yucasin we anticipated to be able to determine at which stage YUC activity would be important. Early yucasin application (day 0) reduced both SE efficiency (the frequency of IZEs producing somatic embryos) and -productivity (average number of somatic embryos produced per IZE) to 0 (Figure 1a), as all IZEs died within the first five days of culture (Figure 1b). Application of yucasin from day 3 onwards resulted in a mild but significant reduction of the SE efficiency (67% compared to 84% in the control), but the productivity was not affected (Figure 1a,b). Yucasin application on day 5 did not significantly affect the SE efficiency, but the SE productivity decreased from 1.4 to 0.5 SEs/IZE. Thus, the IPyA → IAA conversion step controlled by YUCCAs is important for the survival of the IZE in tissue culture, and plays a role during SE, however it is not crucial for SE initiation. The reduction in SE productivity following yucasin application at day 5 was the result of the appearance of more fused embryos (embryonic clusters) and shoot-like structures as opposed to individual somatic embryos in the yucasin treated IZEs as compared to control IZEs. As we are unaware of the stability of yucasin, we presume that it causes a stronger effect when freshly applied on day 5 during the embryo development phase. In conclusion, YUC activity is required for survival of IZEs and for proper development of induced embryonic cells into individual somatic embryos, but not for SE initiation.

To further study the effect of yucasin on 2,4-D treated IZEs, we used the *DR5::GUS* auxin response reporter (Ulmasov et al., 1997; Friml et al., 2003). IZEs of an *Arabidopsis DR5::GUS* line were incubated on SEIM for 4hr with or without 100µM yucasin, or on SEIM without 2,4-D and subsequently stained for GUS activity. As a control, IZEs were included that were freshly isolated from the ovule and

were directly stained for GUS activity. In the control IZEs, *DR5::GUS* was clearly expressed in the root and cotyledons tips and in provascular tissues in cotyledons and the hypocotyl, as described before (Friml et al., 2003).This expression pattern was more pronounced in the SEIM incubated IZEs (Figure 1c,d), and slightly weaker in the absence of 2,4-D, but significantly reduced when IZEs were incubated on SEIM with yucasin (Figure 1c,d). The most striking difference was that all SEIM incubated IZEs showed a strong *DR5::GUS* expression in the hypocotyl, whereas this was only observed in a few yucasin (11%), or hormone free SEIM (8%) treated IZEs (Figure 1d). The results confirm that short-term 2,4-D treatment enhances the auxin response, and that this enhancement is dependent on YUCCA-mediated auxin biosynthesis that is essential for IZE survival during the first few days on SEIM.

YUCCAs are involved in somatic embryo development

To confirm the role of *YUCCA* genes in IZE survival and somatic embryo development, we analyzed promoter reporter lines for several *YUCCAs* in IZEs that were incubated for 0, 3, 5 and 7 days on SEIM medium. Representative microscopy images and frequency of observations are shown in Figure S1 and Table S1 and a schematic representation of the expression observed in more than 20% of the IZEs tested is shown in Figure 2a. Since somatic embryos are mostly developing from the SAM or the proximal adaxial side of cotyledons of an IZE, we expected *YUCCA* genes directly involved in SE to be specifically induced in these tissues of the IZE on days 5 and 7. *YUC2* and *YUC10* were not or barely expressed in IZEs at any time point, in any tissue (Figure S1, Table S1). However, for *YUC4*, *YUC6*, *YUC8* and *YUC9* an interesting dynamic expression pattern was observed, suggesting their involvement in somatic embryo development. *YUC4* was weakly expressed in the epidermis throughout the IZE and more strongly in the SAM on day 0 and day 3 (Figure S1, Figure 2a). On day 5, expression was not observed in SE regions but was enhanced in the SAM and the cotyledon- and root tips, followed by its confinement to the SAM and the proximal region of the cotyledons on day 7. *YUC6* expression was confined to the provascular tissue of the IZE, starting at day 0, disappearing on day 3, and returning on day 5 with particularly strong expression below the areas of SE initiation on day 7. Since somatic embryos do not develop from the provascular tissue but from the epidermal layer (Raghavan, 2004; Kurczyńska et al., 2007) it is unlikely that *YUC6* is directly involved in SE. However, based on its temporal expression, it is likely to be important for IZE survival and somatic embryo development. *YUC8* and *YUC9* have a similar expression pattern in which expression on day 0, 3 and 5 is confined to the cotyledons tips. On day 7 both reporters are observed in the proximal area of the cotyledons as well as

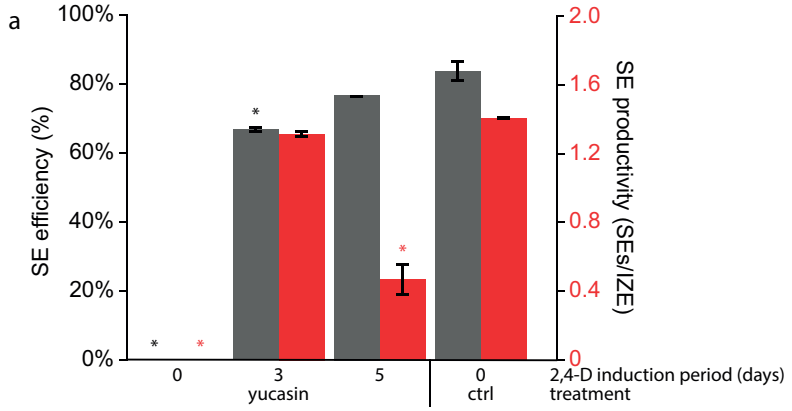

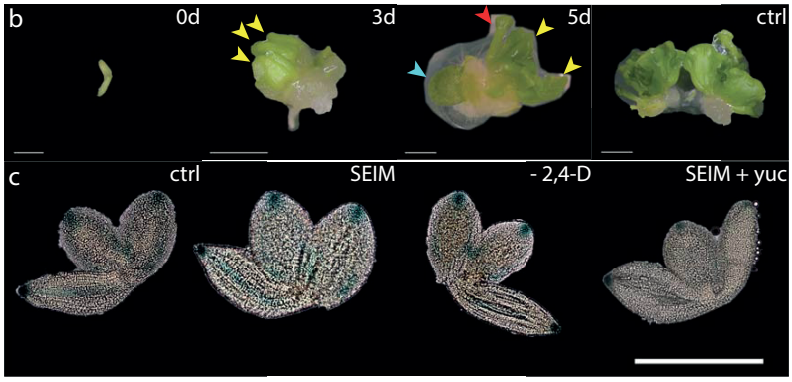

d

	DR5::GUS EXPRESSION				
	TIPS COTYLEDONS		HYPOCOTYL		
	WEAK	STRONG	WEAK	STRONG	*n*
Control	20%	80%	44%	56%	41
SEIM	12%	88%	0%	100%	41
SEIM – 2,4-D	26%	74%	92%	8%	38
SEIM + YUC	78%	22%	89%	11%	27

FIGURE 1 - Effect of yucasin on SE initiation in *Arabidopsis* IZEs.

a) SE efficiency (grey bars) and productivity (red bars) of *Arabidopsis* IZEs cultured on SEIM to which 100µM yucasin was added at the start (0) or at 3 or 5 days after the start of the 14 days incubation period. Control IZEs (0 ctrl) were incubated for 14 days on SEIM without yucasin. Bars represent average values of duplicate experiments with n = 48, error bars indicate SEM. Asterisks denote a significant difference between control and treatment (χ^2-test, $p<0.05$ for SE efficiencies, and Welch *t*-test, $p<0.05$ for SE productivities). b) Representative images of a control IZE (ctrl) or IZEs treated with yucasin after 0, 3 and 5 days of the start of culture. Red arrowheads point at individual somatic embryos, yellow arrowheads point at embryogenic structures, and blue arrowheads indicate shoot-like structures. Scale bar represents 1mm. c) Effect of yucasin on *DR5::GUS* expression in IZEs. Untreated *DR5::GUS* IZEs (ctrl), or *DR5::GUS* IZEs incubated for 4hr on SEIM medium (SEIM), on SEIM without 2,4-D (-2,4-D), or on SEIM supplemented with 100µM yucasin (SEIM + yuc) were stained overnight for GUS activity. Scale bar represents 50µm. Please note that for presentation purposes the original background of the IZE images in b and c was removed. Independent images were placed on a black background. d) IZEs as shown in c were scored for either weak or strong expression in the cotyledon tips and hypocotyl.

the hypocotyl, and expression in the cotyledons tips is only observed in *YUC9*. All four discussed YUCs are strongly expressed on day 7 and weakly or not in prior time points. Therefore we believe that these *YUCs* are most likely involved in somatic embryo development rather than initiation.

A phylogenetic tree of the *Arabidopsis YUCCA* gene family showed that the genes can be grouped into two main clades that are likely to be the result of an early gene duplication event (Figure 2a, Cheng et al., 2007). Interestingly, we noticed that clade members shared expression patterns: e.g. clade 1 *YUCCAs* were either not (*YUC2* and *YUC10*) or only faintly expressed (*YUC4*), or their expression was limited to the vasculature (*YUC6* and *YUC11*) (Figure 2a,b), whereas expression of clade 2 *YUCCAs* was either limited to cotyledon tips (*YUC7, YUC8* and *YUC9*) or was detected in most tissues of the IZE at day 7 (*YUC5*, *YUC8, YUC9*) (Figure 2a,b). This finding corroborates the earlier conclusion by Cheng and coworkers (Cheng, 2006; Cheng et al., 2007) that the sub-functionalization of *YUCCAs* following the early gene duplication that formed the two clades was maintained after subsequent duplication events. Unfortunately, we were not able to study *YUC1* and *YUC3* expression due to malfunctioning of the designed reporter lines.

To correlate *YUC* gene expression patterns with their functionality, we examined available mutant combinations for SE efficiency. It is important to note here that because of our experimental system, our analysis was limited to mutants that developed fertile plants and embryos. Based on the yucasin experiments we expected to see reduced IZE survival, or a slight but significant reduction in SE efficiency (from 80 to 60%). Furthermore, we chose our mutant lines based on a dynamic expression pattern in which expression would increase over time or peak at day 3 or day 5 in regions of SE initiation. This excluded *YUC5* and thus we continued with y*uc8 yuc9* double- and *yuc2 yuc4/+ yuc6* triple loss-of-function mutants that were tested as representatives of respectively clade 1 and clade 2. The *yuc1 yuc10 yuc11* triple loss-of-function mutant was included as negative control, as the corresponding genes were not expressed during IZE-derived SE, or in tissues not directly involved in SE, In addition, the *yuc3* mutant was taken along as part of the *yuc3 yuc9* double mutant, despite the fact that the *YUC3* gene was not included in our expression studies, since it was found to be a target of *BBM* induced SE (Heidman, 2015) and shown to be involved in zygotic embryogenesis (Robert et al., 2013).

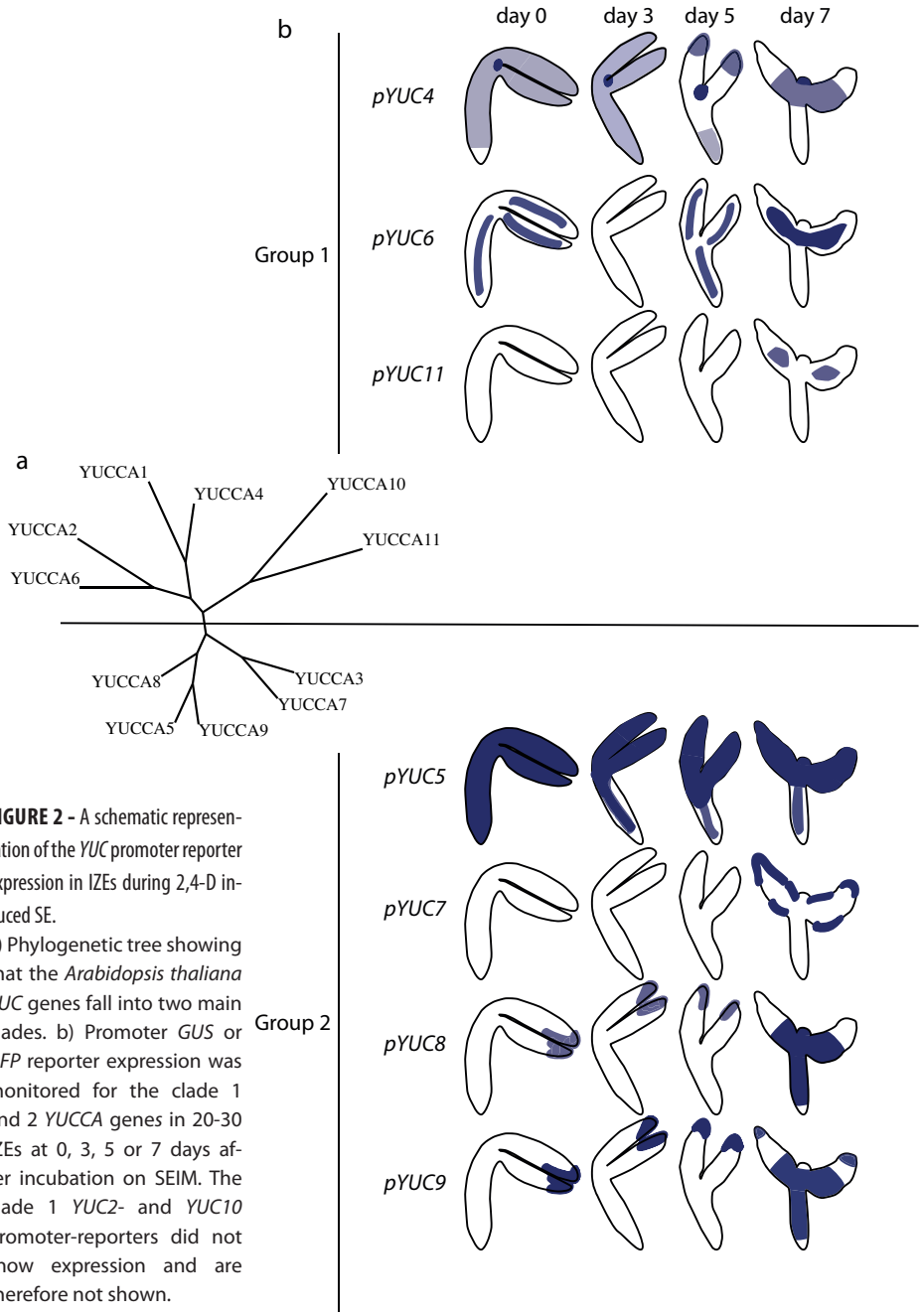

FIGURE 2 - A schematic representation of the *YUC* promoter reporter expression in IZEs during 2,4-D induced SE.
a) Phylogenetic tree showing that the *Arabidopsis thaliana YUC* genes fall into two main clades. b) Promoter *GUS* or *GFP* reporter expression was monitored for the clade 1 and 2 *YUCCA* genes in 20-30 IZEs at 0, 3, 5 or 7 days after incubation on SEIM. The clade 1 *YUC2*- and *YUC10* promoter-reporters did not show expression and are therefore not shown.

For 4 of the 5 tested mutant combinations, including the *yuc1 yuc10 yuc11* negative control, the SE efficiency did not significantly differ from wild type (Figure 3a). Interestingly, however, the *yuc2 yuc4/+ yuc6* triple mutant led to a similar reduction in SE efficiency (81% to 63% SE efficiency) as yucasin treatment, and several mutant IZEs continued with seedling germination programme rather than developing callus or somatic embryos (Figure 3b, blue arrows). As a result, additional shoot or root structures could be found next to somatic embryos on the same explant (Figure 3b). Only few somatic embryos were produced per explant, but if they were present, the somatic embryos exerted a similar phenotype as the wild type.

Previous research on early stage zygotic embryogenesis has shown that *YUCCAs* play a significant role in local auxin biosynthesis that is crucial for embryo development (Cheng, 2006; Cheng et al., 2007; Robert et al., 2013, 2015). Our results confirm this and suggest that at least endogenous auxin production mediated by *YUCCAs* is not needed for SE initiation, but rather for the early survival of IZEs on SEIM and later on for the proper development of individual somatic embryos.

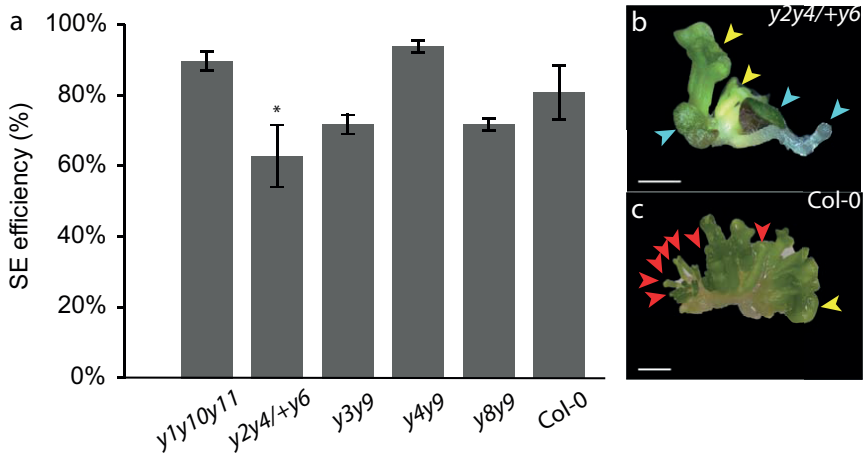

FIGURE 3 - The effect of *yucca* loss-of-function mutations on SE initiation in *Arabidopsis* IZEs.

a) SE efficiency for different *yuc* loss-of-function mutant combinations. Bars represent average values of duplo experiments with n=48 for homozygous lines and n=96 for segregating lines, error bars indicate SEM. Asterisks denote significant differences between wild type (Col-0) and mutant (χ^2-test, $p<0.05$). (b,c) Representative phenotype of the *yuc2 yuc4/+ yuc6* triple mutant (b) and wild-type (Col-0) (c) IZEs following standard SE culture. Red arrowheads point towards individual somatic embryos, yellow arrowheads to embryonic structures and blue arrowheads to shoot structures. Please note that for presentation purposes the original background of the IZE images in b and c was removed and replaced by a black background. Scale bar represents 1mm.

Auxin biosynthesis by TAA1/TAR is required for cell division and proliferation during SE.

Our results indicated that *YUCCAs* are not directly involved in SE initiation. Therefore we set out to investigate whether TAA1/TAR enzymes involved in the Trp → IPyA conversion step have a role during SE initiation. We used the inhibitor L-kynurenine to block the enzymatic activity of TAA1/TAR enzymes. In contrast to the yucasin experiments (Figure 1a), SE efficiency was significantly reduced from 84% in the control treatment to 8%, 3% and 30% for respectively L-kynurenine treatments starting at day 0, 3 and 5 (Figure 4a). Inhibition of the TAA1/TAR enzymes by L-kynurenine resulted in small calli with root and shoot structures, independent of the time point of L-kynurenine application (Figure 4b). In addition, we studied SE initiation by using the embryonic cell fate reporter *pWOX2::NLS-YFP* combined with the auxin response reporter *DR5::RFP* (Chapter 2, Breuninger et al., 2008) during L-kynurenine treatment. IZEs of an *Arabidopsis* line containing both reporters were incubated on SEIM for 3 days and transferred to SEIM with 100µM L-kynurenine or to hormone free medium for 48hr. As a control, a 5 days SEIM culture was included. In the L-kynurenine treated IZEs we did not observe cells marked by *WOX2*, which indicated that SE initiation was completely prohibited. In Chapter 2 we have shown that an elevated auxin response followed by a local minimum is required for SE initiation. This dynamic change was absent in the L-kynurenine treated IZEs. Instead, we observed a reduced expression of *DR5::RFP*, similar to the hormone free treatment (Figure 4c). These results suggested that the Trp → IPyA conversion by TAA1/TARs is essential to SE initiation by enhancing endogenous auxin levels. We noticed that the IZEs treated with L-kynurenine were smaller and hypothesized that this was a result of a defect or reduction in cell division. To investigate this, we performed histological analysis on the base of cotyledons of IZEs that were grown for 5 days on SEIM, and IZEs grown for 3 days on SEIM and subsequently for 2 days on SEIM with 100µM L-kynurenine. In the SEIM cultured IZEs, periclinal and anticlinal symmetric cell divisions were abundantly observed in the (sub)epidermal layer at the base of the cotyledons. Such divisions have been reported to be an indication of SE development (Kurczyńska et al., 2007). In contrast, in the L-kynurenine-treated IZEs the number of cell divisions was limited and most divisions seemed asymmetric (Figure 5b,d). In conclusion, the observed lower auxin response and the disturbed cell divisions producing small calli suggests that *TAA1/TARs*-mediated auxin biosynthesis is triggering an elevated auxin response that is required for appropriate cell division and proliferation during SE initiation.

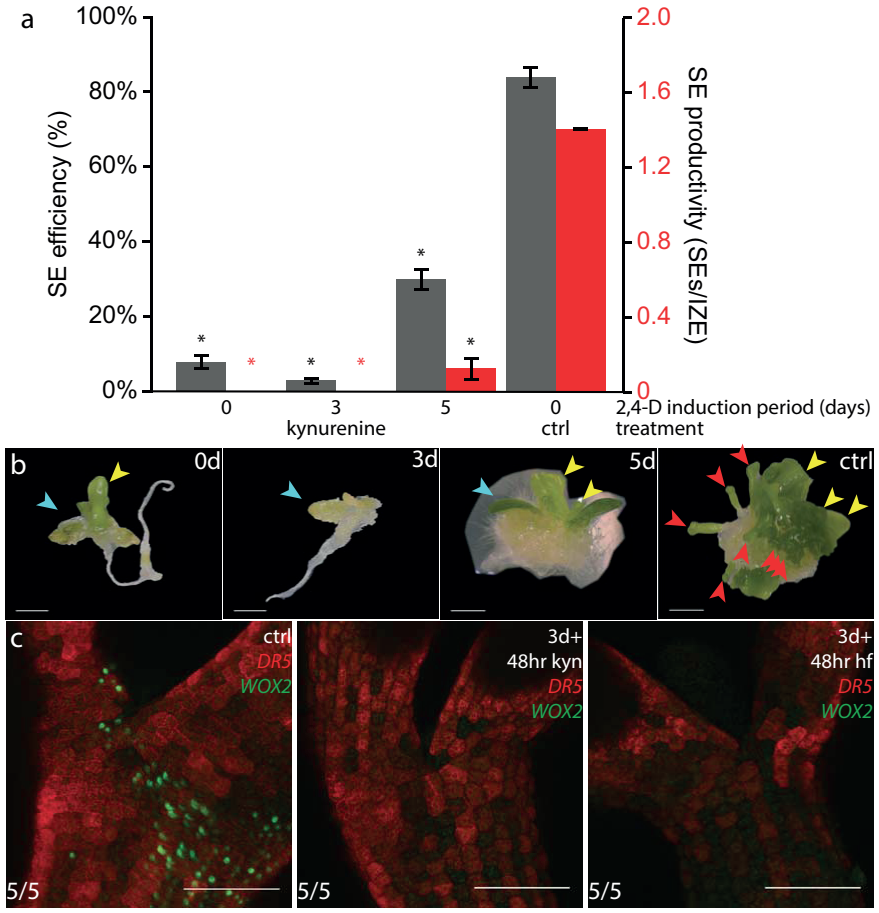

FIGURE 4 - Effect of L-kynurenine on SE initiation in *Arabidopsis* IZEs.
a) SE efficiency (grey bars) and productivity (red bars) of *Arabidopsis* IZEs cultured on SEIM to which 100µM L-kynurenine was added from the start (0) or at 3 or 5 days after the start of incubation. Control IZEs were incubated on SEIM without L-kynurenine (0 ctrl). Bars represent mean values from duplicate experiments with n = 48, error bars indicate SEM. Asterisks denote significant differences between control and treatment. SE efficiencies were compared using the χ^2 test ($p<0.05$), and SE productivities were compared using the Welch *t*-test ($p<0.05$). b) Representative images of phenotype with yucasin treatment after 0, 3 and 5 days and control (ctrl). Red arrowheads point at individual somatic embryos, yellow arrow heads point at embryogenic structures and blue arrow heads indicate shoot-like structures. Please note that for presentation purposes the original background of the IZE images in b and c was removed and replaced by a black background. Scale bar represents 1mm. c) Representative CLSM images of *pWOX2::NLS-YFP* (green) *DR5::RFP* (red) IZEs cultured for 3 days on SEIM followed by 2 days on SEIM in the absence (ctrl) or presence of 100µM L-kynurenine (kyn), or on hormone free (hf) medium. Scale bar represents 50µm.

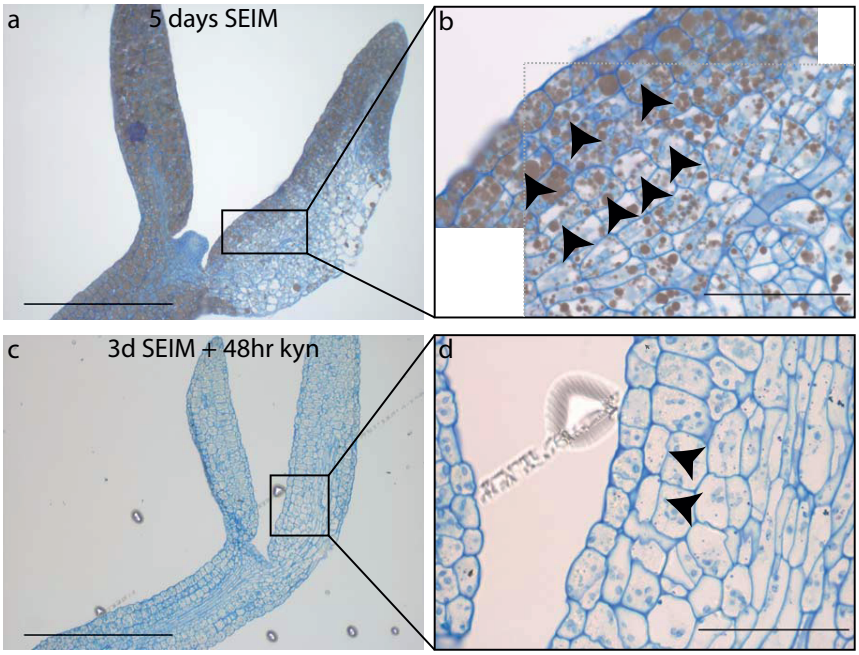

FIGURE 5 - Effect of L-kynurenine treatment on cell divisions in cotyledons of *Arabidopsis* IZEs.
a-b) Representative longitudinal section of an IZE after 5 days SEIM culture (n=5) or c-d) 3days SEIM culture followed by 48hr SEIM culture with 100µM L-kynurenine (n=5). Black arrow heads point at periclinal divisions,. Scale bar in a) and c) represent 250 µm, scale bar in b) and d) represent 50µm. Sections were stained with TBO (blue) for visualizing cells and osmium (brown) was used to color the IZE during embedding and sectioning. Thin sections were made using a microtome at 2µm.

As we observed that L-kynurenine treatment resulted in callus rather than SE development, we investigated whether mutations in the *TAA1/TARs* genes would result in similar phenotypes. To our surprise, however, *wei8-1 tar1-1 tar2-2/+* triple mutant IZEs segregating for the *tar2-2* allele did not show a significant reduction in SE efficiency and productivity compared to wild-type IZEs. We found that the IZEs with the *mp*-like phenotype typical for *wei8-1 tar1-1 tar2-2* homozygous progeny (20 of the 192 IZEs tested) were still able to develop embryogenic calli with somatic embryos similar as wild-type IZEs (Figure 6b, red arrows). We have used a mother plant heterozygous for the *tar2-2* allele, because the availability of IZEs with a *mp*-phenotype was limited. We therefore presumed that the lack of significant differences in phenotype was because at least 75% of IZEs derived from the *wei8-1 tar1-1 tar2-2/+* plant still carried the wild-type *TAR2* allele. We continued with analyzing the auxin response in the triple *wei8-1 tar1-1 tar2-2/+* background to find an explanation for our observations.

Analysis of *DR5::GUS* reporter expression in the triple *wei8-1 tar1-1 tar2-2/+* background showed major differences on day 5 and 7 when SE initiation was expected to occur (Figure 6c,d). Whereas all wild-type IZEs showed a relatively homogeneous *DR5::GUS* expression on both day 5 and day 7 (respectively n=26 and n=31), at day 5 a reduced number of mutant IZEs showed expression in the cotyledons tips (58%), cotyledons base (88%) and root tip (78%) compared to wild-type (respectively 77%, 100%, 85%). On day 7 *DR5::GUS* expression in the mutant IZEs was limited to callus and root tip (Table S3, Figure 6d).

It must be noted that the auxin response restored itself in the root tip at day 7, but was mainly observed in callus that developed in the triple mutant background. As there is still a clear auxin response in the triple mutant, this may explain why *wei8-1 tar1-1 tar2-2/+* did not result in significant differences for SE. The SE initiation still occurs, albeit at a slower rate caused by the reduced auxin response.

In accordance with this slower initiation and development of the somatic embryos, the *wei8-1 tar1-1 tar2-2/+* embryonic calli that developed were smaller (Figure 6d). To confirm this, we scored the frequency of big, small and no calli development after 7 days SEIM culture. In the *DR5::GUS* control 70% of the IZEs developed big calli and only 30% small calli (n=30). In contrast, *wei8-1 tar1-1 tar2-2/+* IZEs developed 31% big calli, 64% small calli and 5% did not develop calli at all (n=59). The lower *DR5* response that was observed together with occurrence of small calli suggests that the *TAA1/TAR*-enhanced auxin response is required for appropriate and efficient cell divisions during SE. Similar cell division defects due to disturbed local auxin homeostasis were also found in embryo and gametophyte development in *Arabidopsis* (Robert et al., 2013; Panoli et al., 2015).

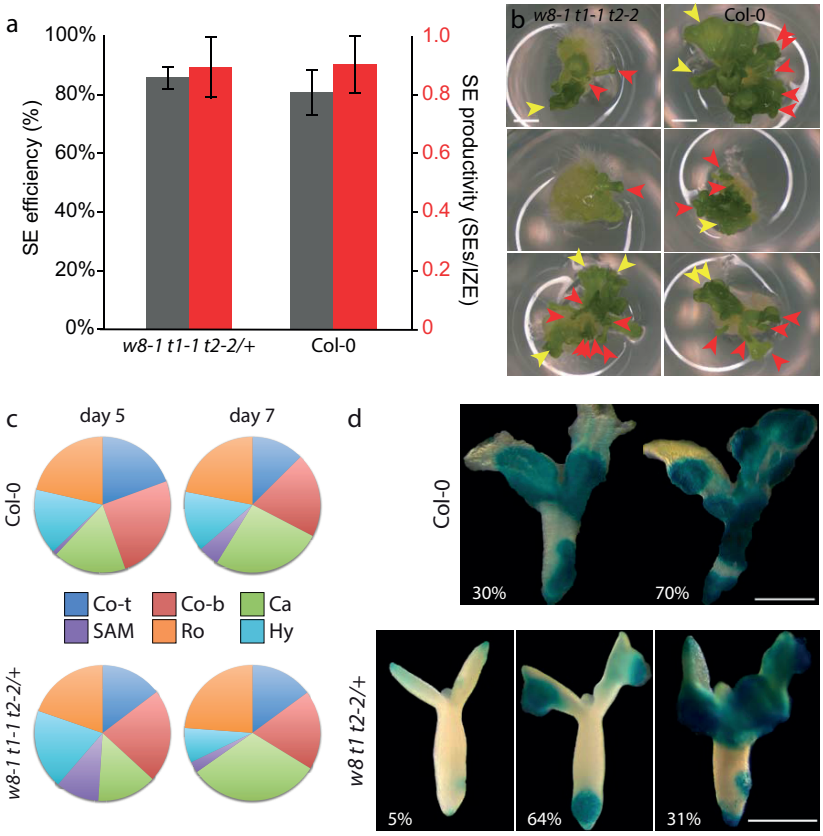

FIGURE 6 - The role of TAA1/TARs during SE initiation in *Arabidopsis* IZEs.
SE efficiency (grey bars) and productivity (red bars) for *wei8-1 tar1-1 tar2-2/+* and Col-0. Bars represent average values of duplicate experiments with n=96, errors bars represent SEM, and asterisks denote significant differences between Col-0 and loss-of-function mutant (χ^2 test, p= 0.05). b) Representative phenotype photos of *wei8-1 tar1-1 tar2-2/+* and Col-0 after standard SE culture. Red arrow heads point towards individual somatic embryos, yellow arrowheads to embryonic structures. Scale bar represents 1mm. c) Graphical representation in pie charts of *DR5::GUS* observations for cotyledon tips (Co-t), cotyledons base (Co-b), callus (Ca), shoot apical meristem (SAM), hypocotyl (Hy) and root (Ro) in Col-0 and *wei8-1 tar1-1 tar2-2/+* after 5 and 7 days standard SEIM culture. d) *DR5::GUS* expression in Col-0 (n=30) and *wei8-1 tar1-1 tar2-2/+* IZE (n=59) after 7 days SEIM culture. Three phenotypic classes were visible after 7 days SEIM culture; IZEs developing big, small or no callus. Percentages denote observations frequencies.

Discussion

The plant hormone auxin controls many aspects of plant development. Many auxin analogs have been made since the 1940s and applied in tissue culture to direct plant regeneration (De Rybel et al., 2009; Simon and Petrášek, 2011; Song, 2014). The synthetic analog 2,4-D is the most abundantly used analog in tissue culture to induce SE. As previous research has shown that 2,4-D causes elevated

levels of auxin (Pasternak, 2002; Michalczuk et al., 1992), we investigated here the role of auxin biosynthesis in SE focusing on two enzymatic steps of the most important Trp dependent pathway, the Trp → IPyA conversion by TAA1/TARs and the IPyA → IAA by YUCCAs.

Using inhibitors for these enzymes we found that the IPyA → IAA conversion has a minor role in SE initiation compared to the Trp → IPyA conversion step. We further demonstrated that most of the *YUCCAs* are not involved in SE initiation, but rather are important during development of the somatic embryo, which is in line with the minor effects of yucasin on SE and a significant reduction in SE productivity on day 5. However, early application of yucasin led to death of IZEs, and the fact that several *YUC* gene candidates have been found to be upregulated in other SE systems (Bai et al., 2013) suggests their importance for the survival of the explants in tissue culture. Besides 2,4-D application, SE can also be induced by ectopic expression of specific transcription factors, such as *LEAFY COTYLEDON1* (*LEC1*), *LEC2, BABYBOOM (BBM)* and *WUSCHEL* (*WUS*) (Lotan et al., 1998; Stone et al., 2001; Boutilier et al., 2002; Zuo et al., 2002). Also in these SE systems, *YUCCA* genes were found to be upregulated. *YUC10* was shown to be upregulated during *LEC1* induced SE (Junker and Bäumlein, 2012; Wójcikowska et al., 2013), whereas *LEC2*- or *BBM*-induced SE led to the upregulation of respectively*YUC1*, *YUC2*, *YUC4*, *YUC10* and *TAA1* (Stone et al., 2008; Wójcikowska et al., 2013) or *YUC3*, *YUC4, YUC8* and *TAA1*) (Heidman, 2015). Thus, an initial rise of auxin mediated by *YUCCAs* in the first 1 to 3 days in SEIM culture seems to be required to maintain embryo viability prior to SE initiation.

However, our results showed that not all *YUCCAs* contribute equally and significantly to SE induction. Firstly, based on our expression analysis we concluded that *YUC2 and YUC11* are not involved during SE initiation and in our SE system, the *yuc2 yuc4/+ yuc6* triple mutant only showed a slight reduction in SE efficiency. This finding is in sharp contrast to a previous study, which reported that *YUCCAs* are essential for SE (Bai et al., 2013). First of all, Bai and co-workers did not test the yucasin inhibitor. Secondly, they detected upregulation of *YUC2* and *YUC11* by qRT-PCR in their system, whereas no expression was observed in our system with GUS reporters. Thirdly, in their hands a *yuc1 yuc2 yuc4 yuc6* quadruple mutant did not show any effect, whereas SE was significantly reduced in a *yuc1 yuc4 yuc10 yuc11* quadruple mutant. In contrast, in our hands only the triple *yuc2 yuc4/+ yuc6* showed a significant effect, whereas the *yuc1 yuc10 yuc11* triple did not. As our *yuc1 yuc10 yuc11* mutant does not include *yuc4* a direct comparison is not possible. More importantly to note is that differences in observations are likely also to be caused by the fact that Bai and coworkers (2013) used a system that studies secondary SE, whereas our system involves the induction of primary

somatic embryos. Both processes may require different auxin mechanisms and can therefore not be compared. What is clear, however, is that YUCCAs act redundantly, and although our data do not completely exclude this redundancy, the yucasin inhibitor results suggest that this pathway is less important for SE initiation. This is in itself a remarkable feature as YUCCAs have been reported to play a key role in zygotic embryogenesis (Cheng, 2006; Stepanova et al., 2007; Robert et al., 2013) and is suggested to be the rate-limiting step of auxin biosynthesis (Zhao, 2014). The auxin biosynthesis is a complicated mechanism and many unknowns remain to be solved such as alternative biosynthesis routes in which YUCCAs may function as well, like the TAM pathway (Ljung, 2013; Mano and Nemoto, 2012; Woodward and Bartel, 2005).

In this chapter we have further shown that SE can be efficiently suppressed by the application of L-kynurenine, a compound that blocks specifically the activity of TAA1/TAR enzymes (He et al., 2011). The dynamic auxin response was absent in L-kynurenine treated IZEs, which corroborates our earlier observation that a dynamic auxin response is required to initiate SE.

However, we found that the loss-of-function mutant *wei8-1 tar1-1 tar2-2/+* did not result in similar phenotypes as the L-kynurenine treatment. One explanation for this is that we cannot measure the effect of the genetic defects because we used a segregating population of the triple mutant and that one functional allele of *TAR2* is sufficient to perform SE similar to wild-type, albeit at slower rate. However, about 20 homozygous triple mutant IZEs could be recognized based on their *mp* phenotype, and these showed somatic embryo development similar to wild-type. To study the functionality of *TAR2*, either more *mp*-like embryos should be studied or its transcriptional as well as translational expression can be studied using reporter lines. In addition, combining reporter assays for *TAA1/TARs* with L-kynurenine treatment would be beneficial to study the specificity of L-kynurenine itself on the TAA1/TAR enzymes during SE initiation. To research the role of TAA1, a new class of TAA1 inhibitors, named "pyruvamines", can be used to perform inhibitor screens (Narukawa-Nara et al., 2016). In addition, other members of the TAA1/TAR family i.e. TAR3 and TAR4 (Tao et al., 2008; Mano and Nemoto, 2012) should also be taken into consideration to fulfill a role in SE initiation. Their role is fairly unknown in plant development thus it would be interesting to use SE to study their function.

We further demonstrated that IZEs in both L-kynurenine and in the *wei8 tar1 tar2/+* knock out developed smaller calli together with a decreased auxin response. This strongly suggests that auxin biosynthesis is required for appropriate cell division during SE, and possibly even for cell wall development, as defects in *WEI8* and *TAR2* have been shown to induce defects in cell wall devel-

opment (Steinwand et al., 2014). It was demonstrated before that defects in cell wall production can lead to callus formation (Nicol et al., 1998; Sato et al., 2001; Ikeuchi et al., 2013; Steinwand et al., 2014). Based on our data it is suggested that auxin biosynthesis is involved during SE initiation in orchestrating cell wall development. Several papers have shown that the auxin biosynthesis-ethylene interaction is of importance to SE and to many other plant development processes (Stepanova et al., 2005; Swarup et al., 2007; Polko et al., 2011; Bai et al., 2013; Nowak et al., 2014). During SE initiation, ethylene levels are decreased and mutations in ethylene signaling or treatment with precursors of ethylene disrupts SE initiation and activate auxin biosynthesis (Jiménez, 2005; Bai et al., 2013; Nowak et al., 2014). *YUC1* and *YUC4* expression is reduced in embryogenic calli treated with the ethylene precursor ACC (Bai et al., 2013). Similarly, *LEC2* activates auxin biosynthesis through *YUCCAs* simultaneous causing ethylene biosynthesis to be inhibited (Wójcikowska et al., 2013). Moreover, a knockout of *ETHYLENE RESPONSE FACTOR022 (ERF022)* has reduced *YUC1* and *YUC4* expression levels during SE (Nowak et al., 2014). Ethylene can regulate organ development by either directly regulating local auxin biosynthesis through *WEI2/WEI7* or indirectly through a signaling pathway, activating auxin transport and biosynthesis (Ruzicka et al., 2007; Stepanova et al., 2008; Li et al., 2006). A detailed analysis of the dynamic auxin response with ethylene application and its inhibitors for biosynthesis aminoethoxyvinylglycine (AVG) (Strader et al., 2010), for signaling silver thiosulfate (STS) (McDaniel and Binder, 2012) and 1-methylcyclopropene (1-MCP) (Hall et al., 2000) would contribute to a more in depth understanding of the auxin biosynthesis – ethylene relationship during SE initiation.

Methods

Plant lines

All *Arabidopsis thaliana* lines described below are in Columbia wild-type (Col-0) background. The *pWOX2::NLS-YFP* line was kindly donated by Thomas Laux and is resistant to phosphinothricin (ppt) (Breuninger et al., 2008). The *DR5::RFP* line was donated by Eva Benkova and is resistant to hygromycin (hyg) (Marhavý et al., 2011). The *yuc1 yuc10 yuc11* and *yuc2 yuc4/+ yuc6* triple mutants were obtained from the original *yuc1 yuc4/+ yuc10 yuc11* and *yuc1/+ yuc2 yuc4/+ yuc6* lines kindly donated by Yunde Zhao (Cheng, 2006; Cheng et al., 2007).

The *YUC2/5/6/7/8/9/10/11* promoter-*GFP-GUS* or *YUC1/4* promoter *NLS-3xGFP* reporter fusion lines are kanamycine (kan) resistant and together with the *yuc3 yuc9* and *yuc4 yuc9* double mutants they were kindly provided by Helene

Robert-Boisivon. The mutant lines *yuc3* (GK-376G12, part of set 436084), *yuc4* (Cheng et al. (2006) and *yuc9* (sail_871_G01) (Robert et al., 2013), *yuc8* (N655757/ SALK_096110C), *yuc9* (sail_871_G01) and *wei8-1 tar1-1 tar2-2/+ DR5::GUS* (N16420/ CS16420) were ordered from NASC.

Genotyping

Sequences of DNA primers used for genotyping are provided in Table S1. All PCR reactions were performed using DreamTaq DNA polymerase (ThermoFisher Scientific, EP0705) on genomic DNA isolated as described by Giraudat (2003), melting temperature and annealing time respectively was 55°C and 60s, unless otherwise stated.

Plant tissue culture and growth conditions

Arabidopsis seeds were surface sterilized and germinated on MA medium (Masson and Paszkowski, 1992) complemented with 1% (w:v) sucrose, and 0.8% (w:v) Daishin agar, pH5.8. For antibiotic selection ppt, hyg or kan was added to the medium after autoclaving at a final concentration of 20mg/mL for ppt and hyg, and of 50mg/mL for kan. Seven to ten days after germination (dag), seedlings were transferred to a mixture of soil and sand, 2 per pot, and grown under a 16hr photoperiod and 70% relative humidity. IZEs were harvested from plants 1-2 weeks after flowering. The siliques were surface sterilized with a 20% bleach/ 70% ethanol solution for 5min. and rinsed at least three times with sterile water. SE-inducing medium (SEIM) consisted of B5 medium, with 4.5µM 2,4-D, 2% (w:v) sucrose and 0.8% (w:v) Daishin agar (Gaj, 2011; Nowak et al., 2012). Hormone free medium was MA medium (Masson and Paszkowski, 1992). Media were sterilized by autoclaving at 120°C for 20min SE induction was performed in sterile 48-wells plates (Greiner cellstar art. nr. 677180) that were filled with 400µL SEIM or hormone free medium using a repeater pipet. IZEs were placed on SEIM (one per well) and incubated overnight at 4°C in the dark followed by incubation at 21°C and under a 16hr photoperiod for a standard period of 14 days, followed by 7 days incubation on hormone free medium (standard SE culture). Yucasin (5-(4-Chlorophenyl)-2,4-dihydro-[1,2,4]-triazole-3-thione, CAS 26028-65-9, Sigma 573769) and L-Kynurenine (Sigma k8625, CAS 2922-83-0) were ordered from Sigma and were added to SEIM from a 50mM stock solution in DMSO to a final concentration of 100µM.

For the SE efficiency studies with inhibitors or mutant IZEs, IZEs synchronized in their developmental stage were obtained by manual pollination. For this purpose, the 2 or 3 oldest but still closed flower buds of primary inflorescence stems were emasculated and pollinated and 12 days after pollination (dap) IZEs were

excised from the ovule using a dissecting microscope. Per two parent plants, 2-3 sets of 2-3 closed flower buds were emasculated.

To keep data comparable between inhibitor experiments, large-scale experiments were set up as follows: the 100µM yucasin, 100µM L-kynurenine and 2,4-D control treatments were performed in duplicate for all 2,4-D pre-induction periods (0, 3 and 5 days). Per treatment, 48 IZEs were used, one IZE per well in a 48-wells plate. For the 3 and 5 days induction, a large pool of IZEs was cultured in multiple 48-wells plates. At day 3 and day 5 48 IZEs were selected randomly out of the different plates for each treatment and transferred to plates containing 2,4-D and 100µM inhibitor. For the day 0 treatment 4 siliques were used to compile 1 plate per treatment (12 IZEs per silique).

The mutant studies were performed by culturing 48 IZEs per genotype in duplicates.

For confocal or light microscopy analysis non-synchronized late IZEs from more or less the same developmental stage were selected based on their size as described by (Gaj, 2011). Broken or damaged IZEs were discarded and not used.

Statistics of SE

To quantify SE, four categories were used to score 1) embryogenic tissue (also referred to as embryogenic callus), if no individual somatic embryos were found but embryogenic tissue developed. Embryogenic tissue was defined as smooth green structures without trichomes, that either looked like fused cotyledons or like fused zygotic embryos 2) SE forming IZEs, if individual somatic embryos were observed that were attached to the IZE by their root pole. In that case, the number of individual somatic embryos was counted. 3) Non-embryogenic callus forming IZEs, if callus was formed that remained white-yellowish without developing somatic embryos or embryogenic tissue 4) Dead IZEs, if the tissue turned white, showed no growth and maintained their original size.

Category 1 and 2 were merged to quantify the number of responding IZEs that produced embryogenic tissue. The SE efficiency was then calculated as (Luo and Koop, 1997)

$$SE\ efficiency = \frac{N_r}{N_t} \quad 100\%$$

N_r = the number of responding explants. N_t = total number of explants tested.

SE productivity was calculated as

$$SE\ productivity = \frac{N_i}{N_t}$$

N_i = the number of individual somatic embryos observed. N_t = the total number of IZEs that were tested (including the ones that died).

Statistics for SE efficiency were performed in Microsoft Excel, using the χ^2-test for association (Holmes et al., 2011). For SE productivity, a Welch *t*-test was performed in Rstudio (Pace, 2015).
For inhibitor studies we compared the control treatments to check whether refreshment of SEIM would contribute to SE efficiency and productivity. The two controls were not statistically different for SE efficiency and productivity (respectively χ^2_{calc}=2.9, and *t*-test p-value 0.524, described in Chapter 2) and for this reason we performed all statistical tests between the treatment and the 0 days control.

GUS staining

Staining for B-glucuronidase (GUS) activity was performed as described by Malamy and Benfey (1997) with the following modifications: The staining solution was made as follows: a K/NaPI buffer was made by adding approximately 50mL 0.5M KH_2PO_4 to 125mL 0.5M Na_2HPO_4 tuntil pH reached 7.0.40mL of this solution was diluted with MilliQ to 200mL, and.subsequently2mL 1M EDTA (pH8.0), 2mL 0.1M $K_4Fe(CN)_6$, 2mL 0.1M ($K_3Fe(CN)_6$ and 200uL 0.1% Triton were added. X-gluc (Duchefa, X1402) was pre-dissolved in DMSO at 100mg/mL and was added to the staining solution at a final concentration of 1mg/mL. The bottle with the solution was wrapped in aluminium foil and stored at 4°C for a maximum of 6 months. Samples were submerged in 1-2mL staining solution and incubated for 3hr at 37°C followed by overnight incubation at room temperature to increase staining. Samples were destained with 0.24M HCL 20% methanol for 15min at 55°C, followed by 15min incubation in 7% (w:v) natriumhydroxide/ 60% ethanol for clearing. Samples were rehydrated through an ethanol series 50% - 30% - 10% - 5%, with 5min incubation between each step. To completely remove chlorophyll from the embryos, samples were then cleared for at least 1hr with a 25% (w:v) chloralhydrate in 50% glycerol solution.
Images were taken with a stereomicroscope Leica DC 500 using the Leica Application Suite v2.8.1 software or a DIC/Nomarski AxioCam using AxioVision40 V4.7.2.0 software and a 10x objective. Image editing was performed with FIJI and Adobe Photoshop CS5.1 and figures were assembled in Adobe Illustrator CS5.1.

Histology

To make thin longitudinal sections of IZEs, samples were fixated overnight at 4°C in 2% (w:v) paraformaldehyde/ 2.5% (v:v) gluteraldehyde/ 1x phosphate buffered saline (PBS, pH7.4, 8g NaCl, 0.2g KCl, 1.44g Na_2HPO_4, 0.24g KH_2PO_4 per liter) and colored with osmium for a few seconds for visibility during the embedding process. Samples were washed twice in PBS for 15min. Samples were then dehydrated through an ethanol serie 70% - 80% - 90% - 96% - 100% for at least one hour per step. Subsequently, samples were incubated twice in propylene oxide for 15min and in a 1:1 propylene:EPON mixture for 2hr at room temperature. The remaining propylene oxide: EPON mix was then added to the samples and left overnight. Samples were embedded by filling up molds with EPON and carefully placing the samples into the molds with the root pointing downwards and cotyledons upwards in the same x,y plane. Samples were then left to dry overnight at 60°C. The EPON embedded samples were cut longitudinal, at 2µm using a microtome and glass knives. The slices were then stained with 1% (w:v) Toluidine Blue O/1% (w:v) borax for 20-25s and covered in a thin layer of EPON with a cover glass on an object glass. Slides were left overnight at 60°C to dry. Photos were taken with a DIC/Nomarski ZEISS AxioCam using AxioVision40 V4.7.2.0 software and a 20x and 100x objective. Image editing was performed with FIJI and Adobe Photoshop CS5.1 and figures were assembled in Adobe Illustrator CS5.1.

Microscopy

Images of (GUS stained) IZEs were taken with Leica DC 500 stereomicroscope using the Leica Application Suite v2.8.1 software or a Zeiss Axioplan DIC/Nomarski microscope equipped with Axiocam MRc5 camera and AxioVision40 V4.7.2.0 software and a 10x objective. Image editing was performed in FIJI and Adobe Photoshop CS5.1 and figures were assembled in Adobe Illustrator CS5.1

Confocal Laser Scanning Microscopy (CSLM) was performed with a ZEISS LSM510 exciter equipped with argon and helium/neon lasers. GFP and YFP were detected using a 488nm band pass filter for excitation and a 500-530nm band pass filter for emission. Simultaneously, chlorophyll background fluorescence was captured with a 650nm long pass emission filter. RFP was excited at 530nm and was captured with a 550-600nm band pass emission filter. Images were captured with ZEISS ZEN2009 software.

Samples were prepared on a microscope slide by embedding IZEs in a thin layer of 0.5% low melting point agarose, and adding a droplet of water before covering with a cover slip.

Construction of phylogenetic tree

Genomic sequences for *YUCCAs* were obtained from the TAIR database (www.arabidopsis.org, visited 2015) and a radial phenogram was constructed using www.phylogeny.fr (Dereeper et al., 2008, 2010; Edgar, 2004; Castresana, 2000; Guindon and Gascuel, 2003; Anisimova and Gascuel, 2006; Chevenet et al., 2006, visited 2015).

Acknowledgements

C.P. was supported by an NWO-TTI-Green Genetics core project grant (NWO 828.11.004) to R.O. from the Earth and Life Sciences Division with financial support from the Netherlands Organisation for Scientific Research (NWO). We thank Gerda Lamers for her help with microscopy.

Supplemental information

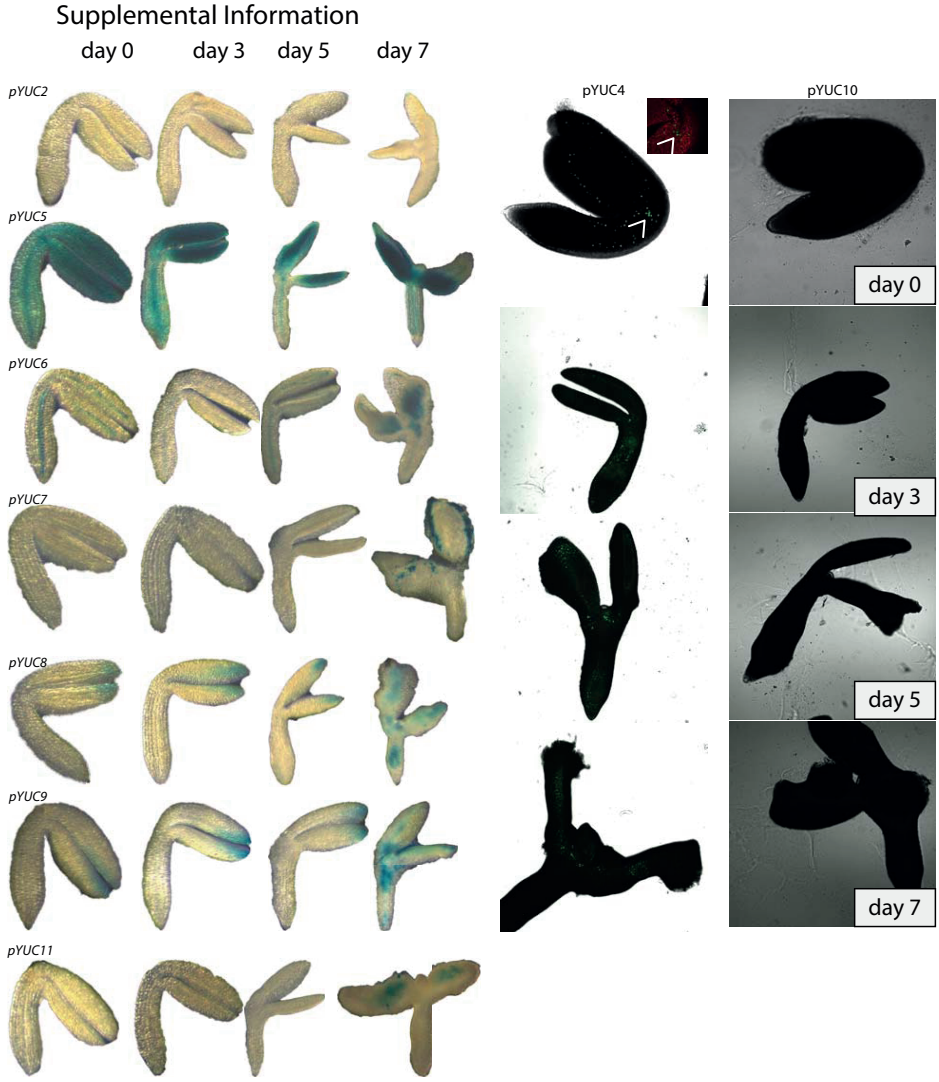

FIGURE S1 - *YUC* promoter expression in IZEs during 2,4-D induced SE. Representative images of GUS or GFP driven by *YUC* promoters in *Arabidopsis* IZEs on day 0, day 3, day 5 and day 7. The white arrowhead marks the shoot apical meristem.

TABLE S1 - *YUC* promoter expression in IZEs during 2,4-D induced SE. Observation frequencies of GUS or GFP driven by *pYUCx* promoters in *Arabidopsis* IZEs on day 0, day 3, day 5 and day 7.

		DAY 0	DAY 3	DAY 5	DAY 7			DAY 0	DAY 3	DAY 5	DAY 7
pYUC2	Cotyledon	4	0	0	0	**pYUC5**	Cotyledon	100	100	100	100
	SAM	0	0	0	0		SAM	100	100	100	100
	Hypocotyl	0	0	0	0		Hypocotyl	100	100	100	100
	Root	0	0	0	0		Root	100	100	100	100
	Callus	0	0	0	0		Callus	0	0	100	100
	n	28	28	28	32		n	34	34	34	34
pYUC4	Cotyledon	100	50	20	40	**pYUC7**	Cotyledon	0	0	0	89
	SAM	100	80	50	80		SAM	0	0	0	6
	Hypocotyl	100	60	10	0		Hypocotyl	0	0	0	6
	Root	0	0	0	0		Root	0	0	0	0
	Callus	0	0	0	80		Callus	0	0	0	83
	n	10	10	10	10		n	27	27	29	35
pYUC6	Cotyledon	29	43	76	100	**pYUC8**	Cotyledon	55	88	100	97
	SAM	0	0	14	100		SAM	0	0	12	79
	Hypocotyl	29	96	76	100		Hypocotyl	0	0	0	76
	Root	29	22	57	27		Root	0	0	0	31
	Callus	0	0	0	100		Callus	0	0	0	97
	n	28	23	37	22		n	31	17	17	29
pYUC10	Cotyledon	0	0	0	0	**pYUC9**	Cotyledon	46	100	96	90
	SAM	0	0	0	0		SAM	0	0	7	25
	Hypocotyl	0	0	0	0		Hypocotyl	0	0	4	60
	Root	0	0	0	0		Root	0	0	21	10
	Callus	0	0	0	0		Callus	0	0	0	45
	n	10	10	10	9		n	24	19	28	20
pYUC11	Cotyledon	0	0	0	56						
	SAM	0	0	0	0						
	Hypocotyl	0	0	0	0						
	Root	0	0	0	0						
	Callus	0	0	0	81						
	n	18	11	26	27						

TABLE S2 - Frequency table for Figure 6e. *DR5::GUS* observations for cotyledon tips (Co-t), cotyledons base (Co-b), callus (Ca), shoot apical meristem (SAM), hypocotyl (Hy) and root (Ro) in Col-0 and *wei8-1 tar1-1 tar2-2/+* after 5 and 7 days standard SEIM culture.

	D5		D7	
Co-t	77%	58%	48%	45%
Co-b	100%	88%	77%	57%
Ca	69%	56%	100%	95%
SAM	4%	41%	19%	8%
Hy	62%	75%	55%	25%
Ro	85%	78%	84%	72%
n	26	64	31	60

TABLE S3 - Plant lines used, with their origin and selection method

PLANT LINE	ORIGIN	SELECTION	ADDITIONAL INFORMATION
pWOX2::NLS:YFP	Breuninger et al. 2008	ppt	
DR5::RFP	Eva Benkova	hyg	
yuc1 yuc10 yuc11	Cheng et al. 2006,2007	PCR	
yuc2 yuc4 yuc6	Cheng et al. 2006,2007	PCR	
yuc3 yuc9	Robert et al. 2013	PCR	yuc3 (GK-376G12, part of set 436084) yuc9 (sail_871_G01)
yuc4 yuc9	Robert et al. 2013	PCR	*yuc4* from Cheng et al. (2006) yuc9 (sail_871_G01)
yuc8	SALK	PCR	N655757/SALK_096110C
yuc9	SALK	PCR	sail_871_G01
wei8-1 tar1-1 tar2-2/+ DR5::GUS	SALK	PCR	N16420/ CS1642
YUC2p:eGFP-GUS	Robert, H.	kan	T3.303.2
YUC4p:3xnGFP	Robert, H.	kan	T4.25W-3.3.1
YUC5p:eGFP-GUS	Robert, H.	kan	T3.104.5
YUC6p:eGFP-GUS	Robert, H.	kan	T3.401.2
YUC7p:eGFP-GUS	Robert, H.	kan	T3.405.5
YUC8p:eGFP-GUS	Robert, H.	kan	T3.204.1
YUC9p:eGFP-GUS	Robert, H.	kan	T3.203.1
YUC10p:3xnGFP	Robert, H.	kan	T4-2.1.1.2
YUC11p:eGFP-GUS	Robert, H.	kan	T3.301.1

TABLE S4 - Primer sequences for genotyping. GSP is gene specific primer, BP is border specific primer. All reactions were carried out with genomic DNA, DreamTaq polymerase, melting temperature = 55ºC, annealing time = 60s, unless otherwise stated.

GENE	PRIMER ORIENTATION	SEQUENCE (5′ - 3′)	REMARKS
yuc1	GSP left	GGTTCATGTGTTGCCAAGGGA	Tm = 61C
	GSP right	CCTGAAGCCAAGTAGGCACGTT	
	Border	LBB1.3 salk	
yuc2	GSP left	CTGCATACAATCCGCTTTCGC	
	GSP right	TTCTTGCATTTTCTCGCTCTACG	
	Border	LBB1.3 salk	
yuc3	GSP left	ATATTGACCATCATACTCATTGC	
	GSP right	TTATAGCCCCTAAAACAGAGCATC	
yuc4	GSP left	CCCTTCTTAGACCTACTCTAC	
	GSP right	GCCCAACGTAGAATTAGCAAG	
	Border	TACGAATAAGAGCGTCCATTTTAGAGTGA	
yuc6	GSP left	CCAGCCTTTGTATTTTCCCGT	
	GSP right	CCGGAAAAAGGGTTCTTGTCG	
	Border	LBB1.3 salk	
yuc8	GSP left	GACTCACTCTTCGACACGGTC	
	GSP right	GAACCGGGTAGCGTAAGACTC	
	Border	LBB1.3 salk	
yuc9	GSP left	TTAAGCAACTGAGATGCATC	Tm = 55C, At = 45s
	GSP right	TAGCATCTGAATTTCATAACCAATCTCGATACAC	
	Border	LB1 sail	
yuc10	GSP left	CCTGAATCTCGCCATCGCGAATC	
	GSP right	CCAAAGAGCTTTTCGTCAACTACC	
	Border	CGTGTGCCAGGTGCCCACGGAATAGT	
yuc11	GSP left	TGTCAACTCCCTCACATGCCA	
	GSP right	CAGATCTCCATCATCGACCTGTGT	
	Border	JMLB1	
wei8-1	GSP left	CATCAGAGAGACGGTGGTGAAC	
	GSP right	GCTTTTAATGAGCTTCATGTTGG	
	Border	DWLB1	
tar1-1	GSP left	CACCATGATGGTTGGGTGTGAAAACTC	
	GSP right	AGGCTCGACGCATTTGAGATC	
	Border	DWLB1	
tar2-2	GSP left	GCACGCAAGTGAAGCTCCAAGC	
	GSP right	ATACTGTGGCCAATAGTAAGCC	
	Border	JMLB1	

LB1 sail	GCCTTTTCAGAAATGGATAAATAGCCTTGCTTCC
LBB1.3 salk	ATTTTGCCGATTTCGGAAC
JMLB1	GGCAATCAGCTGTTGCCCGTCTCACTGGTG
DWLB1	CATACTCATTGCTGATCCATGTAGATTTCC

References

Anisimova, M. and Gascuel, O. (2006). Approximate likelihood-ratio test for branches: a fast, accurate, and powerful alternative. Syst. Biol. **55**: 539–552.

Bai, B., Su, Y.H., Yuan, J., and Zhang, X.S. (2013). Induction of somatic embryos in *Arabidopsis* requires local *YUCCA* expression mediated by the downregulation of ethylene biosynthesis. Mol. Plant **6**: 1247–1260.

Boutilier, K., Offringa, R., Sharma, V.K., Kieft, H., Ouellet, T., Zhang, L., Hattori, J., Liu, C., van Lammeren, A.A.M., Miki, B.L.A., Custers, J.B.M., and van Lookeren Campagne, M.M. (2002). Ectopic expression of *BABY BOOM* triggers a conversion from vegetative to embryonic growth. Plant Cell **14**: 1737–1749.

Breuninger, H., Rikirsch, E., Hermann, M., Ueda, M., and Laux, T. (2008). Differential expression of *WOX* Genes mediates apical-basal axis formation in the *Arabidopsis* embryo. Dev. Cell **14**: 867–876.

Castresana, J. (2000). Selection of conserved blocks from multiple alignments for their use in phylogenetic analysis. Mol. Biol. Evol. **17**: 540–552.

Cheng, Y. (2006). Auxin biosynthesis by the *YUCCA* flavin monooxygenases controls the formation of floral organs and vascular tissues in *Arabidopsis*. Genes Dev. **20**: 1790–1799.

Cheng, Y., Dai, X., and Zhao, Y. (2007). Auxin synthesized by the *YUCCA* flavin monooxygenases is essential for embryogenesis and leaf formation in *Arabidopsis*. Plant Cell **19**: 2430–2439.

Chevenet, F., Brun, C., Bañuls, A.-L., Jacq, B., and Christen, R. (2006). TreeDyn: towards dynamic graphics and annotations for analyses of trees. BMC Bioinformatics **7**: 439.

Dereeper, A., Audic, S., Claverie, J.-M., and Blanc, G. (2010). BLAST-EXPLORER helps you building datasets for phylogenetic analysis. BMC Evol. Biol. **10**: 8.

Dereeper, A., Guignon, V., Blanc, G., Audic, S., Buffet, S., Chevenet, F., Dufayard, J.-F., Guindon, S., Lefort, V., Lescot, M., Claverie, J.-M., and Gascuel, O. (2008). Phylogeny.fr: robust phylogenetic analysis for the non-specialist. Nucleic Acids Res. **36**: W465–W469.

Edgar, R.C. (2004). MUSCLE: multiple sequence alignment with high accuracy and high throughput. Nucleic Acids Res. **32**: 1792–1807.

Friml, J., Vieten, A., Sauer, M., Weijers, D., Schwarz, H., Hamann, T., Offringa, R., and Jürgens, G. (2003). Efflux-dependent auxin gradients establish the apical-basal axis of *Arabidopsis*. Nature **426**: 147–153.

Gaj, M.D. (2001). Direct somatic embryogenesis as a rapid and efficient system for in vitro regeneration of *Arabidopsis thaliana*. Plant Cell. Tissue Organ Cult. **64**: 39–46.

Gaj, M.D. (2011). Somatic embryogenesis and plant regeneration in the culture of *Arabidopsis* thaliana (L.) Heynh. immature zygotic embryos. Methods **710**: 257–265.

Giraudat, J. (2003). Practical course on genetic and molecular analysis of *Arabidopsis*. In EMBO course, J. Giraudat, ed (EMBO), pp. 1–21.

Guindon, S. and Gascuel, O. (2003). A simple, fast, and accurate algorithm to estimate large phylogenies by maximum likelihood. Syst. Biol. **52**: 696–704.

Hall, A.E., Findell, J.L., Schaller, G.E., Sisler, E.C., and Bleecker, A.B. (2000). Ethylene perception by the ERS1 protein in *Arabidopsis*. Plant Physiol. **123**: 1449–1458.

He, W., Brumos, J., Li, H., Ji, Y., Ke, M., Gong, X., Zeng, Q., Li, W., Zhang, X., An F., Wen, X., Li, P., Chu, J., Sun, X., Yan, C., Yan, N., Xie, D-D., Raikhel, N., Yang, Z., Stepanova, A., Alonso, J.M., and Guo H. (2011). A small-molecule screen identifies L-kynurenine as a competitive

inhibitor of TAA1/TAR activity in ethylene-directed auxin biosynthesis and root growth in *Arabidopsis*. Plant Cell **23**: 3944–3960.

Heidman, I. (2015). Applied and fundamental aspects of *BABY BOOM*-mediated regeneration. Thesis, Wageningen Univ.

Holmes, D., Moody, P., and Dine, D. (2011). Research methods for biosciences 2nd ed. O. university Press, ed (Oxford University Press).

Ikeuchi, M., Sugimoto, K., and Iwase, A. (2013). Plant callus: mechanisms of induction and repression. Plant Cell **25**: 3159–3173.

Jiménez, V.M. (2005). Involvement of Plant Hormones and Plant Growth Regulators on in vitro somatic embryogenesis. Plant Growth Regul. **47**: 91–110.

Junker, A. and Bäumlein, H. (2012). Multifunctionality of the *LEC1* transcription factor during plant development. Plant Signal. Behav. **7**: 1718–1720.

Korasick, D. A., Enders, T. A., and Strader, L.C. (2013). Auxin biosynthesis and storage forms. J. Exp. Bot. **64**: 2541–2555.

Kurczyńska, E.U., Gaj, M.D., Ujczak, A., and Mazur, E. (2007). Histological analysis of direct somatic embryogenesis in *Arabidopsis thaliana* (L.) Heynh. Planta **226**: 619–628.

Li, J., Dai, X., and Zhao, Y. (2006). A role for *AUXIN RESPONSE FACTOR19* in auxin and ethylene signaling in *Arabidopsis*. Plant Physiol. **140**: 899–908.

Ljung, K. (2013). Auxin metabolism and homeostasis during plant development. Development **140**: 943–950.

Lotan, T., Ohto, M., Yee, K.M., West, M. A., Lo, R., Kwong, R.W., Yamagishi, K., Fischer, R.L., Goldberg, R.B., and Harada, J.J. (1998). *Arabidopsis LEAFY COTYLEDON1* is sufficient to induce embryo development in vegetative cells. Cell **93**: 1195–1205.

Luo, Y. and Koop, H.U. (1997). Somatic embryogenesis in cultured immature zygotic embryos and leaf protoplasts of *Arabidopsis thaliana* ecotypes. Planta **202**: 387–396.

Malamy, J.E. and Benfey, P.N. (1997). Organization and cell differentiation in lateral roots of *Arabidopsis thaliana*. Development **124**: 33–44.

Marhavý, P., Bielach, A., Abas, L., Abuzeineh, A., Duclercq, J., Tanaka, H., Pařezová, M., Petrášek, J., Friml, J., Kleine-Vehn, J., and Benková, E. (2011). Cytokinin modulates endocytic trafficking of PIN1 auxin efflux carrier to control plant organogenesis. Dev. Cell **21**: 796–804.

Mano, Y. and Nemoto, K. (2012). The pathway of auxin biosynthesis in plants. J. Exp. Bot. 63: 2853–2872.

McDaniel, B.K. and Binder, B.M. (2012). *ETHYLENE RECEPTOR1* (*ETR1*) is sufficient and has the predominant role in mediating inhibition of ethylene responses by silver in *Arabidopsis thaliana*. J. Biol. Chem. **287**: 26094–26103.

Michalczuk, L., Ribnicky, D.M., Cooke, T.J., and Cohen, J.D. (1992). Regulation of indole-3-acetic acid biosynthetic pathways in carrot cell cultures. Plant Physiol. **100**: 1346–1353.

Nicol, F., His, I., Jauneau, A., Vernhettes, S., Canut, H., and Höfte, H. (1998). A plasma membrane-bound putative endo-1,4-β-D-glucanase is required for normal wall assembly and cell elongation in *Arabidopsis*. EMBO J. **17**: 5563–5576.

Nishimura, T., Hayashi, K.-I., Suzuki, H., Gyohda, A., Takaoka, C., Sakaguchi, Y., Matsumoto, S., Kasahara, H., Sakai, T., Kato, J.-I., Kamiya, Y., and Koshiba, T. (2014). Yucasin is a potent inhibitor of YUCCA, a key enzyme in auxin biosynthesis. Plant J. **77**: 352–66.

Nowak, K., Wójcikowska, B., and Gaj, M.D. (2014). *ERF022* impacts the induction of somatic embryogenesis in *Arabidopsis* through the ethylene-related pathway. Planta **241**: 967–985.

Nowak, K., Wojcikowska, B., Szyrajew, K., and Gaj, M.D. (2012). Evaluation of different embryogenic systems for production of true somatic embryos in *Arabidopsis*. Biol. Plant. **56**: 401–408.

Pace, L. (2015). Beginning R: an introduction to statistical programming (Apress).

Panoli, A., Martin, M.V., Alandete-Saez, M., Simon, M., Neff, C., Swarup, R., Bellido, A., Yuan, L., Pagnussat, G.C., and Sundaresan, V. (2015). Auxin import and local auxin biosynthesis are required for mitotic divisions, cell expansion and cell specification during female gametophyte development in *Arabidopsis thaliana*. PLoS One **10**: e0126164.

Pasternak, T.P. (2002). The role of auxin, pH, and stress in the activation of embryogenic cell division in leaf protoplast-derived cells of alfalfa. Plant Physiol. **129**: 1807–1819.

Polko, J.K., Voesenek, L.A.C.J., Peeters, A.J.M., and Pierik, R. (2011). Petiole hyponasty: an ethylene-driven, adaptive response to changes in the environment. AoB Plants **2011**: plr031–plr031.

Raghavan, V. (2004). Role of 2,4-dichlorophenoxyacetic acid (2,4-D) in somatic embryogenesis on cultured zygotic embryos of *Arabidopsis*: cell expansion, cell cycling, and morphogenesis during continuous exposure of embryos to 2,4-D. Am. J. Bot. **91**: 1743–1756.

Reinhardt, D., Pesce, E.-R., Stieger, P., Mandel, T., Baltensperger, K., Bennett, M., Traas, J., Friml, J., and Kuhlemeier, C. (2003). Regulation of phyllotaxis by polar auxin transport. Nature **426**: 255–260.

Robert, H.S., Crhak Khaitova, L., Mroue, S., and Benkova, E. (2015). The importance of localized auxin production for morphogenesis of reproductive organs and embryos in *Arabidopsis*. J. Exp. Bot. **66**: 5029–5042.

Robert, H.S., Grones, P., Stepanova, A.N., Robles, L.M., Lokerse, A.S., Alonso, J.M., Weijers, D., and Friml, J. (2013). Local auxin sources orient the apical-basal axis in *Arabidopsis* embryos. Curr. Biol. **23**: 2506–2512.

Ruzicka, K., Ljung, K., Vanneste, S., Podhorska, R., Beeckman, T., Friml, J., and Benkova, E. (2007). Ethylene regulates root growth through effects on auxin biosynthesis and transport-dependent auxin distribution. Plant Cell **19**: 2197–2212.

De Rybel, B., Audenaert, D., Beeckman, T., and Kepinski, S. (2009). The past, present, and future of chemical biology in auxin research. ACS Chem. Biol. **4**: 987–998.

Sato, S., Kato, T., Kakegawa, K., Ishii, T., Liu, Y-G., Awano, T., Takabe, K., Nishiyama, Y., Kuga, S., Sato, S., Nakamura Y., Tabata, S., and Shibat D. (2001). Role of the putative membrane-bound endo-1,4-beta-glucanase KORRIGAN in cell elongation and cellulose synthesis in *Arabidopsis thaliana*. Plant Cell Physiol. **42**: 251–263.

Sawchuk, M.G. and Scarpella, E. (2015). Control of vein network topology by auxin transport. BMC Biol. **13**: 94.

Simon, S., Kubeš, M., Baster, P., Robert, S., Dobrev, P.I., Friml, J., Petrášek, J., and Zažímalová, E. (2013). Defining the selectivity of processes along the auxin response chain: a study using auxin analogues. New Phytol. **200**: 1034–1048.

Simon, S. and Petrášek, J. (2011). Why plants need more than one type of auxin. Plant Sci. **180**: 454–460.

Song, Y. (2014). Insight into the mode of action of 2,4-dichlorophenoxyacetic acid (2,4-D) as an herbicide. J. Integr. Plant Biol. **56**: 106–113.

Steinwand, B.J., Xu, S., Polko, J.K., Doctor, S.M., Westafer, M., and Kieber, J.J. (2014). Alterations in auxin homeostasis suppress defects in cell wall function. PLoS One **9**: e98193.

Stepanova, A.N., Hoyt, J.M., Hamilton, A.A., and Alonso, J.M. (2005). A link between ethylene and auxin uncovered by the characterization of two root-specific ethylene-insensitive mutants in *Arabidopsis*. Plant Cell **17**: 2230–2242.

Stepanova, A.N., Robertson-Hoyt, J., Yun, J., Benavente, L.M., Xie, D.-Y., Dolezal, K., Schlereth, A., Jürgens, G., and Alonso, J.M. (2008). TAA1-mediated auxin biosynthesis is essential for hormone crosstalk and plant development. Cell **133**: 177–191.

Stepanova, A.N., Yun, J., Robles, L.M., Novak, O., He, W., Guo, H., Ljung, K., and Alonso, J.M. (2011). The *Arabidopsis* YUCCA1 flavin monooxygenase functions in the indole-3-pyruvic acid branch of auxin biosynthesis. Plant Cell **23**: 3961–3973.

Stone, S.L., Braybrook, S. A, Paula, S.L., Kwong, L.W., Meuser, J., Pelletier, J., Hsieh, T.-F., Fischer, R.L., Goldberg, R.B., and Harada, J.J. (2008). *Arabidopsis LEAFY COTYLEDON2* induces maturation traits and auxin activity: Implications for somatic embryogenesis. Proc. Natl. Acad. Sci. **105**: 3151–3156.

Stone, S.L., Kwong, L.W., Yee, K.M., Pelletier, J., Lepiniec, L., Fischer, R.L., Goldberg, R.B., and Harada, J.J. (2001). *LEAFY COTYLEDON2* encodes a B3 domain transcription factor that induces embryo development. Proc. Natl. Acad. Sci. USA **98**: 11806–11811.

Strader, L.C., Chen, G.L., and Bartel, B. (2010). Ethylene directs auxin to control root cell expansion. Plant J **64**: 874–884.

Su, Y.H. and Zhang, X.S. (2014). The hormonal control of regeneration in plants. Curr. Top. Dev. Biol. **108**: 35–69.

Swarup, R., Perry, P., Hagenbeek, D., Van Der Straeten, D., Beemster, G.T.S., Sandberg, G., Bhalerao, R., Ljung, K., and Bennett, M.J. (2007). Ethylene upregulates auxin biosynthesis in *Arabidopsis* seedlings to enhance inhibition of root cell elongation. Plant Cell **19**: 2186–2196.

Tao, Y. et al. (2008). Rapid synthesis of auxin via a new tryptophan-dependent pathway is required for shade avoidance in plants. Cell **133**: 164–176.

Ulmasov, T., Murfett, J., Hagen, G., and Guilfoyle, T.J. (1997). Aux/IAA proteins repress expression of reporter genes containing natural and highly active synthetic auxin response elements. Plant Cell **9**: 1963–1971.

Wójcikowska, B., Jaskóła, K., Gąsiorek, P., Meus, M., Nowak, K., and Gaj, M.D. (2013). *LEAFY COTYLEDON2* (*LEC2*) promotes embryogenic induction in somatic tissues of *Arabidopsis*, via *YUCCA*-mediated auxin biosynthesis. Planta **238**: 425–40.

Won, C., Shen, X., Mashiguchi, K., Zheng, Z., Dai, X., Cheng, Y., Kasahara, H., Kamiya, Y., Chory, J., and Zhao, Y. (2011). Conversion of tryptophan to indole-3-acetic acid by TRYPTOPHAN AMINOTRANSFERASES and YUCCAs in *Arabidopsis*. Proc. Natl. Acad. Sci. USA **108**: 18518–23.

Woodward, A.W. and Bartel, B. (2005). Auxin: regulation, action, and interaction. Ann. Bot. **95**: 707–735.

Zhao, Y., Christensen, S.K., Fankhauser, C., Cashman, J.R., Cohen, J.D., Weigel, D., and Chory, J. (2001). A role for flavin monooxygenase-like enzymes in auxin biosynthesis. Science 291: 306–309.

Zuo, J., Niu, Wu, Q.-W., Frugis, G., and Chua, N-H. (2002). The *WUSCHEL* gene promotes vegetative-to-embryonic transition in *Arabidopsis*. Plant J. **30**: 349–359.

Chapter 4

Somatic embryogenesis initiation in *Arabidopsis* requires *SOLITARY ROOT/IAA14*-regulated dynamic auxin responses similar to lateral root initiation

Cheryl Philipsen[1,2],
Vera Veltkamp[1,3],
Tanja van den Nadort[1,4],
Remko Offringa[1]

[1] *Molecular and Developmental Genetics, Institute of Biology Leiden, Leiden University, Sylviusweg 72, 2333BE, Leiden, the Netherlands*
[2] *Current affiliation: Dümmen Orange, P.O. Box 26, 2678ZG, de Lier, the Netherlands*
[3] *Current affiliation: Plant Research International, P.O. Box 7, 1600AA Wageningen, the Netherlands*
[4] *Current affiliation: Leiden University Medical Centre, P.O. Box 9600, 2300 RC Leiden, the Netherlands*

Abstract

Somatic embryogenesis (SE), a process where embryos are induced on somatic plant tissues, is used for crop micropropagation to obtain genetically identical and uniform plants. SE is commonly induced by incubating explant tissues on high concentrations of the synthetic auxin analog 2,4-dichlorophenoxyacetic acid (2,4-D). Although previous research in *Arabidopsis* has revealed several genetic candidates involved in SE, the molecular mechanism by which 2,4-D induces SE is still largely unknown. Here we used a combination of chemical biology, mutants and promoter reporter lines to map the auxin response components involved in 2,4-D-induced SE on *Arabidopsis* immature zygotic embryos (IZEs). We employed the auxin antagonist auxinole, blocking the formation of TRANSPORT INHIBITOR RESISTANT1/AUXIN SIGNALING F-BOX (TIR1/AFB) co-receptor complex, and found that this co-receptor complex was required for SE initiation. Furthermore, we found that the activating *AUXIN RESPONSE FACTOR* (*ARF*) sister pairs *ARF7/19* and *ARF6/8* were both required for efficient SE initiation as well. Interestingly, SE was almost completely blocked in the semi-dominant *solitary root-1* (*slr-1*) mutant, indicating that 2,4-D-induced SE and lateral root initiation in *Arabidopsis* share the same auxin response module. The auxin response mutants that were blocked in SE also showed a reduced 2,4-D-induced root callus development, suggesting that this phenotype could be used to pre-select mutants affected in SE. Based on our results we propose a model in which *SLR/IAA14*–regulated dynamic auxin responses are required for both lateral root and embryonic founder cell specification and the subsequent cell divisions starting respectively lateral root and somatic embryo development.

Introduction

Somatic embryogenesis (SE) is a fascinating process in plants by which embryo development is induced on differentiated somatic tissues. In *Arabidopsis*, SE can be efficiently induced on immature zygotic embryos (IZEs) by culturing these IZEs on solid medium containing high concentrations of 2,4-dichlorophenoxyacetic acid (2,4-D), a synthetic analogue of the plant hormone auxin (Gaj, 2011). Subsequently, two SE programs can be observed: 1) direct SE (DSE) referring to somatic embryos formed directly from the epidermal cell layer of late IZEs, and 2) indirect SE (ISE) where somatic embryos are formed from embryonic callus that originates from the sub-epidermal layers of young IZEs (Kurczyńska et al., 2007; Raghavan, 2004). Similar to SE, plant regeneration via organogenesis can also occur directly from somatic cells or indirectly via a callus phase. Callus can be produced from a single differentiated cell and many of the derived callus cells are totipotent, being able to regenerate the whole plant body (Ikeuchi et al., 2013). Callus development during plant regeneration can be divided into three phases, which may also occur during SE. Firstly, in the dedifferentiation phase, somatic cells adopt a stem cell state in response to exogenously applied hormones. In the second phase, the callus cells are reprogrammed and determined to form a specific organ depending on the hormone balance in the medium. Several callus types exist that are classified as rooty, shooty, or embryonic callus, depending on the organs they regenerate, or as friable callus that does not regenerate organs. The third or morphogenesis phase of the regeneration process involves the actual formation of the new organs and occurs independent of exogenously applied hormones (Su and Zhang, 2014). Evidence has emerged that during the dedifferentiation phase, somatic cells are not completely dedifferentiated to an omnipotent stem cell state, but rather resemble the stem cells in the root pericycle that give rise to lateral root formation (Atta et al., 2008; Sugimoto et al., 2010; Ikeuchi et al., 2013). Cell dedifferentiation and cell fate specification involve the molecular regulation and action of the natural auxin indole-3-acetic acid (IAA).

Auxin is perceived in the nucleus of plant cells by the TRANSPORT INHIBITOR RESISTANT1/AUXIN SIGNALING F-BOX (TIR1/AFB) F-box proteins and the AUXIN/INDOLEACETIC ACID (AUX/IAA) auxin co-receptors. The *Arabidopsis* genome encodes 6 TIR1/AFB proteins, which together with one of the 29 AUX/IAA proteins from a hydrophobic binding pocket for auxin. TIR1/AFBs interact with other proteins (ASK1, CUL1, RBX) to form the $SCF^{TIR1/AFB}$ E3 ubiquitin protein ligase complex. In the presence of auxin, this complex recruits the Aux/IAA co-receptors and labels these repressor proteins by ubiquitination for degradation by the

26S proteasome (Maraschin et al., 2009; Dharmasiri et al., 2005a, 2005b; Parry et al., 2009). Most Aux/IAAs consist of three conserved domains. The N-terminal domain I (DI) is required for transcriptional repression and recruits co-repressor proteins like TOPLESS (TPL) and the middle domain II (DII) is responsible for protein stability and interacts directly with auxin and the TIR1/AFB auxin co-receptors (Wang and Estelle, 2014). Finally, through their conserved C terminal domain Aux/IAAs interact with Auxin Response Factors (ARFs) that bind to the auxin response elements (AuxREs) in the promoters of auxin responsive genes (Weijers and Wagner, 2016). Recently, evidence has emerged that both Aux/IAAs and ARFs form a type I/II Phox and Bem1p (PB1) protein-protein interaction domain in their C-terminus that is required for this interaction (Korasick et al., 2014).

The auxin-dependent Aux/IAA degradation releases repression of ARFs and allows transcriptional activation of auxin responsive genes. Each TIR1/AFB receptor has different binding affinities for specific Aux/IAA proteins (Calderón Villalobos et al., 2012; Parry et al., 2009). Furthermore, each TIR1/AFB – Aux/IAA co-receptor pair has a different binding affinity for the different natural or synthetic auxins. The affinity for each (synthetic) auxin and co-receptor has not been elucidated yet.

The *Arabidopsis* genome encodes 22 full-length ARFs and three of partial length, (Guilfoyle and Hagen, 2007). The full length ARFs consist of different functional protein domains, including a B3 DNA-binding domain (DBD) and a middle domain that through its amino acid sequence determines whether an ARF acts as a repressor or activator. Based on promoter reporter assays in protoplasts, five *Arabidopsis* ARFs (ARF5-8 and ARF19) were identified as transcriptional activators and the remaining ARFs as transcriptional repressors (Tiwari et al., 2003). The transcriptionally activating ARFs possess an glutamine-enriched middle region that acts as activation domain (AD), whereas repressing ARFs have P,S, and T rich middle region that in some ARFs even contains an EAR repression domain (RD). Recent research revealed extra domains, two dimerization domains (DDs) flanking the DBD, and a Tudor-like ancillary domain in the C-terminal region of the flanking domain (FD). Tudor domains have been shown to bind methylated histones but the methylated domain is lacking in ARFs and thus its function remains unknown (Guilfoyle, 2015; Wright and Nemhauser, 2015; Adams-Cioaba et al., 2012). The DDs facilitate binding of ARFs as dimers to the AuxREs. The ARF - AuxRE binding is sequence specific and multiple motifs have been identified, from which the generic TGTCTC sequence was deduced that has been used to generate the *DR5* promoter that is abundantly used to monitor auxin responses

in plants (Ulmasov et al., 1997) and the more recently discovered specific TGTCGG (Boer et al., 2014).

Four of the activating ARFs can be grouped in sister pairs based on structural- and functional-similarities. The ARF6/8 pair is involved in growth, anther maturation and fruit initiation, and the ARF7/19 pair in lateral root initiation (Okushima et al., 2005; Guilfoyle and Hagen, 2007).

The large diversity in ARFs and Aux/IAAs combined with TIR/AFBs can result in a huge array of diverse, yet specific auxin responses. In total, 6 TIR1/AFBs, 29 Aux/IAAs and 23 ARFs can lead to 4002 hypothetical different auxin responses, which in turn will result in a different onset or attenuation of auxin responsive genes. In addition, expression of auxin responsive genes can be dependent on the degradation dynamics of Aux/IAAs, as was recently shown for IAA14 (Guseman et al., 2015).

The complexity of the mechanism by which different auxin response modules act to coordinate plant development is well illustrated by lateral root development. IAA28 has been described to specify lateral root (LR) founder cell identity and LR initiation is then induced by the SOLITARY ROOT (SLR) /IAA14 – ARF719 module (Fukaki et al., 2002, 2005). Together with the downstream BODENLOSS (BDL)/IAA12 -MONOPTEROS (MP)/ARF5 module it regulates lateral root initiation by specifying cell fate similar to hypophysis specification during zygotic embryogenesis (De Smet et al., 2010; Rademacher et al., 2012). Emergence of the LR through the outer cell layers of the root is subsequently facilitated by SHORT HYPOCOTYL2 (SHY2)/IAA3 together with auxin influx transporter LIKE- AUX1 3 (LAX3) (Goh et al., 2012; Swarup et al., 2008).

Due to the many possibilities of auxin responses the question arises which specific TIR1/AFBs, Aux/IAAs and ARFs act in concert to initiate SE. Here we used reporter lines to identify which auxin response components are expressed during SE, and subsequently tested loss- and gain-of-function mutants of individual auxin response components in our SE system to verify their involvement in the process. By using the direct SE induction system, we show that the TIR/AFB co-receptors and all *Arabidopsis* activating *ARF* genes are expressed during SE initiation. We also demonstrate that ARF sister pairs *ARF7/19* and *ARF6/8* are required with a specific role for the IAA14- ARF7/19 lateral root module in SE. Based on this we show that 2,4-D induced root callus development can be used as a quick test system to identify candidate genes involved in SE. Based on our results, we propose a mechanism in which *SLR/IAA14*–regulated dynamic auxin responses are required for both lateral root and embryonic founder cell specification starting respectively lateral root and somatic embryo development.

Results

The TIR1/AFB-mediated auxin response is required for SE initiation

To investigate whether the TIR1/AFBs are required for SE, single *Arabidopsis tir1-1, afb1, afb2 and afb3* loss-of-function mutant alleles were tested for the efficiency of SE induction from immature zygotic embryos (IZEs, Chapter 2). In short, IZEs obtained 12 days after pollination were cultured for 14 days on 4.5µM 2,4-D and subsequently transferred to hormone free medium to allow somatic embryos to grow out. IZEs from the mutant alleles did not show a significantly different SE efficiency compared to wild-type IZEs (Figure S1), which is probably due to genetic redundancy (Parry et al., 2009). Using translational GUS reporters we explored the expression of *TIR1*, *AFB1*, *AFB2* and *AFB3* during SE (Parry et al., 2009, Figure 1). Interestingly, *TIR1* and *AFB2* showed specific differential expression at the base of the cotyledons, the sites where somatic embryos (SEs) mostly occurred in our SE system, with no or only very weak expression on days 0 and 3, and a significantly increased expression on days 5 and 7 after the start of incubation. *AFB1* also showed enhanced expression at sites of SE initiation, but its expression in IZEs was already relatively high at day 0 and 3. Morphological defects in flower and silique development of triple and quadruple *tir1/afb* mutant plants prevented the availability and use of IZEs from these mutant lines. To overcome TIR1/AFB redundancy and circumvent the morphological defects, we blocked TIR1/AFB-mediated signalling by applying the auxin antagonist auxinole (Hayashi et al., 2012, 2008). Immediate treatment of IZEs with 50 or 100µM auxinole resulted in death of the IZEs (Figure 2a, e, Table S1). IZEs that were pre-induced on SEIM for 3 or 5 days before transfer to SEIM plates supplemented with 100µM auxinole for respectively 11 or 9 days also mostly died (Figure 2a, d, g), whereas transfer to medium with 50µM auxinole resulted in viable IZEs that showed a significant decrease in SE efficiency (Figure 2a, c, f, Table S1). Surviving auxinole-treated IZEs formed white callus from which root and shoot structures regenerated (Figure 2c, d, f, g). Simultaneous analysis of the embryonic cell fate reporter *pWOX2::NLS-YFP* (Breuninger et al., 2008) and the *DR5::RFP* auxin response reporter showed that in IZEs that were induced for 3 days on SEIM and were subsequently treated for 48hr with 100µM auxinole the expression of the reporters was comparable to that in IZEs incubated on hormone free medium (Figure 2h-j). These results showed that the 2,4-D-triggered TIR1/AFB-mediated auxine response is required for IZE survival on SEIM medium as well as for the 2,4-D induced auxin response that triggers SE.

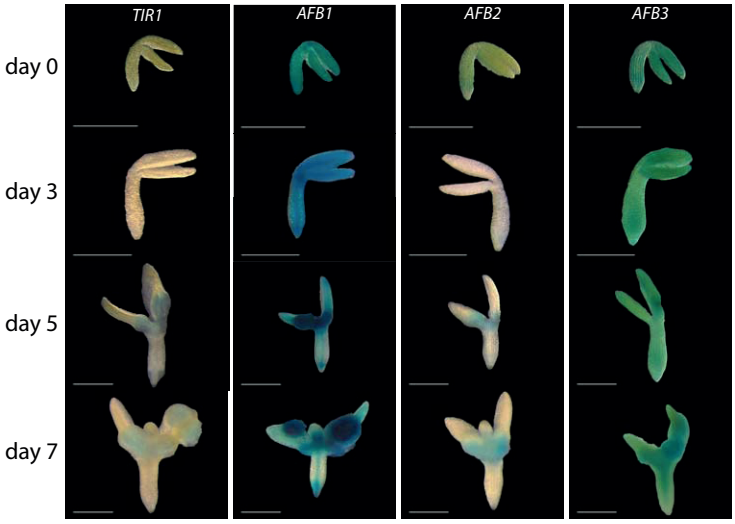

FIGURE 1 - *TIR1/AFB* genes are expressed during *Arabidopsis* SE initiation.
Expression of *TIR1/AFB* genes in IZEs after 0, 3, 5 and 7 days incubation on SEIM, as reported by translational *pTIR1::TIR1-GUS*, *pAFB1::cAFB1-GUS*, *pAFB2::cAFB2-GUS* and *pAFB3::cAFB3-GUS* fusions, Representative images are shown (n=30). Scale bar is 500µm. Please note that for presentation purposes the original background of the IZE images was removed and replaced by a black background.

The activating ARF sister-pairs ARF6/8 and ARF7/19 are involved in SE initiation

Since the auxin response observed during SE initiation must be mediated by activating *ARFs*, we used corresponding promoter-GFP fusions to see which of the corresponding *ARF* genes were expressed and induced in the relevant regions during SE initiation (Figure 3). This analysis showed that, surprisingly, the expression of all five activating *ARF* genes was expressed during SE initiation, and that all five *ARF* genes were expressed at day 7 in the proximal side of the cotyledon where SEs arose. *ARF5* (Figure 3a,d) and *ARF6* (Figure 3b,e) were expressed in the entire IZE on day 5 and day 7, whereas *ARF8* was only expressed in a few cells in the basal and proximal site of the cotyledons of the IZE (Figure 3c,f). *ARF7* expression started at day 7 in the cotyledons and in callus developing on the cotyledons (Figure 3g-j). *ARF19* was expressed in a few cells in the cotyledons and in the proximal area of the cotyledons on day 5 (Figure 3k-n). Results are summarized in a schematic representation of the IZE after 5 and 7 days of SEIM culture (Figure 3o).

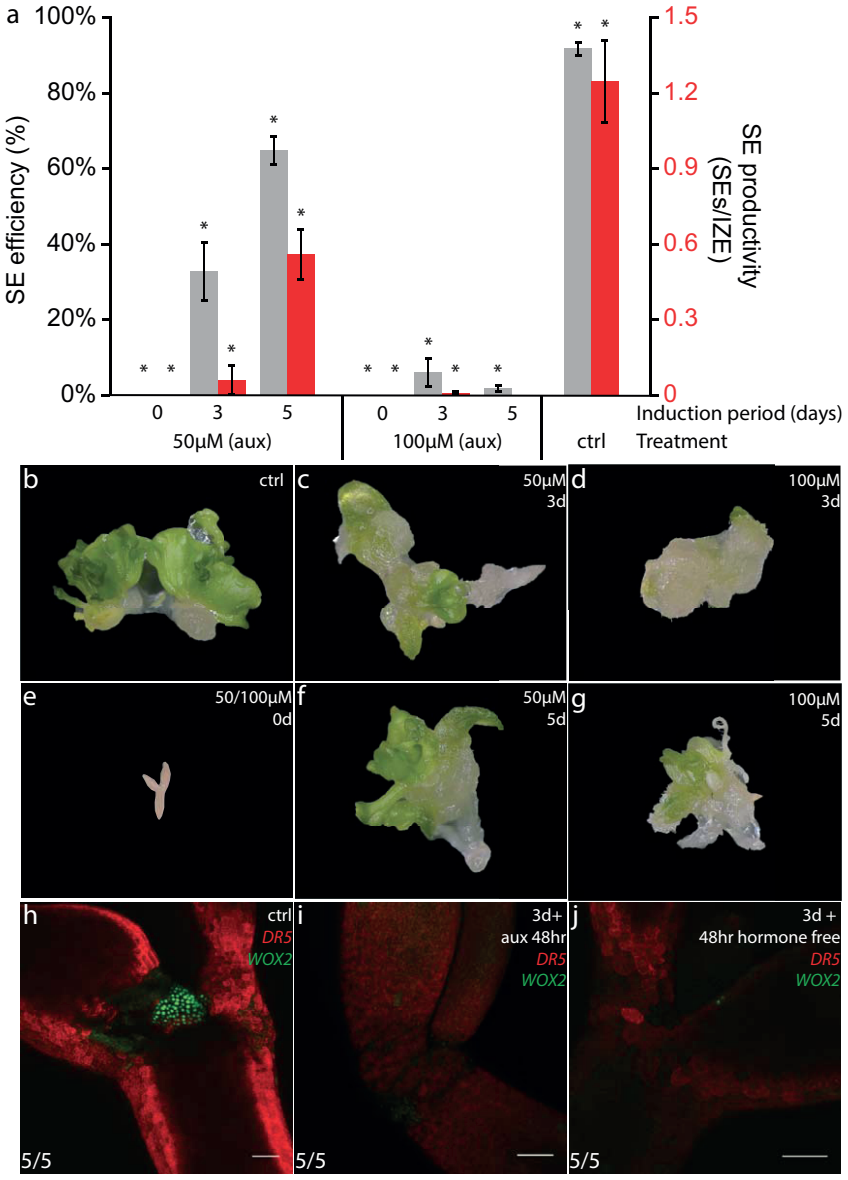

FIGURE 2 - TIR1/AFB-mediated auxin signalling is essential for SE initiation in *Arabidopsis* IZEs.
a) SE efficiency (grey bars) and -productivity (red bars) for control (ctrl) and auxinole (50µM and 100µM) treatments. Bars represent averages of duplo experiments (n=48 per experiment) with the SEM indicated by error bars, * denotes statistical difference between control (ctrl) and treatment (χ^2-test, $p<0.05$ for SE efficiencies, and Welch *t*-test, $p<0.05$ for SE productivities). b-g) Representative phenotypes of IZEs following control (b, ctrl), or 50µM (c,f) and 100µM (d,g) auxinole treatment after 0 (e), 3 (c,d), or 5 (f,g) days of pre-incubation on SEIM. h-j)) Representative confocal images of the SAM and cotyledons of *pWOX2::NLS-YFP DR5::RFP* IZEs incubated on SEIM for 5 days (h, ctrl),or for an additional 48hr on SEIM with 100µM auxinole (i, SEIM) or on hormone free medium (j). Scale bar is 50µm.

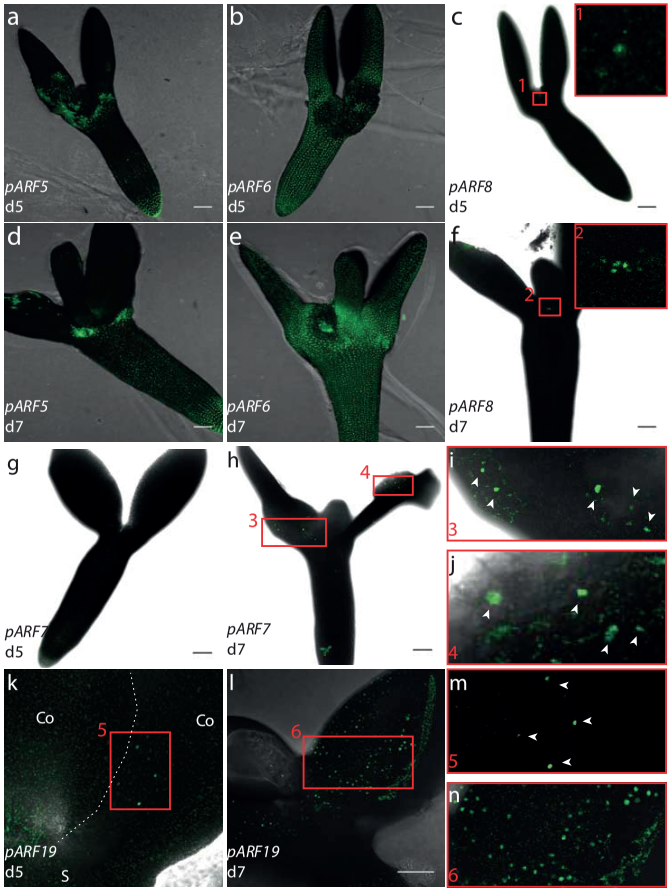

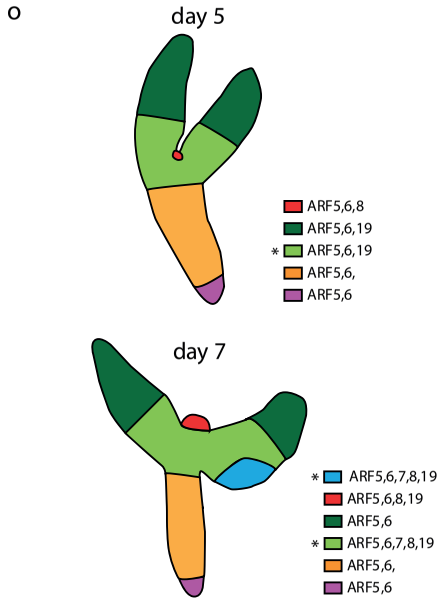

FIGURE 3 - The expression of all five *Arabidopsis* genes encoding activating *ARFs* is enhanced during 2,4-D induced SE initiation.

a-n) Representative CSLM images showing *pARF5::3nGFP* (a,d), *pARF6::3nGFP* (b,e), *pARF8::3nGFP* (c,f), *pARF7::3nGFP* (g-j), and *pARF19::3nGFP* (k-n) IZEs on day 5 (a-c, g, k, m) and day 7 (d-f, h-j, l, n) of culture on SEIM. Red-boxed images in (c) and (f) are magnifications of the regions in boxes (1) and (2), those in (i) and (j) are magnifications of boxes 3 and 4 in (h), and those in (m) and (n) are magnifications of boxes 5 and 6 in (k) and (l), respectively. Scale bar is 100µm, 10-20 IZEs were analysed per timepoint. Dashed lines outline the IZE, Co = cotyledon and S = Sam, arrowheads point towards nuclear GFP. o) Schematic representation of the spatial expression of the indicated ARF genes in IZEs after 5 or 7 days on SEIM. Asterisks indicate regions of SE initiation.

Subsequently, we analysed the SE efficiency of the corresponding T-DNA insertion mutants. A single mutation of *arf6-1* did not result in decreased SE efficiency (Figure 4a) and because of the sterile phenotype of the *arf6 arf8* double mutant we decided to specifically suppress *ARF6* and *ARF8* expression in the embryo by expressing miRNA167 (Wu et al., 2006) under control of the cell division-specific *RPS5A* promoter using a GAL4-*UAS* promoter transactivation system (Weijers et al., 2001). Emasculated flowers of the *Arabidopsis* line *UAS::miRNA167a* were pollinated with *RPS5A::GAL4* pollen. The resulting F1 *RPS5A>>miRNA167a* IZEs showed a significant reduction in the SE efficiency (55%, Figure 4a,b) compared to wild-type IZEs (90%, Figure 4a,c).

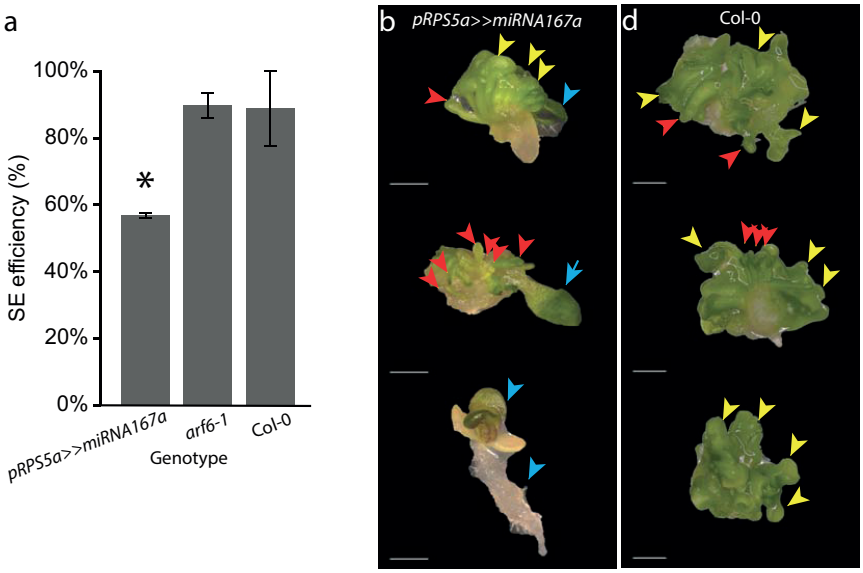

FIGURE 4 - ARF activators ARF6 and ARF8 are both required for SE initiation.
a) SE efficiencies for silenced ARF6/8 by *pRPS5a>>miRNA167a* in F1, *arf6-1* and Col-0 IZEs after standard SE culture. Bars represent averages of duplo experiments (n=48 per experiment) with the SEM indicated by error bars, * denotes statistical difference between control (ctrl) and treatment (χ^2-test, $p<0.05$ for SE efficiencies. b) Representative phenotype images of *pRPS5a>>miRNA167a* and Col-0 IZEs are shown. Root/shoot tissue is indicated with blue arrowheads, embryogenic tissue with yellow arrowheads and individual somatic embryos with red arrowheads, scale bar is 1mm. Please note that for presentation purposes the original background of the IZE images was removed and replaced by a black background.

Two different double mutant combinations were used to study the role of *ARF7* and *ARF19* in SE. Both *arf7-1 arf19-1* and *arf7-1 arf19-2* IZEs showed a significant reduction in SE development compared to wild-type IZEs (Figure 5a). Double mutant IZEs varied in phenotype after SEIM incubation, ranging from IZEs with anthocyanin accumulation in the cotyledons that produced white callus

(Figure 5b), IZEs that started germinating based on cotyledon development and produced callus (Figure 5c), and IZEs that produced somatic embryos (Figure 5d). In general, the *arf7 arf19* double mutant IZEs produced smaller calli and developed more roots and shoots compared to wild-type IZEs (Figure 5e-g). Expression of the auxin response reporter *DR5::RFP* was significantly reduced in the *arf7-1 arf19-1* double mutant compared to wild-type IZEs (Figure 5h-k). Simultaneously, the embryo cell fate reporter *pWOX2::NLS-YFP* in *arf7-1 arf19-1* double mutant IZEs showed reduced expression in the base of the cotyledons (Figure 5o), but stronger expression in the root-hypocotyl junction (Figure 5r) compared to wild-type IZEs (Figure 5n, q). This *pWOX2::NLS-YFP* expression pattern was similar to what was observed in wild-type IZEs incubated on hormone free media (Figure 5l, m, p, s).

In Chapters 2 and 3 we showed that an elevated auxin response followed by a local minimum is first required in the cotyledons of the IZEs to induce SE as marked by *WOX2::NLS-YFP* expression. Our findings here suggest that *ARF7* and *ARF19* are responsible for the overall auxin response induction that represses the embryo fate in the hypocotyl, and is probably required for SE initiation in the cotyledons in regions with a moderate auxin response.

The SLR/IAA14 - ARF7/19 lateral root module is important for SE initiation.

ARF7 and *ARF19* are well known to function together with *SLR/IAA14* during lateral root initiation, and to check whether *SLR/IAA14* is also involved in SE initiation, we analysed the *iaa14-1* loss-of-function allele, the semi-dominant *slr-1* allele that expresses a stabilized version of the SLR/IAA14 protein (Fukaki et al., 2002), and an intragenic suppressor of this allele (*slr-1R1*). Both *iaa14-1* and *slr-1R1* showed wild-type SE efficiencies (80%), whereas the SE efficiency was significantly decreased (10%) for *slr-1* mutant IZEs, which mostly produced white callus with only a few protuberances (Figure 6a,b). Additionally, we analysed *SLR/IAA14* expression using the *pIAA14::GUS* and *pIAA14::mIAA14:GFP* reporter lines, with the latter one expressing a stabilized version of the IAA14-GFP fusion protein (Fukaki et al., 2002). Both reporters showed that the expression of the *IAA14* gene is specifically upregulated on day 7 at the proximal side of the cotyledons, the tissue where SE is initiated in regions of moderate auxin response (Figure 6f-i). The analysis of the mutant alleles indicated that a degradable IAA14 protein is a prerequisite for SE initiation. However, the induction of *IAA14* expression at the site of SE initiation suggested that IAA14 may possibly be required to generate regions of moderate auxin response.

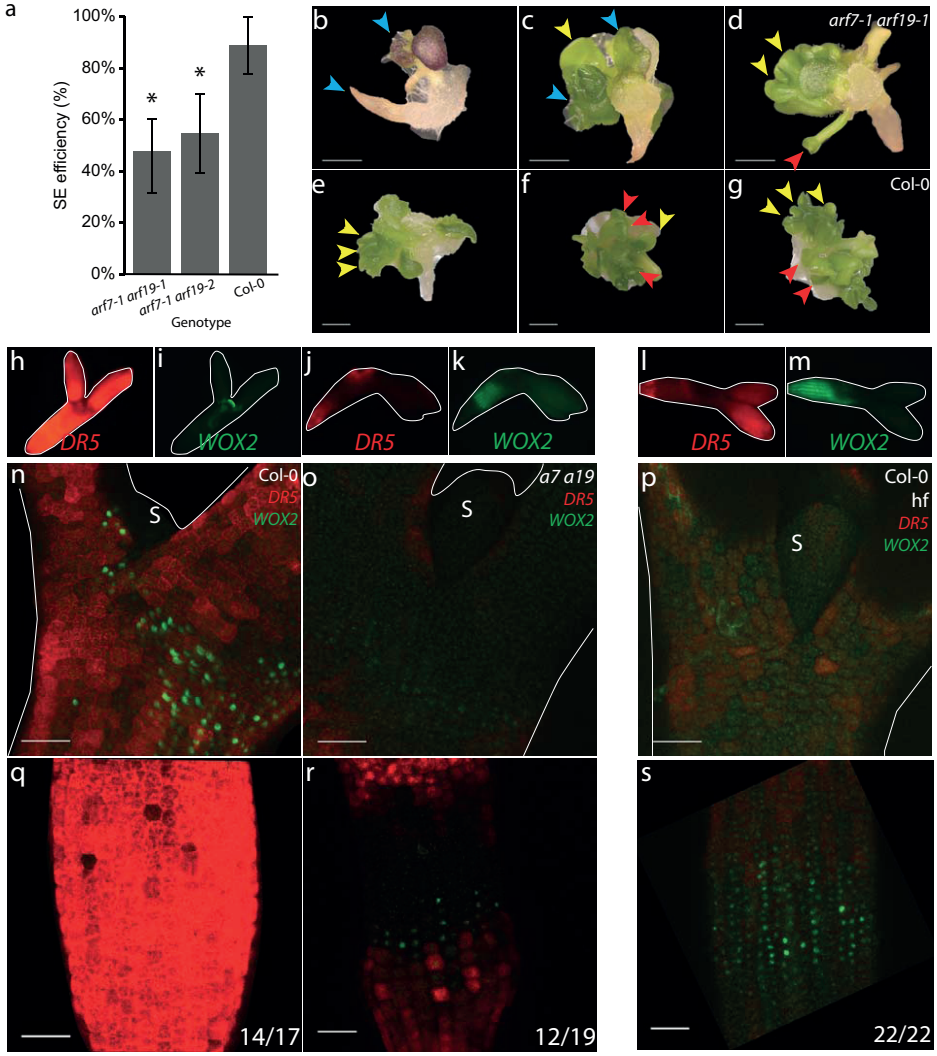

FIGURE 5 - *ARF7/ARF19*-mediated auxin response required for SE initiation in *Arabidopsis* IZEs.

a) SE efficiencies for *arf7-1 arf19-1*, *arf7-1 arf19-2* and Col-0. Bars represent averages of duplo experiments (n=48 per experiment) with the SEM indicated by error bars, * denotes statistical difference between control and treatment (χ^2-test, p<0.05 for SE efficiencies, and Welch *t*-test, p<0.05 for SE productivities). b-g) Representative images of *arf7-1 arf19-1* (b-d) and Col-0 (e-g) IZEs after SE culture, with root/shoot tissue (blue arrowheads), embryogenic tissue (yellow arrowheads) and individual somatic embryos (red arrowheads) indicated, scale bar is 1mm. h-s) Representative CSLM images of *pWOX2::NLS-YFP DR5::RFP* IZEs in Col-0 (h,i,n,q) or *arf7-1 arf19-1* (j,k,o,r) background. in base of cotyledons (n,o) and root-hypocotyl junction (q,r) after 5 days SEIM culture. (l,m,p,s) Col-0 induced for 3 days on SEIM followed by 48hr hormone free (hf) treatment in cotyledons (p) and root-hypocotyl junction (s). Scale bar is 50µm, observation frequencies are indicated in the bottom right corner of (n-s).

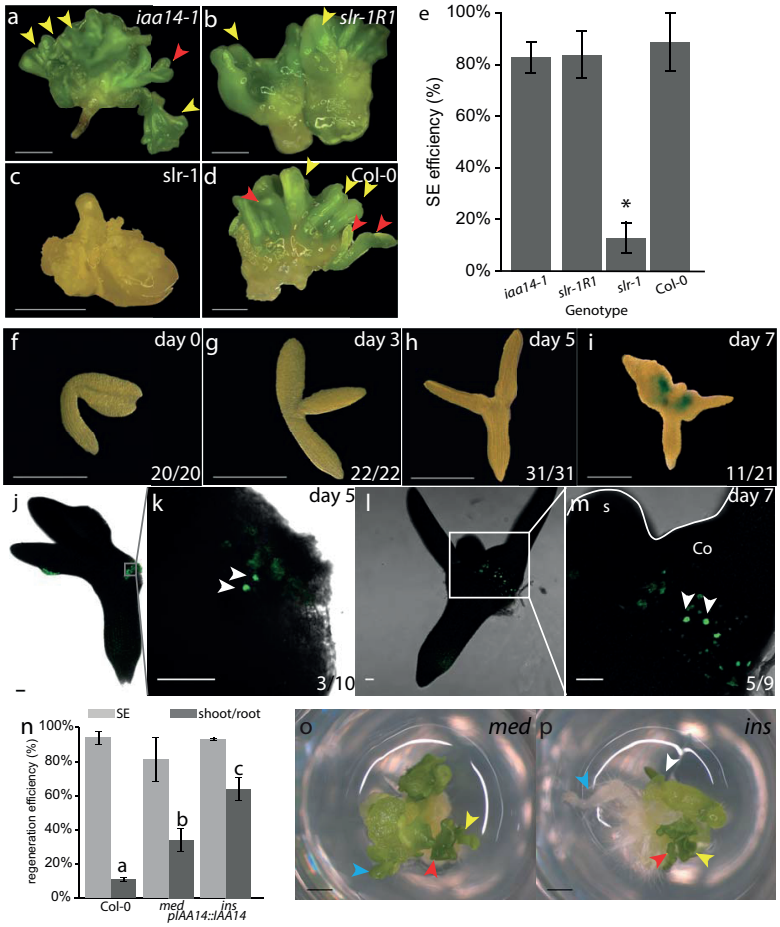

FIGURE 6 - Auxin-induced SE initiation in *Arabidopsis* IZEs requires the expression of auxin-degradable SLR/IAA14.
a-d) Representative images of *iaa14-1* (a), *slr-1R1* (b), *slr-1* (c), and Col-0 (d) IZEs after standard SE culture, scale bar is 1mm. e) SE efficiencies for *iaa14-1*, *slr-1R1* and *slr-1* mutant alleles and Col-0. Bars represent averages of duplo experiments (n=48 per experiment) with the SEM indicated by error bars, * denotes statistical difference between control and treatment (χ2-test, $p<0.05$ for SE efficiencies, and Welch *t*-test, $p<0.05$ for SE productivities). f-i) GUS stained *pIAA14::GUS* IZEs after 0, 3, 5, 7 days in SEIM culture, n=20-31 IZEs per timepoint. Scale bar indicates 500µm, observation frequencies are indicated in the bottom right corner. j-m) GFP signal in *pIAA14::mIAA14-GFP* after 5 days (j,k) and 7 days (l,m) in SEIM culture. Scale bar indicates 50µm, observation frequencies are indicated in the bottom right corner, S = SAM, Co = cotyledon. White arrowheads point at *pIAA14::mIAA14-GFP* expression. n) Regeneration efficiencies of *pIAA14::IAA14 medium (med)* and *pIAA14::IAA14 insensitive* (ins) IZEs. Light grey bars indicate the SE efficiency, and dark grey bars indicate the shoot/root regeneration efficiency. Bars represent averages of duplo experiments (n=48 per experiment) with the SEM indicated by error bars, letters denote statistical difference between control and med (a,b), control and ins (a,c), med and ins (b,c) (χ2-test, $p<0.05$ for SE efficiencies). o,p) Representative images of *pIAA14::IAA14 med* and *ins* IZEs after standard SE culture. Arrowheads in a-d) and o,p) indicate root/shoot tissue (blue arrowheads), embryogenic tissue (yellow arrow heads) and individual somatic embryos (red arrowheads), scale bar is 1mm. Please note that for presentation purposes the original background of the IZE images in (a-d, f-i) was removed and replaced by a black background.

Previously, it was shown that the Aux/IAA turnover rate determines the pace of an auxin-regulated developmental process such as lateral root formation (Guseman et al., 2015). The turnover rate of Aux/IAAs is dependent on the degradation rate of the protein, which can be influenced by the stability of the protein structure (Guseman et al., 2015), by the type of auxin present and its concentration, and by its affinity for the specific TIR1/AFB co-receptors present in the cell (Calderón Villalobos et al., 2012; Lee et al., 2014). The stability of the Aux/IAA proteins is largely dependent on the degron domain DII. To test whether the turnover rate of IAA14 played a role in SE initiation we analysed IZEs expressing mutated versions of IAA14, respectively medium (*iaa14med*) and insensitive (*iaa14ins*) under control of their native *IAA14* promoter (Guseman et al., 2015). The *iaa14med* version has a point mutation changing glycine to glutamic acid in the 72nd position of the DII domain (G72E) and the *iaa14ins* version contains a substitution changing proline to serine in the 81st position of the DII domain (P81S), which is comparable to the original *slr-1* mutation (P82S) (Fukaki et al., 2002; Guseman et al., 2015). Surprisingly, we observed wild-type SE efficiencies for both mutant lines (80-90%), but a significant increase in the shoot/root regeneration efficiency for *iaa14med* (34%) and *iaa14ins* (64%) IZEs compared to wild-type IZEs (11%) (Figure 6n-p). The discrepancy with the original *slr-1* mutation might be explained by the fact that no wild-type IAA14 protein is present in the *slr-1* mutant and that the *slr-1* mutant protein is expressed from its native promoter, whereas the expression of *iaa14med* and *iaa14ins* is controlled by a 2kb *IAA14* promoter region that is inserted at another location of the genome of wild-type *Arabidopsis*. Although this was sufficient to repress lateral root development, the *iaa14ins* line did not fully mimic the *slr-1* SE deficient phenotype (Figure S2, S3), and possibly the *iaa14ins* construct under the IAA14 promoter is not sufficiently expressed in IZEs to significantly reduce the SE efficiency (Fukaki et al., 2002).
Still, the enhanced organogenesis observed in the *iaa14med* and *iaa14ins* lines correlated nicely with the stability of the mutant proteins, and the steep reduction in SE efficiency with *slr-1* mutant IZEs suggests that the regeneration process can be modulated by repression of the auxin response, with weak repression leading to organogenesis, and strong repression to callus formation.

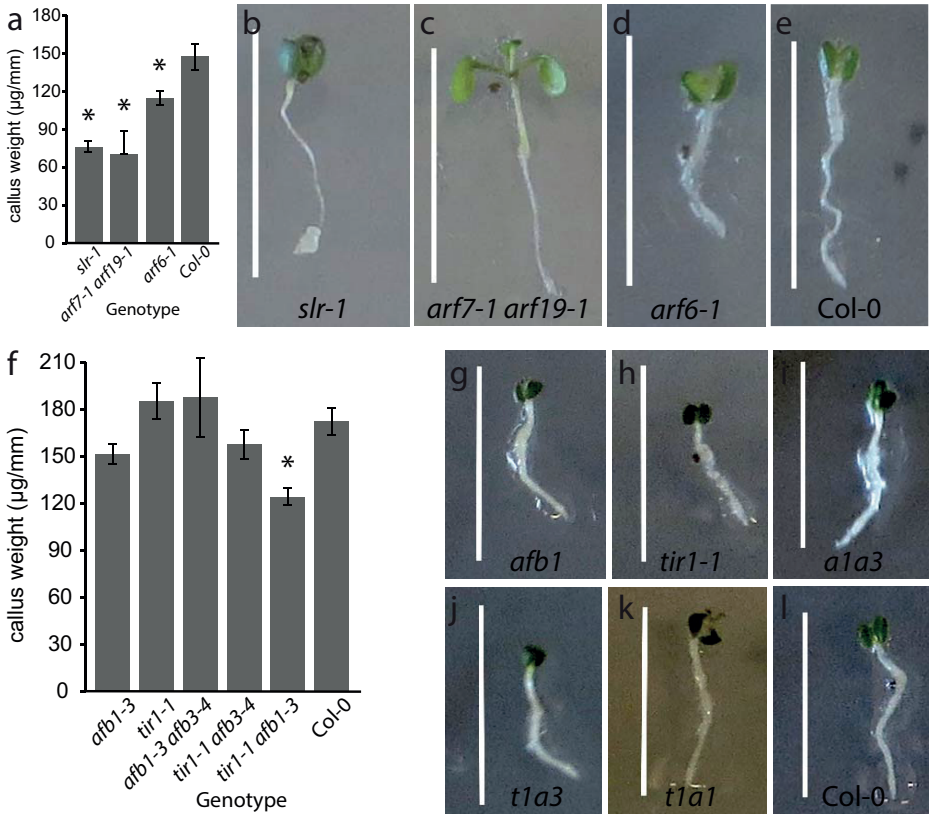

FIGURE 7 - Auxin-induced root callus development as a phenotypic screen for *Arabidopsis* mutants defective in SE.
a, f) Quantification of weight per mm root length for the *slr-1*, *arf7-1 arf19-1*, *arf6-1* mutants (a) and several single and double *tir1/afb* mutants (f) after incubation for 4 days on hormone free medium followed by 4 days on SEIM. Bars represent averages of a single experiment (n=35-50), with the SEM indicated by errors bars.* denotes statistical differences between a mutant line and wild-type Col-0 (Welch *t*-test, $p<0.05$) b-e, g-l) Representative images of *slr-1* (b) *arf7-1 arf19-1* (c) *arf6-1* (d) *afb1-3* (g) *tir1-1* (h) *afb1-3 afb3-4* (i), *tir1-1 afb3-4* (j) *tir1-1 afb1-3* (k) and Col-0 (l). Scale bar is 1cm.

Root callus formation as an easy phenotypic pre-screen to identify candidate genes involved in SE initiation

To determine the SE efficiency for many different *Arabidopsis* mutant backgrounds is a time-consuming, laborious process, because it requires the availability of fertile flowering plants (which is problematic for several important mutant backgrounds) and accurate timing of manual emasculation, pollination of flowers and harvesting of the IZEs from the ovules. In this chapter we showed that lateral root deficient mutants were impaired in SE. In addition, several groups have shown that lateral root deficient mutants are defective in 2,4-D-induced

root callus development (DiDonato et al., 2004; Sugimoto et al., 2010; Fan et al., 2012). This together with the involvement of the IAA14-ARF7/19 auxin signalling module in SE initiation suggested strong similarities between root callus development and lateral root- and SE initiation. We therefore tested whether besides lateral root initiation also 2,4-D-induced root callus development could be used as an easy pre-screen to identify candidate genes involved in SE initiation.

For our experiments we used the SE and lateral root deficient mutants *slr-1* and *arf7 arf19* as a negative control and Col-0 and the single *arf6-1*, *tir1-1* and *afb1*-1 mutants as a positive control (no effect on SE initiation). Furthermore, we tested the *afb1-3 afb3-4* and *tir1-1 afb3-4* double mutants, as based on the strong effect of auxinole on IZE survival and SE imitation we expected to see an effect here on callus development. Four days old seedlings grown on hormone free medium were transferred to SEIM and after four days the shoot was removed, weight and length of the remaining hypocotyl and root was measured and the weight per mm root length was calculated for 35-50 seedlings per genotype. Matching with our expectations, *slr-1* and *arf7-1 arf19-1* seedlings showed a significant reduction in root callus development as compared to wild-type seedlings (Figure 7a). In *slr-1* seedlings callus development was restricted to the root tip, whereas in *arf7-1 arf19-1* seedlings callus development was reduced over the entire root length (Figure 7b) compared to wild-type seedlings (Figure 7e). Unexpectedly, *arf6-1* also showed a significant reduction in the weight per mm root (Figure 7d), whereas no effect on lateral root initiation (Figure S4) or SE initiation was observed. The role of the ARF6/8 pair in both lateral and adventitious root initiation is well described (De Rybel et al., 2010; Gutierrez et al., 2012). From this we concluded that 2,4-D-induced root callus formation might be a more sensitive method to assess the involvement of a gene in SE or lateral root initiation.

Similar to our results for SE initiation (Figure S1), the *tir1-1* and *afb1-3* single and the *afb1-3 afb3-4* double mutants did not affect root callus development. However, the double *tir1-1 afb1-3* did show a significantly reduced callus weight per mm compared to Col-0. Although we have not tested this double mutant for SE initiation, our results are in line with the auxinole inhibitor experiments, and thus corroborate the redundant action of the TIR1/AFBs during SE initiation. These results suggest that root callus development can be used as a relatively easy and quick pre-screen to identify candidate genes involved in SE. A major advantage of this system is that it allows testing of mutants that due to fertility problems do not produce homozygous mutant embryos and it reduces time from nine weeks to 8 days to get the first indication for candidate genes involved in SE initiation.

Discussion

In contrast to the natural auxin IAA or other auxin-like compounds, only the synthetic auxin 2,4-D is able to induce SE in various plant species using specific tissues as explants. A general molecular pathway has been elucidated for auxins, yet specificity for each type of auxin remains to be elucidated. Auxin is perceived in plant cells by TIR1/AFB – Aux/IAA co-receptor pairs, which lead to the degradation of the Aux/IAA repressor proteins and the subsequent activation of auxin responsive gene expression by derepression of the activating ARFs that formed heterodimers with the degraded Aux/IAA protein. Here we investigated which auxin signalling components are specifically involved in 2,4-D-induced SE on *Arabidopsis* IZEs.

SE is dependent on TIR1/AFB mediated signalling

In this chapter we showed by using the auxin antagonist auxinole that TIR1/AFB signaling is important for IZE survival on SEIM and for SE initiation. GUS reporter expression analysis showed that all TIR1/AFBs are expressed in the IZE during SE initiation, and that specifically the expression of *TIR1* and *AFB2* is induced in the tissues that form SEs. Our results are in line with the recent report that *miR393*-mediated repression of *TIR1/AFB* expression leads to reduced SE efficiencies (Wójcik and Gaj (2016). In contrast to our results, however, Wojick and Gaj (2016) found a significant reduction in the SE efficiency and productivity in the *tir1-1* and *afb2-3* single mutants, whereas in our hands the same single mutant alleles were not significantly affected. In fact, Wojick and Gaj (2016) reported that the effect of the single mutant alleles is similar or even stronger than that of *miR393* overexpression. Although this result seems quite counterintuitive, since *miR393* overexpression is expected to target *TIR1*, *AFB2* and *AFB3* genes, it might relate to the weak phenotypes that were previously reported for the *miR393* overexpression lines (Parry et al., 2009). The different results obtained with the *tir1-1* and *afb2-3* single mutants are likely to be due to differences in the methodology of IZE selection for the experiments and how the SE efficiency was scored. Based on the gene expression pattern and the root callus induction assay, we did identify the involvement of *TIR1, AFB1* and *AFB2* in SE initiation. Because of their strong functional redundancy, it will however be difficult to disentangle the role of each individual *TIR1/AFB* gene in the SE initiation process.

Lateral root formation and SE initiation share auxin signalling components

When looking at auxin signalling components downstream of the TIR1/AFBs, we found to our surprise that all activating *ARFs* (5,6,7,8 and 19) were expressed in

2,4-D treated IZEs at the base of the cotyledons, the sites where SEs mostly occur during SE induction. Unfortunately, our experimental system did not allow to analyse the effect of some of the corresponding mutants, as either homozygous mutant embryos were defective and could not be grown to flowering plants producing viable IZEs (*mp/arf5*, Hardtke and Berleth, 1998), or the homozygous plants were completely sterile (*arf6 arf8,* Nagpal et al., 2005). The role of the *ARF6/ ARF8* gene pair could however be assessed by down regulating their expression using *miRNA167a* overexpression under the control of the *RPS5a* promoter (Wu et al., 2006; Weijers et al., 2001). Generated F1 *RPS5a>>miRNA167a* IZEs showed significantly reduced SE efficiencies, and since the single *arf6-1* mutant did not show this reduction, it is likely that *ARF6* and *ARF8* function redundantly in the SE initiation process, similar to their redundant role in anther dehiscence (Nagpal et al., 2005) or adventitious root formation (Gutierrez et al., 2009). Recently, the importance of *ARF6* and *ARF8* was also shown for a secondary SE system in liquid medium (Su et al., 2016).

For the other activating *ARF* pair *ARF7/19* mutant embryos could be tested, because both *arf7-1 arf19-1* and *arf7-1 arf19-2* double mutant did not lead to embryo lethality or infertility. Interestingly, both *arf7 arf19* double loss-of-function mutants showed a significant reduction in SE efficiency from 90% to 50%. *ARF7* and *ARF19* act in lateral root initiation together with *SLR/IAA14* (Fukaki et al., 2002, 2005), and when we tested IZEs of the semi-dominant *slr-1* allele encoding a stabilized version of the SLR protein they showed an even stronger strong reduction in the SE efficiency (10%) compared to the *arf7 arf19* double mutant IZEs. This suggests that the SLR/IAA14 protein may also repress other activating ARFs involved in SE initiation. A recent study on Aux/IAA - ARF interactions has indeed shown that SLR/IAA14 can interact with all activating ARFs, including ARF6 and ARF8 (Piya et al., 2014). This then makes it likely that both ARF7/19 and ARF6/8 pairs are involved in SE initiation, and that SLR/IAA14 is the central Aux/IAA regulating this process. The induction of *pIAA14::GUS* expression in the same region where SEs are formed is in line with its role as modulator of auxin response during SE initiation. By simultaneous analysis of the auxin response and embryo cell fate in the *arf7 arf19* background, we showed that an *ARF7/ ARF19*-dependent elevated auxin response is required to suppress embryo cell fate identity in the IZE, and that this subsequently leads to the generation of regions with a reduced auxin response where somatic embryos are initiated. Interestingly, such an auxin response minimum was also reported during LR founder cell specification (Dubrovsky et al., 2011). The coinciding upregulation of IAA14 expression make it tempting to speculate that this Aux/IAA is possibly

involved in generating regions of reduced auxin response where SEs are initiated.

A common model for LR and SE founder cell specification and start of development

Based on our observations and the similarities between the lateral root and SE pathway we propose a model in which an overall elevated auxin response activated by TIR1, AFB1 and AFB2 and mediated by ARF7/19 (and possibly ARF6/8) is required to reset the specified cell fate in both LR and SE systems. Our finding that an elevated auxin response was absent in the *arf7 arf19* background during SE initiation supports this hypothesis. Generation of a subsequent auxin response minimum, possibly assisted by enhanced SLR/IAA14 expression or stability, defines a developmental window for either LR or SE founder cell specification followed by the first cell division that respectively marks LR- or SE initiation (Figure 8). Interestingly, in both the zygote and lateral root founder cells a lowering and localized auxin response is required to undergo an asymmetric cell division (Scheres et al., 1994; Swarup et al., 2008; Robert et al., 2013; Yoshida et al., 2014), but whether SE starts with a similar asymmetric cell division and auxin distribution remains to be shown. Our results and those of Gliwicka et al. (2013) showed that also *ARF5* is expressed during SE, however a role for this this gene could not be established in our study. We propose that *ARF5* fulfils a similar role as in LR initiation and development, in which the *IAA12/BDL – ARF5* module acts downstream of *IAA14 – ARF7/ARF19*, where similar to its role during zygotic embryogenesis the IAA12/13 – ARF5 module might be involved in specification of the hypophysis (Weijers et al., 2006; Schlereth et al., 2010) and the provascular tissue (Hardtke and Berleth, 1998) in the somatic embryo. Experiments in which a non-repressible *ARF5* (Krogan et al., 2012) is introduced into the semi-dominant *slr* mutant could possibly reveal whether *ARF5* plays a role in SE initiation or that it rather is involved in downstream processes. Moreover, a non-repressible *ARF7* or *ARF19* could possibly reveal the importance of SLR/IAA14 in generating the regions of reduced auxin response in which SE is initiated.

In summary, our results show that lateral root initiation is similar to SE initiation in that an auxin maximum followed by a minimum is required to initiate SE or lateral root development, and the auxin responses in both systems are modulated by the same SLR/IAA14-controlled module. Based on this similarity we propose that the 2,4-D root callus induction assay (DiDonato et al., 2004; Sugimoto et al., 2010; Fan et al., 2012) could be used as a relatively quick phenotypic screen, as a first step in identifying gene candidates involved in SE.

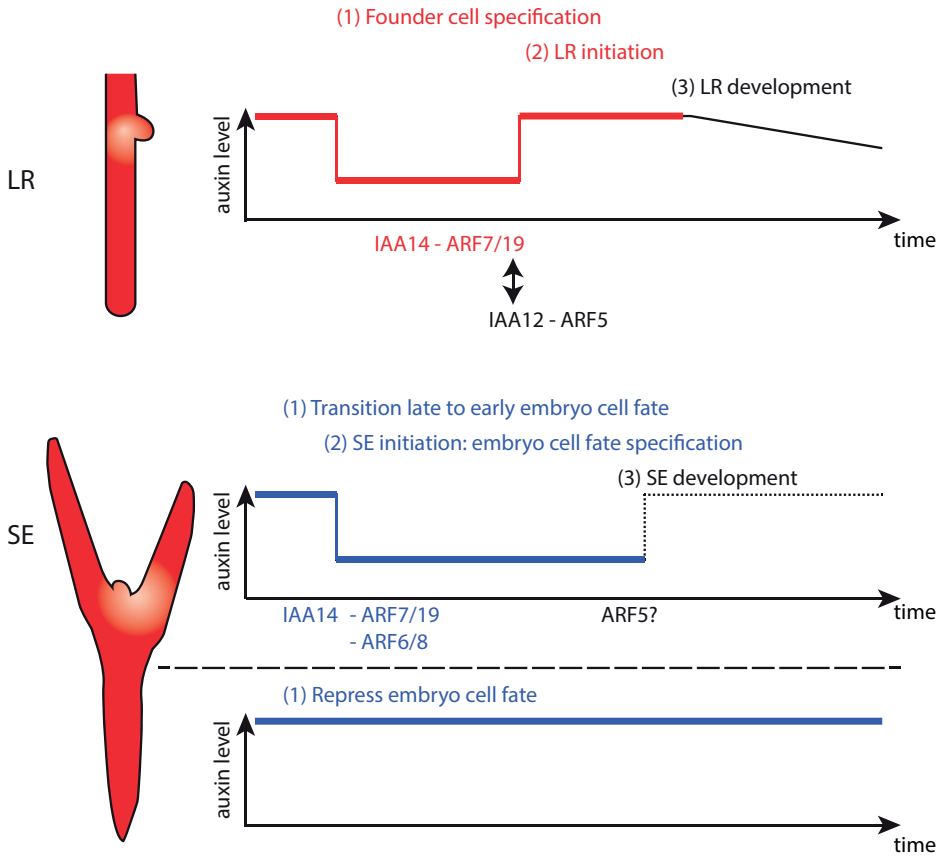

FIGURE 8 - Model for the involvement of auxin and auxin signalling components in lateral root and somatic embryogenesis initiation.

An initial auxin response maximum involving ARF7/19 and possibly also ARF6/8 is required to induce cell reprogramming, after which local auxin response minima in the root pericycle or IZE epidermis specify the lateral root or embryonic founder cells. Possibly, the enhanced expression of IAA14 is responsible for these transient local auxin minima by repressing the activity of ARF7/19 and possibly also ARF6/8. Subsequent degradation of the IAA14 repressor allows these activating ARFs to reactivate the auxin response, which triggers (asymmetric) division of the founder cells leading to lateral root (LR) development- or somatic embryogenesis (SE). To initiate LR, a second module IAA12- ARF5/MP is required to trigger the process, and ARF5 is possibly involved in SE as well. After the start of the developmental program, a gradual decrease in auxin levels allows patterning and growth of the developing root. At present, the specific details of the auxin response during SE (dashed line), after SE initiation is not yet known.

Methods

Plant lines and genotyping

All *Arabidopsis thaliana* lines described are in the Columbia (Col-0) background and summarized in Table S3. The *pWOX2::NLS:YFP* line was kindly

donated by Thomas Laux and is resistant to phosphinothricin (ppt) (Breuninger et al., 2008). The *DR5::RFP* line was donated by Eva Benkova and is resistant to hygromycin (hyg) (Marhavý et al., 2011). The collection of kanamycin (kan) resistant *pARFxx::SV40x3GFP* lines was kindly provided by Dolf Weijers (Rademacher et al., 2011). Hidehiro Fukaki donated *slr-1*, *slr-1R1*, *pIAA14::GUS*, and *pIAA14::IAA14m:GFP* (Fukaki et al., 2002). Jennifer Nemhauser kindly provided *pIAA14::IAA14 G79E (iaa14med), pIAA14::IAA14 P81S (iaa14ins)* (Guseman et al., 2015). Jason Reed kindly donated the *UAS::miR167a* line (Wu and Reed, unpublished) and the *pRPS5a::GAL4* was previously described (Weijers et al., 2001). Mark Estelle donated the *tir1-1 afb1-3 afb2-3/+ afb3-4* quadruple mutant from which segregating double mutants were selected, and the *pTIR1::cTIR1-GUS pAFB1::cAFB1-GUS*, *pAFB2::cAFB2-GUS*, and *pAFB3::cAFB3-GUS* reporter lines (Parry et al., 2009). The *iaa14-1* (N25214/CS25214), *arf7-1 arf19-1* (N24629), *arf7-1 arf19-2* (N24630), *arf6-1* (N24606) mutants were obtained from NASC (www.arabidopsis.info) and are described respectively in Overvoorde et al. (2005) and Okushima et al. (2005). Single *tir1-1* (N3798), *afb1-3* (N662878), *afb2-3* (N637151), and *afb3* (N657515) mutant lines were obtained from NASC as well.

Genotyping

Sequences of DNA primers used for genotyping are provided in Table S2, All PCR reactions were performed using DreamTaq DNA polymerase (ThermoFisher Scientific, EP0705) on genomic DNA isolated as described by Giraudat (2003), melting temperature and annealing time was 55°C and 60s, unless otherwise stated.

Plant tissue culture and growth conditions

Arabidopsis seeds were surface sterilized and germinated on MA medium (Masson and Paszkowski, 1992) complemented with 1% (w:v) sucrose, and 0.8% (w:v) Daishin agar, pH5.8. For antibiotic selection ppt, hyg or kan was added to the medium after autoclaving at a final concentration of 20mg/mL for ppt and hyg, and of 50mg/mL for kan. Seven to ten days after germination (dag), seedlings were transferred to a mixture of soil and sand, 2 per pot, and grown under a 16hr. photoperiod and 70% relative humidity. IZEs were harvested from plants 1-2 weeks after flowering. The siliques were surface sterilized with a 20% bleach/70% ethanol solution for 5min. and rinsed at least three times with sterile water.

SE-inducing medium (SEIM) consisted of B5 medium, with 4.5µM 2,4-D, 2% (w:v) sucrose and 0.8% (w:v) Daishin agar (Gaj, 2011; Nowak et al., 2012). Hormone free medium was MA medium (Masson and Paszkowski, 1992). Media were sterilized

by autoclaving at 120°C for 20min. SE was performed in sterile 48-wells plates (Greiner cellstar art. nr. 677180) that were filled with 400µL SEIM or hormone free medium using a repeater pipet. IZEs were placed on SEIM (one per well) and incubated overnight at 4°C in the dark followed by incubation at 21°C under a 16hr photoperiod for a standard period of 14 days, followed by 7 days incubation on hormone free medium (standard SE culture). Auxinole was kindly donated by Ken-Ichiro Hayashi (Hayashi et al., 2008, 2012) and was added to SEIM from a 50mM stock solution in DMSO to final concentrations of 50µM and 100µM.

For the SE efficiency studies with inhibitors or mutant IZEs, IZEs synchronized in their developmental stage were obtained by manual pollination. For this purpose, the 2 or 3 oldest but still closed flower buds of primary inflorescence stems were emasculated and pollinated and 12 days after pollination (dap) IZEs were excised from the ovule using a dissecting microscope. Per two parent plants, 2-3 sets of 2-3 closed flower buds were emasculated.

To keep data comparable between inhibitor experiments, large-scale experiments were set up as follows: the 50µM and 100µM auxinole and 2,4-D control treatments were performed in duplicate for all 2,4-D pre-induction periods (0, 3 and 5 days). Per treatment, 48 IZEs were used, one IZE per well in a 48-wells plate. For the 3 and 5 days induction, a large pool of IZEs was cultured in multiple 48-wells plates. At day 3 and day 5 48 IZEs were selected randomly out of the different plates for each treatment and transferred to plates containing 2,4-D and 100µM inhibitor. For the day 0 treatment 4 siliques were used to compile 1 plate per treatment (12 IZEs per silique).

The mutant studies were performed by culturing 48 IZEs per genotype in duplicates.

For confocal or light microscopy analysis non-synchronized late IZEs from more or less the same developmental stage were selected based on their size as described by (Gaj, 2011). Broken or damaged IZEs were discarded and not used.

Statistics of SE

To quantify SE, four categories were used to score 1) embryogenic tissue (also referred to as embryogenic callus), if no individual somatic embryos were found but embryogenic tissue developed. Embryogenic tissue was defined as smooth green structures without trichomes, that either looked like fused cotyledons or like fused zygotic embryos 2) SE forming IZEs, if individual somatic embryos were observed that were attached to the IZE by their root pole. In that case, the number of individual somatic embryos was counted. 3) Non-embryogenic callus forming IZEs, if callus was formed that remained white-yellowish without

developing somatic embryos or embryogenic tissue 4) Dead IZEs, if the tissue turned white, showed no growth and maintained their original size.

Category 1 and 2 were merged to quantify the number of responding IZEs that produced embryogenic tissue. The SE efficiency was then calculated as (Luo and Koop, 1997)

$$SE\ efficiency = \frac{N_r}{N_t} \quad 100\%$$

N_r = the number of responding explants. N_t = total number of explants tested.

SE productivity was calculated as

$$SE\ productivity = \frac{N_i}{N_t}$$

N_i = the number of individual somatic embryos observed. N_t = the total number of IZEs that were tested (including the ones that died).

Statistics for SE efficiency were performed in Microsoft Excel, using the χ^2-test for association (Holmes et al., 2011). For SE productivity, a Welch *t*-test was performed in Rstudio (Pace, 2015).
For inhibitor studies we compared the control treatments to check whether refreshment of SEIM would contribute to SE efficiency and productivity. The two controls were not statistically different for SE efficiency and productivity (respectively χ^2_{calc}=2.9, and *t*-test p-value 0.524, described in Chapter 2) and for this reason we performed all statistical tests between the treatment and the 0 days control.

Root callus assay

To induce root callus, seeds were germinated and grown on hormone free medium for four days and subsequently transferred to SEIM for another four days. After a total of 8 days culture the plates, including a scale, were photographed with a compact camera Canon PowerShot SX260 HS. The root length was measured using FIJI. To measure root weight, the shoot was removed and the weight of the root, including callus that developed, were measured. The root weight per mm was calculated in Microsoft Excel and the Welch *t*-test in Rstudio was used to calculate statistical differences (Pace, 2015).

GUS staining

Staining for B-glucuronidase (GUS) activity was performed as described by Malamy and Benfey (1997) with the following modifications: The staining solution was made as follows: a K/NaPI buffer was made by adding approximately 50mL 0.5M KH_2PO_4 to 125mL 0.5M Na_2HPO_4 tuntil pH reached 7.0.40mL of this solution was diluted with MilliQ to 200mL, and.subsequently2mL 1M EDTA (pH8.0), 2mL 0.1M $K_4Fe(CN)_6$, 2mL 0.1M ($K_3Fe(CN)_6$ and 200uL 0.1% Triton were added. X-gluc (Duchefa, X1402) was pre-dissolved in DMSO at 100mg/mL and was added to the staining solution at a final concentration of 1mg/mL. The bottle with the solution was wrapped in aluminium foil and stored at 4°C for a maximum of 6 months. Samples were submerged in 1-2mL staining solution and incubated for 3hr at 37°C followed by overnight incubation at room temperature to increase staining. Samples were destained with 0.24M HCL 20% methanol for 15min at 55°C, followed by 15min incubation in 7% (w:v) natriumhydroxide/ 60% ethanol for clearing. Samples were rehydrated through an ethanol series 50% - 30% - 10% - 5%, with 5min incubation between each step. To completely remove chlorophyll from the embryos, samples were then cleared for at least 1hr with a 25% (w:v) chloralhydrate in 50% glycerol solution.

Microscopy

Images of (GUS stained) IZEs were taken with a Leica DC 500 stereomicroscope using the Leica Application Suite v2.8.1 software or a Zeiss Axioplan DIC/Nomarski microscope equipped with Axiocam MRc5 camera and AxioVision40 V4.7.2.0 software and a 10x objective. Image editing was performed in FIJI and Adobe Photoshop CS5.1 and figures were assembled in Adobe Illustrator CS5.1

Confocal Laser Scanning Microscopy (CSLM) was performed with a ZEISS LSM510 exciter equipped with argon and helium/neon lasers. GFP and YFP were detected using a 488nm band pass filter for excitation and a 500-530nm band pass filter for emission. Simultaneously, chlorophyll background fluorescence was captured with a 650nm long pass emission filter. RFP was excited at 530nm and was captured with a 550-600nm band pass emission filter. Images were captured with ZEISS ZEN2009 software.

Fluorescence combined with Differential Interference Contrast (DIC) microscopy was performed with a Zeiss Axioplan DIC/Nomarski microscope equipped with Axiocam MRc5 camera and AxioVision40 V4.7.2.0 software and a 10x objective, red and green filters were used to capture RFP and GFP images, respectively.

Samples were prepared on a microscope slide by embedding IZEs in a thin layer of 0.5% low melting point agarose, and adding a droplet of water before covering with a cover slip.

Acknowledgements

C.P. was supported by an NWO-TTI-Green Genetics core project grant (NWO 828.11.004) to R.O. from the Earth and Life Sciences Division with financial support from the Netherlands Organisation for Scientific Research (NWO). We thank Gerda Lamers for her help with microscopy.

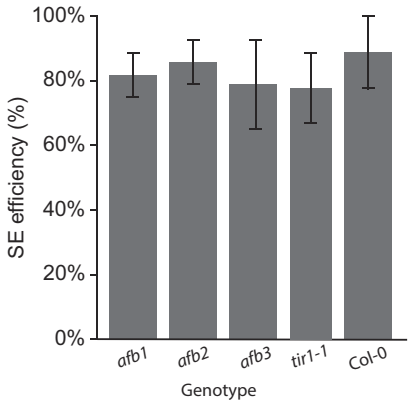

FIGURE S1 - SE efficiencies for single *tir1/afb* mutant and wild-type IZEs. Bars represent duplo experiments (n=48) with the SEM indicated by error bars. No statistical difference was observed between mutant and wild-type IZEs. ($\chi 2$ test , $p<0.05$).

TABLE S1 - Frequency (%) of IZEs not surviving when induced on SEIM supplemented with 50 or 100µm auxinole starting day 3 and 5 in culture. As a control, IZEs cultured on SEIM were included. Frequencies are averages of duplo experiments (n=48 per experiment).

2,4-D induction period (days)	**0**		**3**		**5**		**ctrl**
auxinole (uM)	50	100	50	100	50	100	0
death (%)	100	100	18	90	1	45	0

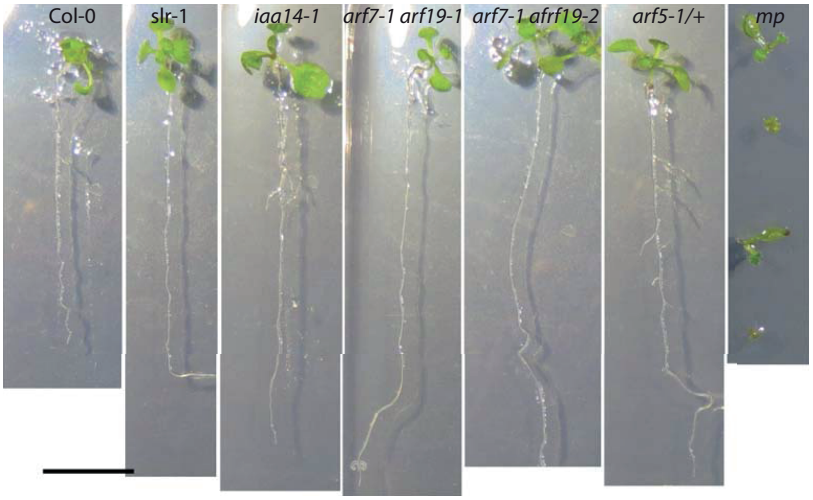

FIGURE S2 - Phenotypes of Col-0, *slr-1*, *iaa14-1*, *arf7-1 arf19-1*, *arf7-1 arf19-2*, *arf5-1/+* and *mp* seedlings germinated and grown for 14 days on hormone free medium. Scale bar is 1cm.

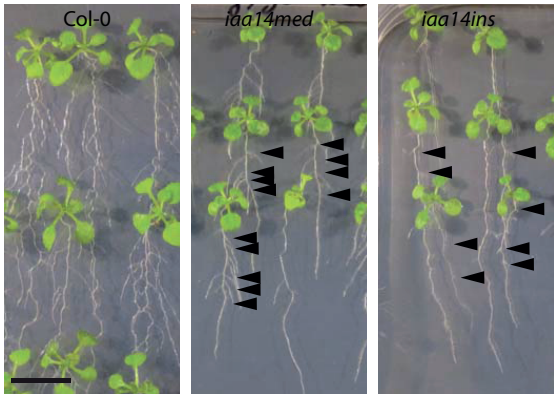

FIGURE S3 - Phenotypes of *iaa14med* (a) *iaa14ins* (b) and Col-0 (c) seedlings germinated and grown for 14 days on hormone free medium. Arrowheads point at lateral roots.. Scale bar is 1cm.

FIGURE S4 - Phenotypes of Col-0 and *arf6*-1. Seedlings were germinated and grown for 10 days on hormone free medium. Scale bar is 1cm.

TABLE S2 - Primers used for genotyping *Arabidopsis* mutant alleles. GSP is gene- specific primer, BP is border-specific primer. All reactions were carried out on genomic DNA, DreamTaq polymerase, Tm = 55ºC, At = 60s, unless otherwise stated.

Gene	Primer orientation	Sequence (5' - 3')	Remarks
arf5-1	GSP left	GAGAGGAAGTAAGCACCCGAC	
	GSP right	TCATTACATCCAGGCTCATCC	
	BP	LBB1.3 salk	
arf6-1	GSP left	GGGAGATTGAGCCTTTAACAACA	Tm=47.9C
	GSP right	TCGCTTCGCAGCTCGTGGTAGCTGCT	
	BP	GAGACATCTCCTTACCACGG	
arf7-1	GSP left	TGCACTCCTCTTTGAACCATC	Tm 58.6C
	GSP right	CACGAGTTCTTGTTTTAGCCG	
	BP	LBB1.3 salk	
arf19-1/arf19-2	GSP left	GTCATATCCAGCGACAGTATG	arf19-1 CP129 + CP124
	GSP right	GAGGTTTGGGGATTGGAAGTTCA	arf19-2 CP128 + CP124
	BP	JMLB1	
tir1-1 **(single)**	GSP left	AGCGACGGTGATTAGGAGGT	CAPS digestion with BsaI
	GSP right	CAGGAACAACGCAGCAAAA	
afb1-3 **(single)**	GSP left	AACGGAAGACTAGGAAGCGAG	SALK_070172
	GSP right	GCAACAGCTTCAAGACCTTTG	
	BP	LBB1.3 salk	
afb2-3 **(single)**	GSP left	TCAACGGTCAAGATCCATCTC	SALK_137151
	GSP right	CTGCAATTAGCGGCAATAGAG	
	BP	LBB1.3 salk	
afb3 **(single)**	GSP left	TGCTTTGCTGATCTTCTAAGG	SALK_016356C
	GSP right	AGGGTCTAAGACGGCTCTCTG	
	BP	LBB1.3 salk	
tir1-1 **(double)**	GSP left	AGCGACGGTGATTAGGAGGT	CAPS digestion with BsaI
	GSP right	CAGGAACAACGCAGCAAAA	
afb1-3 **(double)**	GSP left	GGCGAAAAGTTCGTCTCTTG	SALK_070172
	GSP right	AAGATCAGGCATTCGGACAG	
	BP	LBB1.3 salk	
afb2-3 **(double)**	GSP left	TTCTCCTTCGATCATTGTCAAC	SALK_137151
	GSP right	TAGCGGCAATAGAGGCAAGA	
	BP	LBB1.3 salk	
afb3-4 **(double)**	GSP left	GGGTCTAAGACGGCTCTCTG	SALK_068787
	GSP right	CAATGGCTGAATTACGGTGA	
	BP	LBB1.3 salk	

LBB1.3 salk	ATTTTGCCGATTTCGGAAC
JMLB1	GGCAATCAGCTGTTGCCCGTCTCACTGGTG

TABLE S3 - *Arabidopsis* plant lines used, with their origin and selection method

Plant line	Origin	SALK/ NASC code	selection marker	additional information
pWOX2::NLS:YFP	T. Laux		ppt	Breuninger et al. 2008
DR5::RFP	E. Benkova		hyg	Marhavý et al. 2011
arf7-1 arf19-1	NASC	N24629	PCR	Okushima et al. 2005
arf7-1 arf19-2	NASC	N24630	PCR	Okushima et al. 2005
tir1-1	NASC	N3798	PCR	Ruegger et al. 1997, 1998
afb1-3	NASC	SALK_070172C / N662878	PCR	
afb2-3	NASC	SALK_137151 / N637151	PCR	
afb3	NASC	SALK_016356C / N657515	PCR	
afb1-3 afb3-4	M. Estelle	SALK_070172 (afb1-3) SALK_068787 (afb3-4)	PCR	Dharmasiri et al. 2005, selected from segregating TirQ
tir1-1 afb3-4	M. Estelle	SALK_068787 (afb3-4)	PCR	Dharmasiri et al. 2005, selected from segregating TirQ
tir1-1 afb1-3	M. Estelle	SALK_070172 (afb1-3)	PCR	Dharmasiri et al. 2005, selected from segregating TirQ
arf5-1	NASC	SALK_023812/ N24605	PCR, *mp* phenotype	
arf6-1	NASC	N24606	PCR	
UAS::miR167a	J. Reed			Wu and Reed, unpublished
pRPS5a::GAL4	J. Reed / R. Offringa			Weijers et al. 2001
pARFxx::SV40x3GFP	D. Weijers		kan	Rademacher, E. PhD thesis (2009)
iaa14-1	NASC	N25214 / CS25214		
slr-1	H. Fukaki		LR phenotype	Fukaki et al. 2002
slr-1R1	H. Fukaki			Fukaki et al. 2002
pIAA14::GUS	H. Fukaki			Fukaki et al. 2002
pIAA14:mIAA14:GFP	H. Fukaki			Fukaki et al. 2002
pIAA14::IAA14 G79E (med)	J. Nemhauser		kan	T3, Guseman et al. 2015

TABLE S3 - *Arabidopsis* plant lines used, with their origin and selection method (continued)

Plant line	Origin	SALK/ NASC code	selection marker	additional information
pIAA14::IAA14 P81S (insensitive)	J. Nemhauser		kan	T3, Guseman et al. 2015
pIAA14::IAA14 G79E (med) DR5::Venus-N7	J. Nemhauser		kan x ppt	T3, Guseman et al. 2015
pIAA14::IAA14 P81S (insensitive) DR5::Venus-N7	J. Nemhauser		kan x ppt	T3, Guseman et al. 2015
pTIR1::cTIR1-GUS (tir1-1)	M. Estelle			Dharmasiri et al 2005, Parry et al. 2009
pAFB1::cAFB1-GUS (afb1-3)	M. Estelle			Dharmasiri et al 2005, Parry et al. 2009
pAFB2::cAFB2-GUS (afb2-3)	M. Estelle			Dharmasiri et al 2005, Parry et al. 2009
pAFB3::cAFB3-GUS (afb3-4)	M. Estelle			Dharmasiri et al 2005, Parry et al. 2009
iaa14-1	NASC	N25214 / CS25214		Overvoorde et al. 2005
slr-1	H. Fukaki		LR phenotype	Fukaki et al. 2002
slr-1R1	H. Fukaki			Fukaki et al. 2002
pIAA14::GUS	H. Fukaki			Fukaki et al. 2002
pIAA14:mIAA14:GFP	H. Fukaki			Fukaki et al. 2002
pIAA14::IAA14 G79E (med)	J. Nemhauser		kan	T3, Guseman et al. 2015
pIAA14::IAA14 P81S (insensitive)	J. Nemhauser		kan	T3, Guseman et al. 2015
pIAA14::IAA14 G79E (med) DR5::Venus-N7	J. Nemhauser		kan x ppt	T3, Guseman et al. 2015
pIAA14::IAA14 P81S (insensitive) DR5::Venus-N7	J. Nemhauser		kan x ppt	T3, Guseman et al. 2015
pTIR1::cTIR1-GUS (tir1-1)	M. Estelle			Dharmasiri et al 2005, Parry et al. 2009
pAFB1::cAFB1-GUS (afb1-3)	M. Estelle			Dharmasiri et al 2005, Parry et al. 2009
pAFB2::cAFB2-GUS (afb2-3)	M. Estelle			Dharmasiri et al 2005, Parry et al. 2009
pAFB3::cAFB3-GUS (afb3-4)	M. Estelle			Dharmasiri et al 2005, Parry et al. 2009

References

Adams-Cioaba, M.A., Li, Z., Tempel, W., Guo, Y., Bian, C., Li, Y., Lam, R., and Min, J. (2012). Crystal structures of the Tudor domains of human *PHF20* reveal novel structural variations on the Royal Family of proteins. FEBS Lett. **586**: 859–865.

Atta, R., Laurens, L., Boucheron-Dubuisson, E., Guivarc'h, A., Carnero, E., Giraudat-Pautot, V., Rech, P., and Chriqui, D. (2008). Pluripotency of *Arabidopsis* xylem pericycle underlies shoot regeneration from root and hypocotyl explants grown in vitro. Plant J. **57**: 626–644.

Boer, D.R., Freire-Rios, A., Van Den Berg, W.A.M., Saaki, T., Manfield, I.W., Kepinski, S., Lopez-Vidrieo, I., Franco-Zorrilla, J.M., De Vries, S.C., Solano, R., Weijers, D., and Coll, M. (2014). Structural basis for DNA binding specificity by the auxin-dependent *ARF* transcription factors. Cell **156**: 577–589.

Breuninger, H., Rikirsch, E., Hermann, M., Ueda, M., and Laux, T. (2008). Differential expression of WOX Genes mediates apical-basal axis formation in the *Arabidopsis* embryo. Dev. Cell **14**: 867–876.

Calderón Villalobos, L.I.A., Lee, S., De Oliveira, C., Ivetac, A., Brandt, W., Armitage, L., Sheard, L.B., Tan, X., Parry, G., Mao, H., Zheng, N, Napier, R., Kepinski, S., and Estelle, M. (2012). A combinatorial TIR1/AFB-Aux/IAA co-receptor system for differential sensing of auxin. Nat. Chem. Biol. **8**: 477–485.

Dharmasiri, N., Dharmasiri, S., and Estelle, M. (2005a). The F-box protein TIR1 is an auxin receptor. Nature **435**: 441–445.

Dharmasiri, N., Dharmasiri, S., Weijers, D., Lechner, E., Yamada, M., Hobbie, L., Ehrismann, J.S., Jürgens, G., and Estelle, M. (2005b). Plant development is regulated by a family of auxin receptor F box proteins. Dev. Cell **9**: 109–119.

DiDonato, R.J., Arbuckle, E., Buker, S., Sheets, J., Tobar, J., Totong, R., Grisafi, P., Fink, G.R., and Celenza, J.L. (2004). *Arabidopsis ALF4* encodes a nuclear-localized protein required for lateral root formation. Plant J. **37**: 340–353.

Dubrovsky, J.G., Napsucialy-Mendivil, S., Duclercq, J., Cheng, Y., Shishkova, S., Ivanchenko, M.G., Friml, J., Murphy, A.S., and Benková, E. (2011). Auxin minimum defines a developmental window for lateral root initiation. New Phytol. **191**: 970–983.

Fan, M., Xu, C., Xu, K., and Hu, Y. (2012). LATERAL ORGAN BOUNDARIES DOMAIN transcription factors direct callus formation in *Arabidopsis* regeneration. Cell Res. **22**: 1169–1180.

Fukaki, H., Nakao, Y., Okushima, Y., Theologis, A., and Tasaka, M. (2005). Tissue-specific expression of stabilized SOLITARY-ROOT/IAA14 alters lateral root development in *Arabidopsis.* Plant J. **44**: 382–395.

Fukaki, H., Tameda, S., Masuda, H., and Tasaka, M. (2002). Lateral root formation is blocked by a gain-of-function mutation in the *SOLITARY-ROOT/IAA14* gene of Arabidopsis. Plant J. **29**: 153–168.

Gaj, M.D. (2011). Somatic embryogenesis and plant regeneration in the culture of *Arabidopsis thaliana* (L.) Heynh. immature zygotic embryos. Methods **710**: 257–265.

Giraudat, J. (2003). Practical course on genetic and molecular analysis of *Arabidopsis*. In EMBO course, J. Giraudat, ed (EMBO), pp. 1–21.

Goh, T., Kasahara, H., Mimura, T., Kamiya, Y., and Fukaki, H. (2012). Multiple *AUX/IAA-ARF* modules regulate lateral root formation: the role of *Arabidopsis SHY2/IAA3*-mediated auxin signalling. Philos. Trans. R. Soc. Lond. B. Biol. Sci. **367**: 1461–1468.

Guilfoyle, T.J. (2015). The *PB1* domain in auxin response factor and Aux/IAA proteins: a versatile protein interaction module in the auxin response. Plant Cell **27**: 33–43.

Guilfoyle, T.J. and Hagen, G. (2007). Auxin response factors. Curr. Opin. Plant Biol. **10**: 453–460.

Guseman, J.M., Hellmuth, A., Lanctot, A., Feldman, T.P., Moss, B.L., Klavins, E., Calderon Villalobos, L.I.A., and Nemhauser, J.L. (2015). Auxin-induced degradation dynamics set the pace for lateral root development. Development **142**: 905–909.

Gutierrez, L., Bussell, J.D., Pacurar, D.I., Schwambach, J., Pacurar, M., and Bellini, C. (2009). Phenotypic plasticity of adventitious rooting in *Arabidopsis* is controlled by complex regulation of *AUXIN RESPONSE FACTOR* transcripts and microRNA abundance. Plant Cell **21**: 3119–3132.

Gutierrez, L., Mongelard, G., Floková, K., Pacurar, D.I., Novák, O., Staswick, P., Kowalczyk, M., Pacurar, M., Demailly, H., Geiss, G., and Bellini, C. (2012). Auxin controls *Arabidopsis* adventitious root initiation by regulating jasmonic acid homeostasis. Plant Cell **24**: 2515–2527.

Hardtke, C.S. and Berleth, T. (1998). The *Arabidopsis* gene *MONOPTEROS* encodes a transcription factor mediating embryo axis formation and vascular development. EMBO J. **17**: 1405–1411.

Hayashi, K.-I., Tan, X., Zheng, N., Hatate, T., Kimura, Y., Kepinski, S., and Nozaki, H. (2008). Small-molecule agonists and antagonists of F-box protein-substrate interactions in auxin perception and signaling. Proc. Natl. Acad. Sci. USA **105**: 5632–5637.

Hayashi, K., Neve, J., Hirose, M., Kuboki, A., Shimada, Y., Kepinski, S., and Nozaki, H. (2012). Rational design of an auxin antagonist of the SCF(TIR1) auxin receptor complex. ACS Chem. Biol. **7**: 590–598.

Holmes, D., Moody, P., and Dine, D. (2011). Research methods for biosciences 2nd ed. Oxford University Press.

Ikeuchi, M., Sugimoto, K., and Iwase, A. (2013). Plant callus: mechanisms of induction and repression. Plant Cell **25**: 3159–3173.

Korasick, D. A, Westfall, C.S., Lee, S.G., Nanao, M.H., Dumas, R., Hagen, G., Guilfoyle, T.J., Jez, J.M., and Strader, L.C. (2014). Molecular basis for AUXIN RESPONSE FACTOR protein interaction and the control of auxin response repression. Proc. Natl. Acad. Sci. USA **111**: 5427–5432.

Krogan, N.T., Ckurshumova, W., Marcos, D., Caragea, A.E., and Berleth, T. (2012). Deletion of *MP/ARF5* domains III and IV reveals a requirement for *Aux/IAA* regulation in *Arabidopsis* leaf vascular patterning. New Phytol. **194**: 391–401.

Kurczyńska, E.U., Gaj, M.D., Ujczak, A., and Mazur, E. (2007). Histological analysis of direct somatic embryogenesis in *Arabidopsis thaliana* (L.) Heynh. Planta **226**: 619–628.

Lee, S., Sundaram, S., Armitage, L., Evans, J.P., Hawkes, T., Kepinski, S., Ferro, N., and Napier, R.M. (2014). Defining binding efficiency and specificity of auxins for SCF TIR1/AFB -Aux/IAA co-receptor complex formation. ACS Chem. Biol. **9**: 673–682.

Luo, Y. and Koop, H.U. (1997). Somatic embryogenesis in cultured immature zygotic embryos and leaf protoplasts of *Arabidopsis* thaliana ecotypes. Planta **202**: 387–396.

Malamy, J.E. and Benfey, P.N. (1997). Organization and cell differentiation in lateral roots of *Arabidopsis thaliana*. Development **124**: 33–44.

Maraschin, F.D.S., Memelink, J., and Offringa, R. (2009). Auxin-induced, SCF(TIR1)-mediated poly-ubiquitination marks AUX/IAA proteins for degradation. Plant J. **59**: 100–109.

Marhavý, P., Bielach, A., Abas, L., Abuzeineh, A., Duclercq, J., Tanaka, H., Pařezová, M., Petrášek, J., Friml, J., Kleine-Vehn, J., and Benková, E. (2011). Cytokinin modulates endocytic trafficking of PIN1 auxin efflux carrier to control plant organogenesis. Dev. Cell **21**: 796–804.

Nagpal, P., Ellis, C.M., Weber, H., Ploense, S.E., Barkawi, L.S., Guilfoyle, T.J., Hagen, G., Alonso, J.M., Cohen, J.D., Farmer, E.E., Ecker, J.R., and Reed, J.W. (2005). Auxin response factors

ARF6 and *ARF8* promote jasmonic acid production and flower maturation. Development **132**: 4107–4118.

Nowak, K., Wojcikowska, B., Szyrajew, K., and Gaj, M.D. (2012). Evaluation of different embryogenic systems for production of true somatic embryos in *Arabidopsis*. Biol. Plant. **56**: 401–408.

Okushima, Y., Overvoorde, P.J., Arima, K., Alonso, J.M., Chan, A., Chang, C., Ecker, J.R., Hughes, B., Lui, A., Nguyen, D., Onodera, C., Quach, H., Smith, A., Yu, G., and Theologis, A. (2005). Functional genomic analysis of the AUXIN RESPONSE FACTOR gene family members in *Arabidopsis thaliana*: unique and overlapping functions of *ARF7* and *ARF19*. Plant Cell **17**: 444–463.

Overvoorde, P.J., Okushima, Y., Alonso, J.M., Chan, A., Chang, C., Ecker, J.R., Hughes, B., Lui, A., Onodera, C., Quach, H., Smith, A., Yu, G., and Theologis, A. (2005). Functional genomic analysis of the *AUXIN/INDOLE-3-ACETIC ACID* gene family members in *Arabidopsis thaliana*. Plant Cell **17**: 3282–3300.

Pace, L. (2015). Beginning R: an introduction to statistical programming (Apress).

Parry, G., Calderon-Villalobos, L.I.A., Prigge, M., Peret, B., Dharmasiri, S., Itoh, H., Lechner, E., Gray, W.M., Bennett, M., and Estelle, M. (2009). Complex regulation of the *TIR1/AFB* family of auxin receptors. Proc. Natl. Acad. Sci. USA **106**: 22540–22545.

Piya, S., Shrestha, S.K., Binder, B., Stewart, C.N., and Hewezi, T. (2014). Protein-protein interaction and gene co-expression maps of ARFs and Aux/IAAs in *Arabidopsis.* Front. Plant Sci. **5**: 1–9.

Rademacher, E.H., Lokerse, A.S., Schlereth, A., Llavata-Peris, C., Bayer, M., Kients, M., Rios, A.F., Borst, J.W., Lukowitz, W., Jürgens, G., and Weijers, D. (2012). Different auxin response machineries control distinct cell fates in the early plant embryo. Dev. Cell **22**: 211–222.

Rademacher, E.H., Möller, B., Lokerse, A.S., Llavata-Peris, C.I., van den Berg, W., and Weijers, D. (2011). A cellular expression map of the *Arabidopsis AUXIN RESPONSE FACTOR* gene family. Plant J. **68**: 597–606.

Raghavan, V. (2004). Role of 2,4-dichlorophenoxyacetic acid (2,4-D) in somatic embryogenesis on cultured zygotic embryos of *Arabidopsis*: cell expansion, cell cycling, and morphogenesis during continuous exposure of embryos to 2,4-D. Am. J. Bot. **91**: 1743–56.

Robert, H.S., Grones, P., Stepanova, A.N., Robles, L.M., Lokerse, A.S., Alonso, J.M., Weijers, D., and Friml, J. (2013). Local auxin sources orient the apical-basal axis in *Arabidopsis* embryos. Curr. Biol. **23**: 2506–2512.

De Rybel, B., Vassileva, V., Parizot, B., Demeulenaere, M., Grunewald, W., Audenaert, D., Van Campenhout, J., Overvoorde, P., Jansen, L., Vanneste, S., Möller, B., Wilson, M., Holman, T., Van Isterdael, G., Brunoud, G., Vuylsteke, M., Vernoux, T., De Veylder, L., Inzé, D., Weijers, D., and Bennett, M.J. (2010). A novel Aux/IAA28 signaling cascade activates GATA23-dependent specification of lateral root founder cell identity. Curr. Biol. **20**: 1697–1706.

Scheres, B., Wolkenfelt, H., Willemsen, V., Terlouw, M., Lawson, E., Dean, C., and Weisbeek, P. (1994). Embryonic origin of the *Arabidopsis* primary root and root meristem initials. Development **2487**: 2475–2487.

Schlereth, A., Möller, B., Liu, W., Kientz, M., Flipse, J., Rademacher, E.H., Schmid, M., Jürgens, G., and Weijers, D. (2010). *MONOPTEROS* controls embryonic root initiation by regulating a mobile transcription factor. Nature **464**: 913–916.

De Smet, I., Lau S.,, Voß, U., Vanneste, S., Benjamins, R., Rademacher, E., Schlerethd, A., De Rybel, B., Vassileva, V., Grunewald, W., Naudts, M., Levesqueh, M.P., Ehrismann, J.S., Inzé, D., Luschnig, C., Benfey P.N., Weijers, D., Van Montagu, M.C.E., Bennett, M.J., Jürgens, G., and Beeckman, T., (2010). Bimodular auxin response controls organogenesis in *Arabidopsis*. Proc. Natl. Acad. Sci. USA **107**: 2705–2710.

Su, Y.H., Liu, Y.B., Zhou, C., Li, X.M., and Zhang, X.S. (2016). The microRNA167 controls somatic embryogenesis in *Arabidopsis* through regulating its target genes *ARF6* and *ARF8*. Plant Cell. Tissue Organ Cult. **124**: 405–417.

Su, Y.H. and Zhang, X.S. (2014). The hormonal control of regeneration in plants. Curr. Top. Dev. Biol. **108**: 35–69.

Sugimoto, K., Jiao, Y., and Meyerowitz, E.M. (2010). *Arabidopsis* regeneration from multiple tissues occurs via a root development pathway. Dev. Cell **18**: 463–471.

Swarup, K., Benková, E., Swarup, R., Casimiro, I., Péret, B., Yang, Y., Parry, G., Nielsen, E., De Smet, I., Vanneste, S., Levesque, M.P., Carrier, D., James, N., Calvo, V., Ljung, K., Kramer, E., Roberts, R., Graham, N., Marillonnet, S., Patel, K., Jones, J.D.G., Taylor, G., Schachtman, D.P., May, S., Sandberg, G., Benfey, P., Friml, J., Kerr, I., Beeckman, T., Laplaze, L., and Bennet, M.J. (2008). The auxin influx carrier LAX3 promotes lateral root emergence. Nat. Cell Biol. **10**: 946–954.

Tiwari, S.B., Hagen, G., and Guilfoyle, T.J. (2003). The roles of auxin response factor domains in auxin-responsive transcription. Plant Cell **15**: 533–543.

Ulmasov, T., Murfett, J., Hagen, G., and Guilfoyle, T.J. (1997). Aux/IAA proteins repress expression of reporter genes containing natural and highly active synthetic auxin response elements. Plant Cell **9**: 1963–71.

Wang, R. and Estelle, M. (2014). Diversity and specificity: auxin perception and signaling through the TIR1/AFB pathway. Curr. Opin. Plant Biol. **21C**: 51–58.

Weijers, D., Franke-van Dijk, M., Vencken, R.-J., Quint, A., Hooykaas, P. J.J., and Offringa, R. (2001). An *Arabidopsis* Minute-like phenotype caused by a semi-dominant mutation in a *RIBOSOMAL PROTEIN S5* gene. Development **128**: 4289–4299.

Weijers, D., Schlereth, A., Ehrismann, J.S., Schwank, G., Kientz, M., and Jürgens, G. (2006). Auxin triggers transient local signaling for cell specification in *Arabidopsis* embryogenesis. Dev. Cell **10**: 265–270.

Weijers, D. and Wagner, D. (2016). Transcriptional responses to the auxin hormone. Annu. Rev. Plant Biol. **67**: 539–574.

Wójcik, A.M. and Gaj, M.D. (2016). *miR393* contributes to the embryogenic transition induced in vitro in *Arabidopsis* via the modification of the tissue sensitivity to auxin treatment. Planta: 231–243.

Wright, R.C. and Nemhauser, J.L. (2015). New tangles in the auxin signaling web. F1000Prime Rep. **7**: 7-19.

Wu, M.-F., Tian, Q., and Reed, J.W. (2006). *Arabidopsis microRNA167* controls patterns of *ARF6* and *ARF8* expression, and regulates both female and male reproduction. Development **133**: 4211–4218.

Yoshida, S., Barbier de Reuille, P., Lane, B., Bassel, G.W., Prusinkiewicz, P., Smith, R.S., and Weijers, D. (2014). Genetic control of plant development by overriding a geometric division rule. Dev. Cell. 29: 75-87.

Summary

Plant clonal propagation can be achieved either through stem cuttings or shoot and subsequent root regeneration, in which cells go through a dedifferentiated state from which they can differentiate again into shoot or root forming cells. Alternatively, vegetative propagation can be established in a single step in which a shoot-root axis, a vascular system and functional meristems are produced by the induction of embryos without fertilization such as somatic embryogenesis (SE). In the model plant *Arabidopsis thaliana*, somatic embryos are efficiently induced by incubating immature zygotic embryos (IZEs) on SE induction medium (SEIM) containing high concentrations of the auxin analogue 2,4-dichlorophenoxyacetic acid (2,4-D). During SE somatic cells are reprogrammed to become totipotent cells, from which a new embryo cell fate is acquired in order to develop somatic embryos. The genetic and molecular mechanism by which 2,4-D induces SE initiation has not been elucidated yet and the aim of this PhD thesis was to identify which components of the auxin response pathway are involved in this developmental process.

Chapter 2 describes the establishment of a standardized system for SE initiation and outgrowth of somatic embryos using 12 days old *Arabidopsis* IZEs. In this system, *pWOX2::NLS-YFP* was used as a marker for embryonic cell fate and the first *WOX2-YFP*-reported embryonic cell clusters could be observed after 5 to 7 days of culture in SEIM. Interestingly, these clusters were located in regions of low auxin response. Cells neighboring these SE initiation regions with low auxin response expressed AUX1 influx carriers, which suggested the low auxin response regions might be generated by auxin influx into these neighboring cells. *aux1 lax* loss-of-function mutant IZEs showed enhanced shoot/root regeneration at the cost of SE, and studies using inhibitors of cellular auxin transport corroborated the important role for auxin influx proteins in SE initiation, whereas auxin efflux proteins only seemed to be important for establishment of the embryonic body pattern later during SE. .

Chapter 3 focuses on the role of auxin biosynthesis in SE. We used combinations of chemical biology, genetics and reporter studies to unravel the Trp-dependent auxin biosynthesis pathway during 2,4-D induced SE initiation. The best-characterized Trp-dependent pathway is the indole-3-pyruvic acid (IPyA) pathway, which includes two enzymatic steps that successively convert Trp into IPyA and IPyA to IAA. The first step comprises the TRYPTOPHAN AMINOTRANSFERASE OF ARABIDOPSIS1 / TRYPTOPHAN AMINOTRANSERASE RELATED1-4 (TAA1/TAR1-4) family of enzymes. The second step includes the YUCCA1-11 (YUC1-11) family enzymes. Histological analysis in combination with the use of YUC- or TAA1/TAR-specific inhibitors suggested that YUC activity is rather required for IZE survival during tissue culture and for later development of the initiated embryo, and that

TAA1/TARs are required to establish a dynamic auxin response that drives cell division during SE initiation.

In **Chapter 4** again a combination of chemical biology, mutants and promoter reporter lines was used to map the auxin response components involved in 2,4-D-induced SE on *Arabidopsis* IZEs. Blocking the formation of TRANSPORT INHIBITOR RESISTANT1/AUXIN SIGNALING F-BOX (TIR1/AFB) co-receptor complex with the auxin antagonist auxinole showed that this co-receptor complex was required for SE initiation. Furthermore, we found that the activating AUXIN RESPONSE FACTOR (ARF) sister pairs ARF7/19 and ARF6/8 were both required for efficient SE initiation. Interestingly, SE was almost completely blocked in the semi-dominant *solitary root-1* (*slr-1*) mutant, indicating that 2,4-D-induced SE and lateral root initiation in *Arabidopsis* share the same auxin response module. The auxin response mutants that were blocked in SE also showed a reduced 2,4-D-induced root callus development, suggesting that this phenotype can be used to pre-select mutants affected in SE. Based on our results we propose a model in which *SLR/IAA14*–regulated dynamic auxin responses are required for both lateral root and embryonic founder cell specification and for the subsequent cell divisions starting respectively lateral root and somatic embryo development.

In conclusion, we propose that lateral root initiation is similar to SE initiation in that an auxin maximum followed by a minimum is required for both processes, and that the auxin responses in both systems are modulated by the same SLR/IAA14 module. Substantial work is still required to outline the details of downstream responses. They possibly include the regulation of auxin biosynthesis through TAA1/TAR and the coordinated expression of AUX1/LAX proteins to establish the dynamic auxin response leading to SE initiation.

Samenvatting

Vegetatieve vermeerdering van planten vindt veelal plaats door middel van stekken, waarbij cellen door een dedifferentiatie fase moeten gaan om vervolgens weer te herdifferentiëren tot wortel- of scheutvormende cellen. Een alternatieve methode van vegetatieve vermeerdering is somatische embryogenese (SE), waarbij in een enkele stap van een wortel-scheut as, een vasculair systeem en functionele meristemen worden geproduceerd. In de modelplant *Arabidopsis thaliana* (zandraket) kan SE efficiënt geïnduceerd worden door onrijpe zygotische embryos (immature zygotic embryos, IZE) te incuberen op SE inductie medium (SEIM) met een hoge concentratie van het auxine analoog 2,4-dichlorofenoxyazijnzuur (2,4-D). Tijdens SE worden somatische cellen "geherprogrammeerd" tot totipotente cellen, waaruit vervolgens vervolgens wordt opnieuw een embryo-identiteit wordt aangenomen, waarna somatische embryo ontwikkeling volgt. Het genetische en moleculaire mechanisme verantwoordelijk voor de initiatie van SE door 2,4-D is nog niet volledig opgehelderd en was het doel van dit promotieonderzoek.

Hoofdstuk 2 beschrijft de ontwikkeling van een gestandaardiseerd systeem voor SE initiatie en uitgroei van somatische embryo's met behulp van 12 dagen oude *Arabidopsis* IZEs. In dit systeem werd *pWOX2::NLS-YFP* gebruikt als een marker voor het aanduiden van de embryo identiteit in cellen en de eerste *WOX2-YFP* gemarkeerde cellen waren zichtbaar na 5 tot 7 dagen in kweek op SEIM. Opvallend was dat deze gemarkeerde clusters van cellen gelokaliseerd waren in regio's van een lage auxine response., Cellen gelegen naast deze SE initiatie regio's met een lage auxine response, tonen expressie van AUX1 influx eiwitten, wat de suggestie wekt dat de lage auxine concentratie regio's vereist voor het genereren van SE initiatie veroorzaakt worden door een verhoogde opname in de aangrenzende cellen. *aux1 lax* verlies-van-functie mutante IZEs toonden een verhoogde scheut/wortel-regeneratie, ten koste van SE, en experimenten met behulp van blokkers voor cellulair auxine transport benadrukten de belangrijke rol voor auxine influx eiwitten in de initiatie van SE, terwijl de auxine efflux eiwitten enkel van belang lijken te zijn tijdens de ontwikkeling van het embryo later tijdens SE.

Hoofdstuk 3 is toegewijd aan de rol van auxine biosynthese in SE. Door een combinatie van chemische biologie, genetica en markers te gebruiken is de Trp-afhankelijke biosynthese route tijdens 2,4-D geïnduceerde SE initiatie ontrafeld. De meest bekende Trp-afhankelijke route is de indole-3-pyruvic acid (IPyA) route waarin twee enzymatische stappen Trp successievelijk naar IPyA en IPyA naar IAA converteren. De eerste enzymatische stap wordt uitgevoerd door de TRYPTOPHAN AMINOTRANSFERASE OF ARABIDOPSIS1 / TRYPTOPHAN AMINOTRANSERASE RELATED1-4 (TAA1/TAR1-4) enzym familie. De tweede stap door

de YUCCA1-11 (YUC1-11) enzym familie. Histologische analyse in combinatie met het gebruik van YUC of TAA1/TAR specifieke inhibitoren suggereert dat YUC activiteit cruciaal is voor de overleving van IZE overleving tijdens de weefselkweek fase en voor de latere ontwikkeling van het somatische embryo, en dat de TAA1/TAR enzymen nodig zijn voor het genereren van een dynamische auxine response, welke de cel deling tijdens SE initiatie te aanstuurt.

In **Hoofdstuk 4** is wederom een combinatie van chemische biologie, genetica en promoter marker lijnen gebruikt om de componenten van de auxine response in kaart te brengen die een rol spelen in 2,4-D geïnduceerde SE in *Arabidopsis* IZEs. Door het blokkeren van het co-receptor complex TRANSPORT INHIBITOR RESISTANT1/AUXIN SIGNALING F-BOX (TIR1/AFB) met de auxine antagonist auxinole lieten we zien dat dit co-receptor complex vereist is voor SE initiatie. Aanvullend vonden we dat de activatie van AUXIN RESPONSE FACTOR (ARF) zuster paren ARF7/19 en ARF6/8 beide vereist zijn voor efficiënte SE initiatie. Aanvullend vonden we dat SE bijna volledig geïnhibeerd is in de semi-dominante *solitary root-1* (*slr-1*) mutant. Deze bevindingen suggereerden dat 2,4-D geïnduceerde SE en laterale wortel ontwikkeling in *Arabidopsis* dezelfde auxine response module gebruiken. De auxine response mutanten die een SE deficiënt fenotype hadden, ontwikkelden ook minder 2,4-D geïnduceerde wortel callus. Dit suggereert dat dit wortel callus fenotype gebruikt kan worden om mutanten te voorselecteren voor SE. Op basis van onze resultaten, stellen wij een SE initiatie model voor waarin *SLR/IAA14*-gereguleerde dynamische auxine responsen zijn vereist om voor zowel laterale wortel als voor somatische embryogene cel differentiatie te bewerkstelligen en voor de daaropvolgende celdelingen welke de ontwikkeling starten van laterale wortels en somatische embryo's.

In conclusie stellen wij dat laterale wortel ontwikkeling vergelijkbaar is met SE initiatie op het gebied van de in beide systemen vereiste auxine maximum gevolgd door een auxine minimum, En dat beide processen worden gestuurd door de *SLR/IAA14* module. Aanzienlijk werk is nog nodig om de processen die worden aangestuurd door *SLR/IAA14* te ontrafelen. Deze processen bevatten mogelijk de regulatie van auxine biosynthese door TAA1/TAR en de gecoördineerde expressie van AUX/LAX transporters welke de dynamische auxine response reguleren die leidt tot SE initiatie.

Dankwoord

De afgelopen jaren heb ik een hoop mensen leren kennen die direct of indirect bijgedragen hebben aan de resultaten beschreven in dit boekje. De eerste persoon die ik graag wil bedanken is mijn voormalige MSc afstudeerstage begeleider, Dr. Chris van Schie (Enza Zaden). Onder zijn begeleiding mocht ik mijn afstudeerstage aan University California San Diego doen en hij stimuleerde mij om met een promotieonderzoek verder te gaan en verwees mij door naar de groep van Dr. Remko Offringa. Remko ben ik zeer dankbaar voor de kans die hij mij gaf om dit onderzoek te doen en voor de inzichten in ontwikkeling van planten en de moleculaire genetica. Tevens ben ik zeer dankbaar voor de mogelijkheid om deel te nemen aan internationale congressen in Hawaii (USA), Norwich (UK) en Versailles (FR) waar ik veel inspirerende wetenschappers heb kunnen spreken die een bron van kennis waren voor mijn project.
Dit project was een samenwerking met de groep van Dr. Kim Boutilier en hen wil ik via deze weg bedanken, voor hun enthousiasme en input in mijn project.

Het promoveren is een substantieel onderdeel van je leven en het hele traject heb ik met veel plezier beleeft samen met mede promovendi. Felix en Daan, onbetwiste borrelgangers. Marloes, altijd opgewekt en positief. Dino, mega gezellig met een nuchtere blik op onderzoek. Senioren Christiaan, Marijn, Martijn en Philippe, het was fijn om jullie als ervaren collega's te hebben! Kasper en Myckel, ook erg bedankt voor het helpen opstarten van moleculair werk in het lab. Yuanwei and Majid, thank you for all the funny comments and jokes that you made and insights into a different culture as well as Omid, thank you for the initial help in the lab.
Much gratitude goes toward Dr. Emma Larsson, from the Swedish University of Agricultural Sciences (SLU) in Uppsala. You gave my project a significant boost when I was stuck. I loved your enthusiasm for auxin responses, your way of thinking and I really appreciated that you were always available for a discussion. I hope we stay in touch!
De rest van de Moleculaire Genetica groep ben ik natuurlijk ook erkentelijk voor de kritieken en suggesties tijdens besprekingen, lab-uitjes en de bijzondere koffietafel gesprekken.

Tijdens mijn promotie heb ik ook een aantal leuke studenten mogen begeleiden: Jo-Janneke, Tanja, Paulina, Kadir en Vera. Allen hebben zij bijgedragen aan dit boekje en aan mijn persoonlijke ontwikkeling als docent en adviseur. Dank voor jullie bijdrage, de eindeloze vragen, post-its en gezelligheid in het lab.

Niet alleen mijn collega's in het lab hebben bijgedragen aan een mooi promotietraject. Vrienden en familie hebben zeker hun bijdrage geleverd met het doorvragen over het 'nut' van mijn onderzoek en wat het betekende als ik een experiment probeerde uit te leggen. Mijn paard weet nu inmiddels ook alles van auxine en geniet nu nog meer van elke grasspriet die ze eet.

En als laatste, mijn steun en toeverlaat, Caspar. Dank voor het aanhoren van al mijn uitdagingen, theorieën, het meedenken en de ondersteuning.

Curriculum vitae

Cheryl Philipsen was born September 12th, 1987 in Den Helder, the Netherlands. She graduated from SG Nieuwediep in 2006 and continued with studying Biology at Utrecht University from which she graduated in 2009. Following the bachelor Biology, Cheryl continued with the masters programme at Utrecht University in Environmental Biology, where she focused on Plant Sciences. As part of her Master study she conducted two internships, one at Utrecht University and one at University California San Diego (UCSD). At Utrecht University, the role of *ETHYLE RESPONSE FACTORS* (*ERFs*) during the hyponasty response in *Arabidopsis* was investigated with the supervision of Dr. Joanna Polko in the Ecophysiology group of prof. L.A.C.J. Voesenek. At UCSD, Multiple Reaction Monitoring (MRM) assays were developed and applied to identify proteins involved in Pathogen-Associated Molecular Pattern (PAMP)- and effector triggered immunity in *Arabidopsis* with the supervision of Dr. Christiaan van Schie in the Developmental Biology group of prof. S. Briggs. After obtaining her Master degree in 2011, Cheryl started her PhD research on the role of the hormone auxin in 2,4-dichlorophenoxyacetic acid (2,4-D)-induced somatic embryogenesis in *Arabidopsis* at the Institute of Biology at Leiden University under the supervision of Dr. Remko Offringa. The work done as a PhD student is described in this thesis. Currently, Cheryl is working as a project lead Plant Physiology at breeding company Dümmen Orange.